



Water, Environment, Landscape Management at
Contaminated Megasite . WELCOME
(EVK1-CT-2001-00103)

WORKPACKAGE 9

DELIVERABLE 9.4

Modeling Sediment transport and Contaminant transport in water systems

Edited by T. Grotenhuis

Authors

M. Mokwa, R. G³owski, R. Kasperek, I. Chmielewska
*Institute of Environmental Engineering
Agricultural University of Wroclaw, Wroclaw,
Poland*

K. Kania, G. Malina
*Institute of Environmental Engineering
Czêstochowa University of Technology, Czestochowa,
Poland*

J. Szdzuj , M. Korcz, J. Bronder
*Institute for Ecology of Industrial Areas, Katowice,
Poland*

M.P.J. Smit, J.T.C. Grotenhuis
*Department of Environmental Technology
Wageningen University and Research Centre, Wageningen,
The Netherlands*

Wageningen, November 2004

Content

1. General introduction	4
2. Contaminant transport by particles	6
2.1 Numerical modelling of contaminated sediment transport: Model of reduction/prevention against contaminant transport.....	6
2.1.1 Objective and scope	7
2.1.2 Characteristics of the lower Widawa river: section from km 8,0 To km 14,0	8
2.1.2.1 Climate, hydrography, hydrology and hydraulics of the riverbed.....	8
2.1.2.2 Bed materials and suspended load	8
2.1.2.3 Types and sources of contaminants.....	10
2.1.3 Incipient motion Criterion and critical parameters	12
2.1.3.1. Bed load	12
2.1.3.2. Suspended load.....	12
2.1.3.3. Incipient motion of sediment, suspension, erosion, sedimentation in the Widawa River	12
2.1.3.4. The grain-size boundary for the suspended and bed load transport	14
2.1.4 The HEC-RAS Model	16
2.1.4.1 Initial measurements required for the model	16
2.1.4.2. Input data and used options for modelling of the Widawa River	17
2.1.4.3. Sediment transport formulas in the HEC-RAS	21
2.1.4.4. Presentation of results.....	26
2.1.5. Results of the contaminated sediment transport modeling	27
2.1.6. Conclusions and recommendations.....	28
2.1.7 Literature	30
2.1.8 Attachments.....	32
Attachment 1	33
2.2 Estimation of Water Erosion Potential and Contaminant Flux at The Tarnowskie Góry Megasite	34
2.2.1 Introduction.....	35
2.2.2 Approach	36
2.2.2.1 Modeling erosion and Megasite management.....	36
2.2.2.2 Calculation of the potential erosion rate	37
2.2.2.3 GIS coverages and data used to model soil erosion	38
2.2.3 Results and conclusion.....	40
2.2.4 References	42
2.2.5 Appendix A. List of map compositions.....	43
3. Contaminant transport in water systems	51
3.1 Heavy metal and inorganic contaminant transport	51
3.1.1 Introduction.....	52
3.1.2 Material and methods	53
3.1.3 Results.....	54
3.1.3.1 Contaminant leaching at different Eh	54
3.1.3.2 Contaminant leaching at different pH	56
3.1.3.3 Contaminant leaching at different L/S ratio	58
3.1.4 Discussion	60
3.1.5 References	63

3.2	Hydrophobic organic contaminant transport.....	65
3.2.1	Introduction.....	66
3.2.2.	Linking bioavailability approach to hydraulic conditions	69
3.2.2.1	Bioavailability approach.....	69
3.2.2.2	Hydraulic conditions	70
3.2.2.3	Linking bioavailability with hydraulics	71
3.2.2.4	Mass transfer in the boundary layer	72
3.2.2.5	Mass transfer within a sediment particle	73
3.2.3	Linking bioavailability and hydraulics: laboratory experiment.....	74
3.2.4	Relevance of the availability-tool to the IMS.....	78
3.2.5	List of publications	79
4.	Relevance sediment and contaminant transport to IMS	80
5.	Appendix 1. Heavy metal and inorganic contaminant transport.....	82

1. General introduction

In the previous deliverables of WP9 a mathematical tool was developed for the determination of the transport of contaminated sediment (D9.3), and a desorption method for the determination of bioavailable Hydrophobic Organic Contaminants (HOC) was described (D9.2). In the development of the desorption tool, samples from the megasites were used that were characterized in D9.1.

In this deliverable an approach is presented to obtain an insight into the transport of contaminated sediment particles, and to find out whether such contaminated sediment may function as a source or a sink of heavy metals, as well as hydrophobic organic contaminants.

The transport of contaminated particles is described in chapter 2. In a specific case the sediment transport was illustrated by the HEC-RAS model whereas in another specific case a risk- screening assessment was performed with the ESEM model for water erosion.

First, the numerical modeling of sediment transport is illustrated by a specific case of the Widawa river (Poland). An analysis and presentation of the minimum set of required input data for the HEC-RAS model for a section of the Widawa river was made. Further verification and adjustment of the HEC-RAS model to simulate of contaminated sediment transport was performed. A simulation of contaminated sediment transport was conducted, and a demo version of the HEC-RAS model for simulating contaminated sediment transport was made.

As contaminated sediments may origin from water erosion due to run-off, an estimation of the water erosion potential and contaminant fluxes at the Tarnowskie Góry Megasite was performed with the ESEM model. The goal of this work was to estimate the water erosion potential of the soil and the potential contaminant flux that can be mobilized as a result of this process. The fluxes of barium and zinc were estimated for the area of the Tarnowskie Góry Megasite. It was shown that the total amount of emission of contaminants is about several hundred times lower than the original load of contaminants contained in the chemical plant landfills, and several times lower than the load of contaminants deposited in the top soils surrounding the Chemical Plant. The evaluation of real load into the sediment system was not conducted, and no hydrological model for the area was made. However, the obtained results may be used in risk management of the site, and for selection of the areas that are suitable for specific remediation activities like phytoremediation to reduce the contaminant fluxes.

The contaminant transport in water systems is described in chapter 3. As in sediments most often a cocktail of heavy metals and organic contaminants can be found, the contaminants mass transport from sediments into water systems was evaluated in two subsequent studies.

First, the effect of pH, redox potential and the liquid over solid ratio (L/S) on the mobility of metals and other inorganic contaminants in sediment was studied. In this study the sediment material was taken from the Stola river, as this river flows through the Tarnowskie Góry megasite. In the sediments high concentrations of heavy metals and inorganic contaminants are observed. Results show that leaching may be

enhanced at low pH as is generally known. However, in the studies with a high ratio of L/S, the situation that may take place during the flooding, a relatively high flux of heavy metals and inorganic contaminants into the water system may occur.

The second part of the transport of contaminants to the water system focused on desorption of hydrophobic organic contaminants (HOC). Here, the bioavailability tool that was developed in deliverable 9.2 is coupled to hydraulic conditions by using a radial diffusion model. As the characterization of the hydraulic conditions in this set up is identical to the hydraulic conditions used in the sediment transport model of HEC-RAS model a first link is made between the transport of sediment particles and the transport of contaminants to the water system. A study was performed with sediments from the Rotterdam harbor megasite in an experimental set up under well controlled hydraulic conditions. Preliminary results showed the promising link between the bioavailability approach and hydraulic conditions. More experiments using different stir-rates and dilution rates, as well as using soils and sediments with different contaminants, are needed to test the validity and robustness of this setup.

In chapter 4 the relevance of the results obtained in this deliverable to the Integrated Management System (IMS) is discussed.

2. Contaminant transport by particles

2.1 Numerical modelling of contaminated sediment transport: Model of reduction/prevention against contaminant transport

Edited by G. Malina

M. Mokwa, R. G³owski, R. Kasperek, I. Chmielewska
Institute of Environmental Engineering
Agricultural University of Wroclaw, Wroclaw, Poland

G. Malina
Institute of Environmental Engineering
Cz stochowa University of Technology, Czestochowa,
Poland

2.1.1 Objective and scope

The main objectives of this work are as follows:

- analysis and presentation of necessary input data for HEC-RAS model for the section of the Widawa river,
- verification and adjustment of HEC-RAS model to the simulation of contaminated sediment transport,
- conducting simulation of contaminated sediment transport,
- making a demo version of HEC-RAS model for simulating contaminated sediment transport.

The execution of the above goals was conducted based on the following tasks:

- characteristics of the Widawa river at the section from km 8,0 to km 14,0 with regard to hydrography, hydrology and hydraulics,
- measurement and analysis of bed material and transported sediments in the Widawa river,
- characteristics of the sources and types of water and sediment contaminants in the Widawa bed,
- assessment of the criteria and parameters of the: start of sediment movement, sediment transport (traction and suspended bedload convection), and sediment settlement (sedimentation) in the Widawa river,
- characteristics of required input data for HEC-RAS model,
- adjustment of the HEC-RAS model to the selected section of the Widawa river with a possibility of its verification for other rivers,
- conducting simulation of contaminated sediment transport,
- analysis and presentation of transport simulation results, and recommendations.

2.1.2 Characteristics of the lower Widawa river: section from km 8,0 To km 14,0

In the valley of Widawa two dikes system exists to protect against flood (Parzonka et al. 2003):

the summer-dike system (dike spacing of 30 – 150 m),

the winter-dike system (dike spacing up to 1-1,5 km).

2.1.2.1 Climate, hydrography, hydrology and hydraulics of the riverbed

In recent years, the mean temperatures in the river basin of lower Widawa amounted to approx. 20°C (in summer period) and to 1.2°C (in winter period) (Banas, 2002). Precipitation varies on average from 24 mm (in winter) to 105°C (in summer). The mean water temperature in the Widawa River oscillated around 11°C (summer: 13-19°C, autumn: 4°C and spring: 6°C).

The Widawa River is the right-bank tributary of the river Odra river inflow at 266.9 km (Parzonka et al. 2003). Drainage area of the Widawa River in inflow cross-section to Odra is equal to 1713.1 km². There is mainly agricultural and forestry activity within the drainage basin. The low sector of the river is regulated and flows through the city of Wroclaw (km 0.0-22.0), and is a part of the Wroclaw Hydrotechnical System. The length of the river is 103.2 km, and the main tributaries are: Studnica, Swierzna, Graniczna, Olesnica and Dobra. In the studied sector of lower Widawa (km 11.2), there is the gauging station Krzyzanowice, where the water level and flow discharge are registered. The flow discharges of the Widawa River are presented in Table 2.1.

Water-surface slope in the sector of lower Widawa in the main channel varies from 0.1‰ to 0.7‰. The total Manning-Strickler coefficient ($K_s = 1/n$) for the Widawa channel varies from 10 m^{1/3}/s to 60 m^{1/3}/s, and depends on season and water levels. A low annual flow is equal to 1.59 m³/s, and an average annual flow is 6.95 m³/s.

Table 2.1 The flow discharge at the gauging station Krzyzanowice

Probability p [%]	Flow discharge Q [m ³ /s]
50	27.0
20	40.3
10	50.1
5	60.0
3	67.2
2	73.2
1	83.7
0,3	103.0

note: p - probability of the specific flow discharge frequency

2.1.2.2 Bed materials and suspended load

In order to estimate the grain composition and the grain size distribution of bed materials some field and laboratory measurements were carried out (Parzonka et al. 2003, Glowski et al. 2004).

Bed materials

In the Widawa River (section between km 0.0 and km 22.5) the material, which form the riverbed, was sampled. It consisted of sands of a mean diameter of $d_{50} = 0.33 - 0.87$ mm (Fig. 1). Main fractions were: $d = 0.1 - 0.25$ mm; $0.25 - 0.5$ mm and $0.5 - 1.0$ mm. No significant variation of the sediment bed composition on the studied river sector was observed. There are two main fractions: $0.25 - 0.5$ mm (52%) and $0.5 - 1.0$ mm (45%).

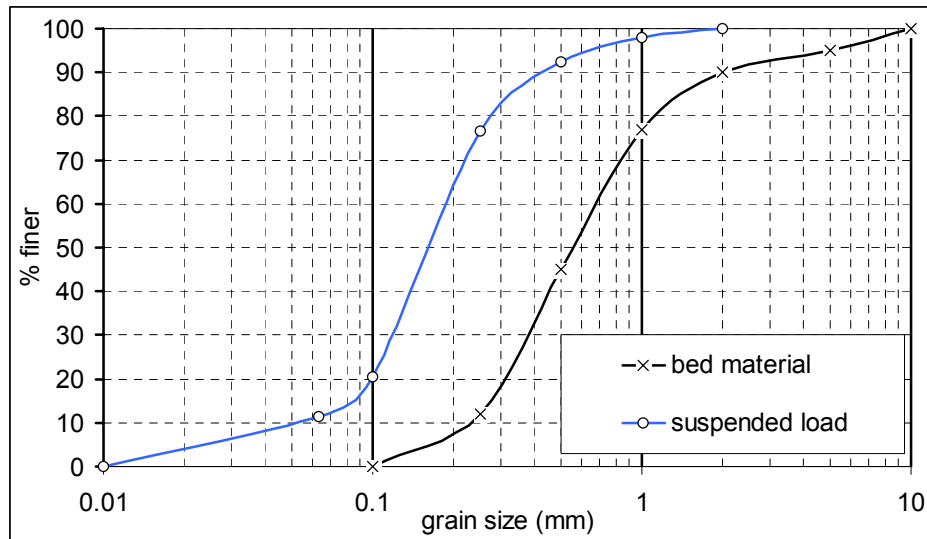


Figure 2.1 The grain size distribution curve of bed material and suspended load in the Widawa River

Suspended load

The grain size of suspended sediments in rivers, and its distribution in the vertical direction, depend on hydrological regime, hydraulic conditions and the type of bed materials. During low water levels and flow velocities usually most of fine fractions are in motion, while at high flows the coarse fractions are moving (Banasiak, 1999; Van Rijn, 1984b).

Based on the field measurements in the Widawa channel at the cross-section in Krzyzanowice performed in 2004 (Glowski et al. 2004), the sediment transport conditions, grain composition and contamination levels were estimated.

The measurements were conducted at low water levels and flows. Water depths varied from 0.45 to 0.55 m, a flow discharge was of $1.5 \text{ m}^3/\text{s}$, and flow velocity of 0.8 m. The transported sediment consisted of the fractions:

- < 0.063 mm (11.3%),
- 0.063 – 0.1 mm (9.1%),
- 0.1 – 0.25 mm (56.1%),
- 0.25 – 0.5 mm (15.9%),
- 0.5 – 1.0 mm (5.6%),
- 1.0 – 2.0 mm (2.0%).

2.1.2.3 Types and sources of contaminants

The potential sources of water contamination within the river basins include the following (Allan, 1995; Banas, 2002; Bieszczad and Sobota, 1998; Dojlido, 1995; Manczak, 1972; O'Neill, 1997; Ongley, 1982; Pawlaczyk-Szpilowa, 1980; Swerpel, 1997; Trybala, 1996):

local waste dumps (surface run-off, effluents, draining by water courses and reservoirs, washing-out during freshets/floods),
precipitation and dustfall (dry and wet deposition) from the atmosphere,
agricultural activity (fertilisers, ballast of mineral fertilisers, pesticides),
industrial districts, industrial plants, electric power plants, heat and power plants, transportation.

In the river basin of Widawa, there were, or are still operating the following facilities, which may cause the contamination of water: distillery and bakery in Działosze, fruit-vegetable processing plant in Dziadowa Kłoda, household and industrial sewage from the wastewater treatment plant in Bierutow, distilleries in Posadowice and Bierutow, SELGRROS in Długolęka; wastewater treatment plants in Mirkow, Dobroszyce, Wrocław-Psie Pole, wastewater treatment plant of sugar factory in Wrocław; Polar-Division Psie Pole and Zakrzów.

Water quality of the Widawa River

The physical-chemical characteristics of the Widawa river was conducted in 2001-2002, including the following parameters: pH, BOD, N-NH₄ (ammonia nitrogen), N-NH₃ (nitrate nitrogen), phosphates, sulfates, chlorides, Na, Mg, Ca, K, Fe, Zn, Cd, Mn, Cr, Cu, Ni, and Pb. In Table 2.2 the characteristic of water is presented, and the water purity class is specified (Banas, 2002).

Table 2.2 Mean values of water contamination in the river Widawa

Parameter	Value (mg/l)	Water purity class ^{*)}
BOD	4	A2
N-NH ₄	6.3	A1
N-NH ₃	14.7	out of class
PO ₄	0.556	A2
SO ₄	12	A1
Cl	46	A1
Na	208	-
Mg	25.7	-
Ca	134	-
K	11.2	-
Fe	1.4	A2-A3
Cr	0.1	out of class
Zn	0.2	A1
Cd	0.002	A1-A2
Mn	0.14	A2
Cu	0.02	A1
Ni	0.06	A1-A2
Pb	0.03	A1

note: ^{*)} Dz.U.2002.204.1728

The suspended load quality

The physical-chemical analysis of suspended load sampled from the Widawa River showed no presence of heavy metals. The smallest fractions, i.e. $d = 0,063-0,1$ mm and $d < 0,063$ mm, contained the most of PO_4 (above 1 mg/l) (Table 2.3). Much less phosphates were present in the coarser sediment (about 0,3 mg/l).

Table 2.3 Contents of phosphates in suspended load in the Widawa River

Fraction d (mm)	Portion of fraction (%)	Content of PO_4 (mg/l)
2-1	2.0	0.31
1-0.5	5.6	0.36
0.5-0.25	15.9	0.63
0.25-0.1	56.1	0.82
0.1-0.063	9.1	1.21
<0.063	11.3	1.49

2.1.3 Incipient motion Criterion and critical parameters

2.1.3.1. Bed load

The zone close to the riverbed is not sampled by suspended load samplers and is termed the un-sampled zone, or the zone of bed load transport (Yang, 1996). Transport in the un-sampled zone includes the rolling and jumping material of the bed load, together with some portion of suspended load. The amount of material transported in this zone can represent a significant fraction of the total load in sand-bed rivers. Bed load is difficult to measure, and at most gauging stations, it is estimated or computed rather than measured directly. Because sediments in arid zones tend to be coarse-grained, bed load generally constitutes a larger part of the total load in streams draining desert areas than those in humid areas. Generally, the bed load consists of coarser material than suspended load. It is formed of coarse sand, gravel and pebbles (stones) with the grain size larger than 1-2 mm.

2.1.3.2. Suspended load

Suspended load refers to these components of sediments, which are transported upwards by turbulent currents and stay in suspension for a significant period of time. In most natural rivers, sediments are mainly transported as suspended load. Generally, this sediment is formed by particles smaller than 1-2 mm (sand, silt and clay). Suspended load transport is a function of the concentration, sediment properties, and local (near-bed) flow parameters (Banasiak, 1999; Mokwa, 2002; Ongley, 1982; Ratomski, 1997; Wisniewski, 1972; Walling and Kane, 1982; Van Rijn, 1984b).

2.1.3.3. Incipient motion of sediment, suspension, erosion, sedimentation in the Widawa River

Incipient motion

The Shields diagram is a widely used method to determine the condition of incipient motion based on bed shear stress (Van Rijn, 1993; Yang, 1996). Points lying above the curve representing the critical condition correspond to a sediment motion, and points below the curve indicate no motion. The critical condition could be related to two dimensionless parameters: the dimensionless shear stress $\theta_{cr} = \tau_{cr} / (\rho_s - \rho)gd_i$ (also known as the Shields parameter), which does not represent the actual shear stress, and the boundary Reynolds number $Re_* = v_* d_i / \nu$.

Bonnefille and Yalin (Van Rijn, 1993; Yang, 1996) expressed the Shields curve in terms of the parameter θ_{cr} and dimensionless particle diameter $D_* = [(s_d - 1)gd_i^3 / \nu^2]^{1/3}$, where $s_d = \rho_s / \rho$ is relative density. The Shields curve can be divided into five sections expressed by the following functions:

$$\begin{aligned}\theta_{cr} &= 0.24D_*^{-1} \quad 1 < D_* \leq 4 \\ \theta_{cr} &= 0.14D_*^{-0.64} \quad 1 < D_* \leq 10 \\ \theta_{cr} &= 0.04D_*^{-0.1} \quad 10 < D_* \leq 20 \\ \theta_{cr} &= 0.013D_*^{0.29} \quad 20 < D_* \leq 150 \\ \theta_{cr} &= 0.055 \quad D_* > 150\end{aligned}$$

Suspension

Before analyzing the main hydraulic parameters, which influence the suspended load, it is necessary to determine the flow conditions, at which initiation of suspension will occur.

The critical flow conditions were determined, at which instantaneous upward turbulent motions of the sediment particles, by means of jumps with lengths of the order of 100 particle diameters, were observed. The experimental results can be represented by $v_{*,cr}/w_s = 4/D_*$ for $1 < D_* \leq 10$; and $v_{*,cr}/w_s = 0.4$ for $D_* \geq 10$, where $v_{*,cr}$ is critical bed-shear velocity according to Shields, and w_s is particle fall velocity of suspended sediment (Van Rijn, 1984a, 1984b).

It is suggested that the criterion of Bagnold may define an upper limit of suspension, whereas the lower limit can be defined by the criterion of Engelund (Molinas and Wu, 1998).

Particle settling velocity

In a clear and still fluid, the particle settling velocity w_s of a single sand particle smaller than ca. 100 μm (i.e. Stokes-range) can be described by $w_s = (s_d - 1)gD_s^2/(18\nu)$, where D_s is parameter expressing the representative particle diameter of suspended sediment particles, which may be considerably smaller than D_{50} of the bed material (Van Rijn, 1984a, 1984b).

For suspended sand particles in the range of 100-1000 μm , the following type of equation, as proposed by Zanke, can be used $w_s = 10\nu/D_s\{[(1+0.01(s_d-1)gD_s^3/(18\nu^2))]^{0.5}-1\}$,

For particles larger than ca. 1000 μm , the following simple equation can be used $w_s = 1.1[(s_d-1)gD_s]^{0.5}$.

For normal flow conditions with particles in the range of 50-500 μm , the reduced particle fall velocity (in a fluid-sediment mixture) can be described by a Richardson-Zaki type equation $w_{s,m} = (1-c)^4 w_s$.

Sedimentation, transportation and erosion

Hjulstrom estimated the relationship between the sediment size and average flow velocity for erosion, transportation, and sedimentation (Yang, 1996). He proposed the relationship for different particle size i.e. from 0.001 to 500 mm.

Calculations for the Widawa River

The results of the sediment movement conditions in the Widawa River were compared in Table 2.4 and Table 2.5. The bed materials were divided into 8 fractions. Table 4 shows the calculations of incipient motion and suspension

parameters for each fraction using the modified Shields curve (Van Rijn, 1984b). In Table 2.5, the velocities of sedimentation, transportation and erosion are compared.

Table 2.4 Parameters describing the sediment transport in lower Widawa

Grain size (mm)	D_*	θ_{cr}	τ_{cr} (Pa)	h_{cr} (m)	$\theta_{susp.}$	τ_{susp} (Pa)	$h_{susp.}$ (m)
10	240	0.055	8.9	1.82	0.20	32.4	6.6
5	120	0.052	4.2	0.86	0.20	16.2	3.3
2	49	0.040	1.3	0.26	0.15	4.90	1.00
1	25	0.033	0.53	0.11	0.12	1.90	0.39
0.5	12	0.031	0.25	0.05	0.08	0.65	0.13
0.25	6	0.044	0.18	0.04	0.08	0.32	0.07
0.1	2.5	0.096	0.16	0.03	0.16	0.26	0.05
<0.063	1.6	0.15	0.15	0.03	0.20	0.20	0.04

Table 2.5 Average flow velocities v_{cr} (m/s) for erosion, transportation and sedimentation of the sediment from lower Widawa

Grain size (mm)	Sedimentation	Transportation	Erosion
10	<0.8	>0.8	>1.8
5	<0.4	>0.4	>0.75
2	<0.16	>0.16	>0.35
1	<0.08	>0.08	>0.25
0.5	<0.04	>0.04	>0.2
0.25	<0.02	>0.02	>0.2
0.1	<0.008	>0.008	>0.22
<0.063	<0.001	>0.001	>0.9

2.1.3.4. The grain-size boundary for the suspended and bed load transport

Bed load. Bed load comprises particles that are carried in a demersal layer of a river by rolling or plane motion with a predominant gravity force. Many researchers include particles that contact riverbeds periodically and move by saltation. However, the opinions on height of lifted particles are inconsistent. Bed load consists of: boulders ($d \in 80\text{-}40\text{mm}$), gravel ($d \in 40\text{-}2\text{mm}$) and sand ($d \in 2\text{-}0.25\text{mm}$). Depending on hydrodynamic conditions, sand fractions can be classified into dragged or afloat materials. Motion of bed load grains is of a stochastic character, and can be defined as a continuous process. Density of solid particles is estimated at $\rho_r = 2650 \text{ kg}\cdot\text{m}^{-3}$, and d_{50} is generally higher than 1.0-1.2 mm. The shape of bed load grains is diverse (spherical, ellipsoidal, planar), and they may settle down on a riverbed in various ways (Morris and Fan, 1998; Yang, 1996).

Suspended load. It refers to particles transported by motion of turbulences that come from a riverbed, or can be formed at the entire flow section. In the majority, suspended load is a product of river basin denudation. Grain diameters range from 0.1 to 1.2mm. According to some researchers, suspended load transport in the European rivers is actually limited to solid particles with diameters of 0.25-0.50mm.

Practically, the upper limit diameter of grains suspended in lowland rivers is estimated at 1.2 mm, which has been confirmed by measurements carried out for the Middle Odra River. A lower limit diameter of 0.1 mm generates great controversy. With reference to literature, the apparent lower limit for suspended load corresponds to a diameter of the finest sand grains, i.e. 0.05mm (0.063mm), which in practice matches the finest sieve mesh in load material determined by screen analysis (Banasiak, 1999; Mokwa, 2002; Olive and Rieger, 1988; Van Rijn, 1984b, 1993; Yang, 1996).

Wash load. It is usually transported in a form of suspension and does not have any contact with a riverbed. It generally comes from the surface flow and consists of dusty materials with grain size of 5-100 μ m, silt wash (0.5 to 10 μ m) and dusty-silt wash (2 to 30 μ m). Grain size limits for wash load are diverse. Nevertheless, it can be assumed that if a lower limit grain size for wash load is estimated at 0.05mm, then it also constitutes an upper limit grain size for suspended load. Suspension of individual and aggregated particles is carried out in a form of laminar flow with Reynolds numbers $Re_d < 1$. Hydraulic properties of wash load depend to a large extent on: concentrations of solid particles, size and shape of grains, density of solid particles, organic matter contents (Allan, 1995; Bieszczad and Sobota, 1998; Dojlido, 1995; Gutra-Korycka and Werner-Wieckowska, 1996; Manczak, 1972; Pawlaczyk-Szpilowa, 1980; Trybala, 1996). Transport of wash load is based on maintaining grains in suspension due to turbulent velocity fluctuations that counterbalance the grain sedimentation. The Froude number of 20 can be considered as a criterion for wash load transport. Transport of the total bottom deposit comprising bed and suspended load is referred to as the total bed material load, whereas the sum of bottom deposit (bed load + suspended load) and wash load, as the total load (Morris and Fan, 1998; O'Neill, 1997).

2.1.4 The HEC-RAS Model

2.1.4.1 Initial measurements required for the model

Geometry:

- general river inventory (walk along river) for estimation of river hydraulic conditions and zones of aggradation/degradation (erosion),
- defining cross-sections of the main channel and the river valley (in order to model the contaminated sediments transport during floods). Number of cross-sections is depended on the length of a typical river sector, for small streams a distance between cross-sections should vary from ca 50 to 100 m,
- in the case of bridges, which usually contract the river width, the number of cross – sections near bridges should be of 5 (2 upstream, 2 downstream and 1 at a bridge),
- study of river scheme (tributaries etc.),
- to set-up the representative river sectors (name of the river, sector, kilometres), where the widening (increased sedimentation of contaminated sediments) and/or contractions of the river bed may occur (increased erosion of bed material with washing-out of contamination).

Hydraulics:

- decision upon selection of cross-sections, and performing the measurements of critical parameters at different water flow conditions (from low to high water levels) (Chmielewska 2004):
 - a) free surface slope I ,
 - b) water depth h ,
 - c) area of flow stream A ,
 - d) water stream width B ,
 - e) flow velocity v at given depths in hydrometric verticals,
 - f) flow discharge Q ,
- selection of roughness coefficients of a river channel based on field measurements and/or literature,
- flow discharge curves at given cross-sections (preferably gauging cross-sections if exist) from low to high discharge rates,
- indicating river sections with low or no flow,
- indicating of existing river embankments.

Sediments:

- sampling of materials from riverbed at selected cross-sections and determination of grain size distribution and physical properties (by division on fractions),
- measurement of suspended and bed load transport by means of samplers at cross-sections and physical-chemical analysis, including contamination,
- for bed materials, suspended and bed load to determine:
 - a) sediment composition, grain size curves, sediment density, grain shape coefficients, water temperature (by division on fractions),
 - b) characteristic diameters (d_{16} , d_{35} , d_{50} , d_{60} , d_{84} , d_{90}) and grading coefficients,

- c) settling velocity of a single particle ω depending on a grain size d , water temperature t , and grain shape coefficients, and its correction depending on sediment concentration C ,
- d) kinematics viscosity coefficient ν ,
- e) start of suspended and bed load movement,
- f) erosion conditions of river muds (if present) in riverbed based on laboratory studies and calculations,
- g) transport intensity of bed and suspended load,
- sampling and physical-chemical analysis of materials from the river catchments (a few samples) for comparison with riverbed materials,
- sampling of sediment samples (unaltered structure) from the riverbed to calculate the concentration degree and sedimentation conditions of contaminated materials (mainly fine suspended load) based on laboratory studies in sedimentation columns.

Remarks and recommendations

For accurate analysis of sediment transport 9 measurements in one cross-section are postulated:

- a) 3 at a zone of low water levels,
- b) 3 at a zone of mean and bank water levels,
- c) 3 at a zone of high (above bank) water levels, i.e. at flooded area.

2.1.4.2. Input data and used options for modelling of the Widawa River

An American HEC: HEC – RAS series model is the basic model used in the world, which is recommended here within a one-dimensional description of the flood hazard zones (Brunner, 2002; Mokwa et al. 2003). It has two elementary advantages:

- it is a verified and reliable model guarded by strong restrictions within the requirements regarding the hydraulic interpretation of movements in the numerical sense - it does not require any additional tests and result checks,
- it belongs to public domain products.

HEC-RAS ver. 3.1.1 is an integrated package of hydraulic analysis programs. The system is capable of performing steady flow and unsteady flow water surface profile calculations. This application takes into account the influence of bridges, culverts, weirs, inline structures, lateral structures, storage areas, pump stations and sediment transport.

Water surface profiles are computed from one cross section to the next by solving the energy equation. Whenever the water surface passes through critical depth, the energy equation is not considered to be applicable. Then program uses the momentum equation (Brunner, 2002).

The HEC-RAS calculation procedures enable the calculation of hydraulic losses at the bridge cross-section based on a drop of water level under the bridge due to changes of a flow cross-section. For high water levels and flows, the HEC-RAS allows for calculations using the energy equation, and separation of hydraulic equations into the forced and free water flows. The forced (pressure) flow occurs when the free surface of water at the bottom of a bridge structure, whereas the free flow takes place when water flows over a bridge. The correct determination of the

free water surface in vicinity of the bridge structure is an essential issue as the bridge significantly dams-up (throttles) water in a river during the high water levels (floods).

Block diagram of the HEC – RAS ver. 3.1.1 algorithm is shown in Figure 2.2

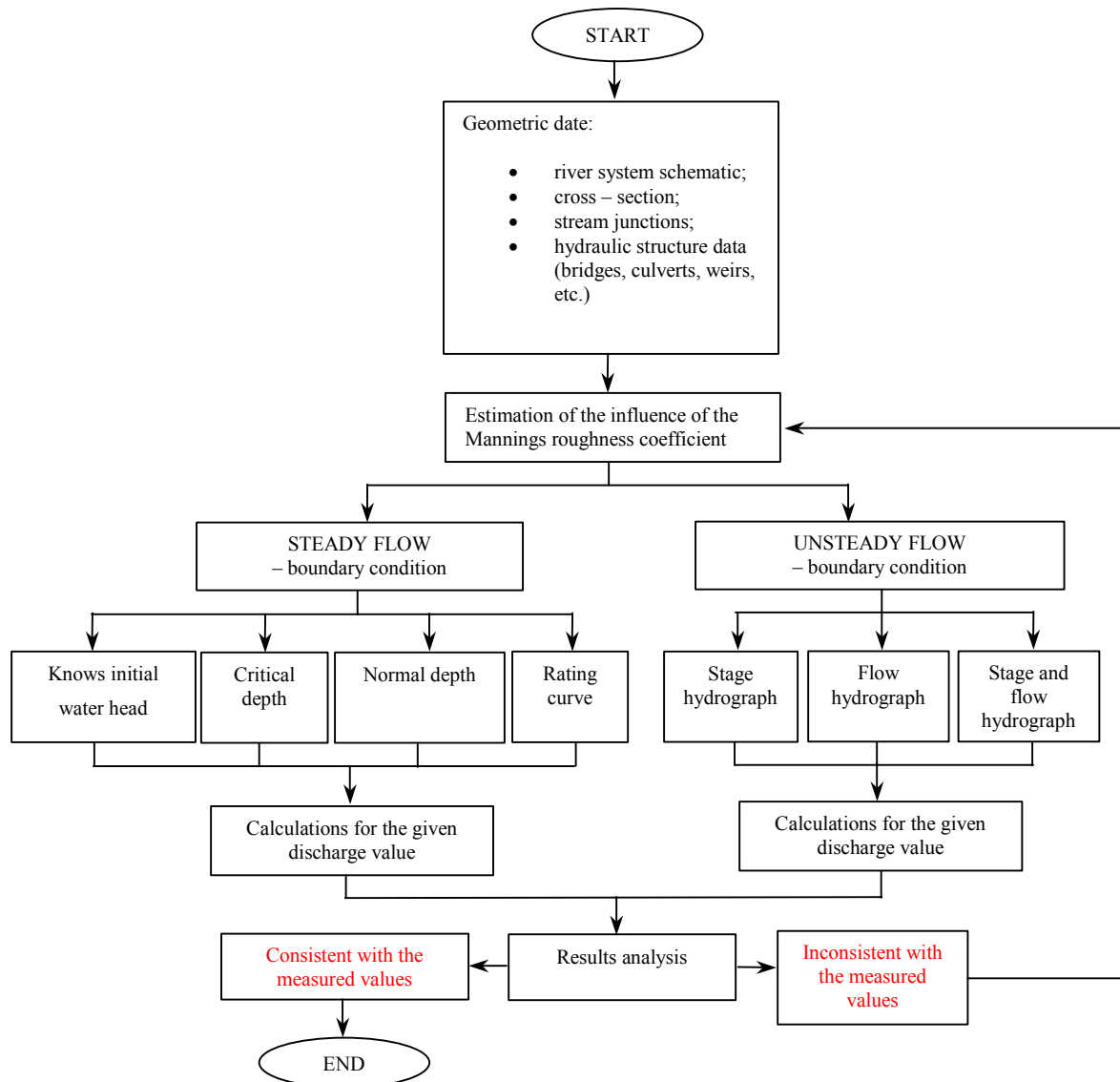


Figure 2.2 Block diagram of the HEC – RAS ver. 3.1.1 algorithm

Computations

1. Geometric data:

- river system schematic,
- information of the stream system (stream junctions),
- cross – section data,
- hydraulic structure data (bridges, culverts, weirs, etc.).

2. Mannings roughness coefficient

In order to determine the Manning's coefficient "n", the flow resistance coefficient $k_d=1/n$ has been determined (on the basis of hydrometric measurements). Due to too high variation of the coefficient k_d , the Manning's coefficient for the main channel was determined by means of the Cowan's method (1956):

$$n = (n_0 + n_1 + n_2 + n_3 + n_4)m_5 \quad (1)$$

where:

- n_0 – n base value for straight, uniform river bed,
- n_1 – correction due to the degree of irregularities of the bed bank and bottom,
- n_2 – correction due to the change in size and shape of the river cross section,
- n_3 – correction due to the occurrence of obstacles, such as: eluvia, boulders, trunks, boughs and logs, and exposed tree roots,
- n_4 - correction due to the vegetation intensity and the extent of the river cross-section cover,
- m_5 - correction due to the extent of the river meanders.

In order to determine the Manning's roughness coefficient "n" for the overbank areas, the following materials were used:

maps:

- topographic maps in 1:10000, 1:25000 scale,
- hydrological map of Poland in 1:50000 scale,
- environmental science map of Poland in 1:50000 scale.

photographs:

- photographs and movies recorded in the field,
- aerial photogrametric photographs.

These materials allowed for determining the areas, to which relevant Manning's roughness coefficients have been assigned.

1. Steady flow date

Values of average low water (SNQ) and average annual (SSQ) discharges were entered to the model, respectively: 1.59 m³/s and 6.95 m³/s.

2. Model calibration

The model was calibrated on the basis of the rating curve from a profile of the Widawa River (from km 8.0 to km 14.0).

Describing of the used sediment transport options in HEC-RAS

The functions enabling the sediment transport calculations are included in the Run menu (start) of the HEC-RAS 3.1. After entering this menu, the user should choose the option of Hydraulic design functions. After selecting it, a new window will open, including one of the modules available in the Type menu of this window. Due to the issues connected with hydraulics and sediment transport, there are two (out of four possible) important modules, i.e. stable channel design... and Sediment transport capacity.... The selection of either of the above modules causes the opening of a new window enabling the choice of the calculation method, input of necessary data, conducting calculations, and presenting the results obtained.

The windows of both of the above modules include four main control buttons to be found on the right side of the window:

Defaults button – restoring the setting of a given window to default values,

Apply button – enabling the input of data, loaded by the user, into the computer memory. The data reside in memory until the user opens the file of the new project or when the user exits the HEC-RAS program.

Compute button – activating calculation procedures for the currently active calculation project,

Report button - enabling the display of a printable window with detailed calculation data.

Stable channel design module

The channel stability can be calculated with the application of three different methods:

- Copeland's,
- Regime,
- Tractive force.

The Copeland' method

To make calculations, the user must select Copeland bar in the window of Stable channel design... module. In the open window of this method, the user can input - into suitable fields – the data necessary for modelling:

- flow – projected flow, it can be two-year water, ten-year-water, bank water, etc.,
- specific gravity - self-explanatory; defaultly, it amounts to 2.65,
- temperature – representative water temperature. The default value has been set at 10 degrees C.,
- valley slope (optional),
- median channel width,
- side slope,
- equation – possibility to select between the Manning or Strickler formula,
- Manning roughness (n) or $1/n = k$ coefficients,
- inflow sediment – button activating a window in which it is possible to input information regarding the concentration of the inflowing sediment, or it can make the HEC – RAS program calculate it. If the user makes the program calculate this quantity, the following data must be provided: supply reach bottom width, supply reach bank height, supply energy slope, side slope – slopes of the right and left side of the feeding section, equation – opportunity to choose between the Manning or Strickler formula for the assessment of roughness of the sloped parts of the feeding cross section, “n” or “k”. The concentration is provided in ppm.

The following buttons are activated after conducting the simulation calculations:

- table button,
- two buttons of the stability curve,
- copy button for geometric characteristic.

Pressing the table button allows viewing the calculation data obtained, among which there are values of shear stresses determining the sediment movement. Using the Stability Curve 1 button results in displaying the stability curve diagram showing the relation of slope to width, demonstrating, for which slope/width values bed aggregation or degradation appears.

The Regime method

In order to make calculations with this method, the user should select the Regime bar in the window of the Stable channel design module. In the open window of this method, the user can input - into suitable fields – the data necessary for modelling:

- flow – it should be a bed-forming flow (m^3/s),
- d_{50} – median particle size (mm),
- sediment concentration (ppm),

- water temperature,
- coefficient for bank scarps after Blench.

After inputting the above data, the compute button is activated. The calculations lead to the determination of values describing the bed stability regime for the depth, width and slope.

The Tractive force method

Making calculations by means of this method requires the selection of the tractive force bar in the window of the Stable channel design module. In the open window of this method, you can input -into suitable fields – the data necessary for modelling:

- projected flow,
- water temperature,
- specific gravity,
- angle of repose,
- side slope,
- equation – opportunity of choice between Manninga or Strickler formula,
- Manning roughness (n) or $1/n = k$ coefficients,
- method – it is possible to choose the calculation method of critical shears of the Lane, Shields method, or after input by the user his own critical mobility parameter,
- ratio d_{50}/d_{75} ,
- D – stable cross section depth,
- B – width in stable cross section bed,
- S – slope of energy grade line at stable cross-section.

After input these data, the compute button is activated. The calculations lead to the determination of the stable shape of the cross-section.

2.1.4.3. Sediment transport formulas in the HEC-RAS

The sediment transport potential computations in the HEC-RAS can only be run once steady or unsteady flow computations have been run. The sediment transport potential for any cross-section can be computed using any of the below sediment transport functions.

Ackers-White (flume studies)

$0.04 < d < 7 \text{ mm}$ $1.0 < s < 2.7$
 $0.07 < V < 7.1 \text{ fps}$ $0.01 < D < 1.4 \text{ ft}$
 $0.00006 < S < 0.037$ $0.23 < W < 4.0 \text{ ft}$
 $46 < T < 89 \text{ degrees F}$

A total load function developed under the assumption that fine sediment transport is best related to the turbulent fluctuations in the water column, and coarse sediment transport - to the net grain shear with the mean velocity used as the representative variable. The transport function was developed in terms of particle size, mobility and transport. A dimensionless size parameter is used to distinguish between the fine, transitional, and coarse sediment sizes. Under typical conditions, fine sediments are silts less than 0.04 mm, while coarse sediments are sands greater than 2.5 mm. Since the relationships developed by Ackers-White are applicable only to non-cohesive sands, greater than 0.04 mm, only transitional and coarse sediments apply. Experiments were conducted with coarse grains up to 4 mm. This function is based on over 1000 flume experiments using uniform, or near-uniform sediments, with flume depths of up to 1.4 m. A range of bed configurations was used, including plane, rippled, and dune forms, however the equations do not apply to upper phase transport (e.g. anti-dunes) with Froude numbers in excess of 0.8. A hiding adjustment factor developed for the Ackers-White method by Profitt and Sutherland (1983), is included in the RAS as an option. The hiding factor is an adjustment to include the effects of a masking of the fluid properties felt by smaller particles due to shielding by larger particles. This is typically a factor when the gradation has a relatively large range of particle sizes, and would tend to reduce the rate of sediment transport in the smaller grade classes.

Engelund-Hansen (flume studies)

$0.19 < d_m < 0.93 \text{ mm}$ $0.65 < V < 6.34$
 $0.19 < D < 1.33 \text{ fps}$ $0.000055 < S < 0.019 \text{ ft}$
 $45 < T < 93 \text{ degrees F}$

It offers a total load prediction, which gives adequate results for sandy rivers with substantial suspended load. It is based on flume data with sediment sizes between 0.19 and 0.93 mm. It has been extensively tested, and found to be fairly consistent with field data.

Laursen (field studies)

$0.08 < d_m < 0.7 \text{ mm}$ $0.068 < V < 7.8 \text{ fps}$
 $0.67 < D < 54 \text{ ft}$ $0.0000021 < S < 0.0018$
 $63 < W < 3640 \text{ ft}$ $32 < T < 93 \text{ degrees F}$

Laursen (flume studies)

$0.011 < d_m < 29 \text{ mm}$ $0.7 < V < 9.4 \text{ fps}$
 $0.03 < D < 3.6 \text{ ft}$ $0.00025 < S < 0.025$
 $0.25 < W < 6.6 \text{ ft}$ $46 < T < 83 \text{ degrees F}$

It offers a total sediment load prediction derived from a combination of qualitative analysis, original experiments and supplementary data. Transport of sediments is primarily defined based on the hydraulic characteristics of mean channel velocity, depth of flow and energy gradient, and on the sediment characteristics of gradation and settling velocity. Contributions by Copeland (Copeland, 1989) extended the

range of applicability to gravel-sized sediments. The overall range of applicability is from 0.011 to 29 mm.

Meyer-Peter Muller (flume studies)

$0.4 < d < 29 \text{ mm}$ $1.25 < s < 4.0$
 $1.2 < V < 9.4 \text{ fps}$ $0.03 < D < 3.9 \text{ ft}$
 $0.0004 < S < 0.02$ $0.5 < W < 6.6 \text{ ft}$

BED LOAD ONLY! A bed load transport function is based primarily on experimental data. It has been extensively tested and used for rivers with relatively coarse sediments. The transport rate is proportional to the difference between the mean shear stress acting on the grain, and the critical shear stress. Applicable particle sizes range from 0.4 to 29 mm with a sediment specific gravity range of 1.25 to in excess of 4.0. This method can be used for well-graded sediments and flow conditions that produce other-than-plane bed forms. The Darcy-Weisbach friction factor is used to define bed resistance. Results may be questionable near the threshold of incipient motion for sand bed channels as demonstrated by Amin and Murphy (1981).

Toffaletti (field studies)

$0.062 < d < 4 \text{ mm}$ $0.095 < d_m < 0.76 \text{ mm}$
 $0.7 < V < 7.8 \text{ fps}$ $0.07 < R < 56.7 \text{ ft}$
 $0.000002 < S < 0.0011$ $63 < W < 3640 \text{ ft}$
 $40 < T < 93 \text{ degrees F}$

Toffaletti (flume studies)

$0.062 < d < 4 \text{ mm}$ $0.45 < d_m < 0.91 \text{ mm}$
 $0.7 < V < 6.3 \text{ fps}$ $0.07 < R < 1.1 \text{ ft}$
 $0.00014 < S < 0.019$ $0.8 < W < 8 \text{ ft}$
 $32 < T < 94 \text{ degrees F}$

It is a modified-Einstein total load function that breaks the suspended load distribution into vertical zones, replicating two-dimensional sediment movement. Four zones are used to define the sediment distribution. They are the upper zone, the middle zone, the lower zone and the bed zone. Sediment transport is calculated independently for each zone, and the summed to arrive at total sediment transport. This method was developed using an exhaustive collection of both flume and field data. The flume experiments used sediment particles with mean diameters ranging from 0.45 to 0.91 mm, however successful applications of the Toffaletti method suggests that mean particle diameters as low as 0.095 mm are acceptable.

Yang (field studies, sands)

$0.15 < d < 1.7 \text{ mm}$ $0.8 < V < 6.4 \text{ fps}$
 $0.04 < D < 50 \text{ ft}$ $0.000043 < S < 0.028$
 $0.44 < W < 1750$ $32 < T < 94 \text{ degrees F}$

Yang (field studies, gravels)

$2.5 < d < 7.0 \text{ mm}$ $1.4 < V < 5.1 \text{ fps}$
 $0.08 < D < 0.72 \text{ ft}$ $0.0012 < S < 0.029$
 $0.44 < W < 1750$ $32 < T < 94 \text{ degrees F}$

It is a total load function developed under the premise that unit stream power is the dominant factor in the determination of the total sediment concentration. The

research is supported by data obtained in both flume and field experiments under a wide range of conditions found in alluvial channels. Principally, the sediment size range is between 0.062 and 7.0 mm, with the total sediment concentrations ranging from 10 ppm to 585,000 ppm. Yang (1984) expanded the applicability of his function to include gravel-sized sediments.

To perform computation of the sediment transport intensity, the user must define one or more segments, where the sediment transport takes place (the so-called 'sediment reaches'). A sediment reach indicates, for which cross-section the sediment transport intensity will be computed, and contains information necessary to perform the computations. Sediment reaches can vary spatially, have different input parameters, as well as temperature, specific gravity, and gradation, or can use diverse simplified sediment transport functions. The sediment reach cannot contain more than one river segment, however, there can be more sediment reaches within one river segment.

When the 'sediment transport potential' window is opened, and if there are not any previously defined sediment reaches for the currently used hd file, the user will be automatically prompted to name a new sediment reach. To create a new reach otherwise, the user should click on File...New Sediment Reach. The user also has the option of copying, deleting and renaming existing sediment reaches under the File menu option. The name selected for the new sediment reach will appear in the Sed. Reach dropdown box, along with all other existing sediment reaches for the particular hydraulic design file.

Once a new sediment reach has been named, the user must define its spatial constraints by selecting the river, the segment (reach), and the bounding upstream and downstream river stations. Next, one of the existing profiles must be selected. A sediment reach can only have one profile associated with it. To compute for more profiles, additional sediment reaches must be created.

Sed.Reach: Indicates which sediment reach is active. This dropdown box lists all existing sediment reaches for the current hydraulic design file.

River: The river where the current sediment reach is located.

Reach: The reach where the current sediment reach is located.

US RS: The upstream bounding river station of the current sediment reach.

DS RS: The downstream bounding river station of the current sediment reach.

Profile: The profile to be used in the sediment transport computations for the current sediment reach.

River Sta: The river station currently displayed on the plot.

Temperature: Temperature of the water. Default is 55 F or 10°C.

Specific Gravity: Specific gravity of the moveable sediments. Default is 2.65.

Bed Sta Left/Right: The cross-section stations that separate the left overbank of the main channel from the right overbank for sediment transport potential computations. Defaults are the main bank stations. These values can be changed for every cross-section within the sediment reach. The selected stations appear on the cross-section plot as yellow nodes, and are bracketed by “MB” (mobile bed) location arrows on the top of the plot.

Concentration of Fine Sediment, ppm: The concentration of fine sediments (wash load) in the current sediment reach. This is an optional value, and is used to adjust the transport rate based on Colby’s findings regarding the effects of fine sediments and temperature on kinematic viscosity, and consequently on the particle settling velocity (Colby, 1964). Values are given in parts of sediment per one million parts of water.

Solve Using: This allows the user to select, which depth- and width-parameters to use in the solution of the transport functions. If “Default” is selected, the program will use the depth/width combination used in the research of the selected function(s). If any of the other depth/width combinations is used, all selected functions will be solved using those specific parameters.

Eff. Depth/Eff. Width: Used in the HEC 6, is the effective depth and effective width. Effective depth is a weighted average depth, and the effective width is calculated from the effective depth to preserve $aD^{2/3}$ for the cross-section:

Hyd. Depth/Top Width: The hydraulic depth is the area of the cross-section divided by the top width.

Hyd. Radius/Top Width: The hydraulic radius is the Area divided by the wetted perimeter. Is equivalent to hydraulic depth for relatively wide, shallow streams.

Functions: The user can select one or more sediment transport functions from the list box. By clicking the checkbox, a check will appear and the RAS will compute for that function. When clicking the name of the function, a brief description of the function, and its applicability, will appear in the text box.

Gradation: This is entered for the left overbank (LOB), main channel (Main) and right overbank (ROB), as defined by the left- and right-bed stations. The user can enter nothing, or up to 500 particle size/percent finer relationships. Typically 5 to 10 gradation points are enough to represent a typical gradation curve. The particle diameter is entered in mm under the column header Diam, mm, and the percentage of the representative sediment that is finer than that particle diameter is entered under the column header %Finer. The RAS then takes this gradation input to determine the fraction of the sediment that is in each standard grade size class. If a zero percent value and/or a 100% value are not entered by the user, the program will assign zero percent to the next lowest grade class and 100% to the next highest grade class. The details can be found in the hydraulic calculation manual for the HEC-RAS program.

Plot/Table: This button displays a plot of the sediment transport potential (intensity) rates for the current sediment reach. It is only enabled once computations for that reach have been performed. In addition to viewing the plots, the table tab can be clicked to view in tabular form.

The user has the option to compute sediment transport potential rates for the currently selected sediment reach (Compute for this Sediment Reach), or for all

existing sediment reaches (Compute for all Sediment Reaches) within the currently opened hydraulic design file.

Defaults: The Defaults button will restore all input boxes for the currently selected sediment reach to the default values.

Apply: The Apply button will be enabled any time when new input has been added, which has not been stored into memory. By clicking on the Apply button, all input for the current sediment reach will be stored to memory.

Compute: The compute button will be enabled once all required input data are entered. Pressing the compute button initiates the computations for the sediment transport potential.

Report: The Report button generates a report summarizing the input and output data.

2.1.4.4. Presentation of results

The model allows the calculation of the grain settling velocity in a liquid with three different methods: Toffaleti's, Van Rijn's and Rubey's. Moreover, it is possible to impose on the HEC-RAS program, after selecting the option: compute, to calculate the sediment transport for smaller grains outside the applicability range of particular models. After approving of the selected calculation model (one of six available ones) by the data input by means of the apply button, the compute button is activated. After conducting calculations the following options are possible:

- After pressing the button of sediment rating curve plot/table, it is possible to view a diagram showing the sediment transport quantity in a selected cross-section for different formulas used in modelling, and to print the calculation results of transport in tons per day in the form of a table,
- Selecting the button of sediment transport profile plot/table enables viewing of a chart of changes in sediment transport quantity along the analysed river. The transport capacities can be also presented in a tabular form. The tables with results can be printed, sent to safe or saved in the form of text files.

The HEC – RAS program belongs to a group of public domain programs, and is continuously developed and updated at the Hydrologic Engineering Center for the U.S. Army Corps of Engineers, therefore it is necessary to keep constant track on the latest, supplemented and revised versions.

2.1.5. Results of the contaminated sediment transport modeling

Modelling of the contaminated sediment transport in the Widawa River was done for a sector between km 8.070 and km 14.590. Hydraulic calculations and the sediment transport potential (intensity) were performed in 21 cross-sections, and for 5 values of the flow discharge: i.e. $1.0 \text{ m}^3/\text{s}$, $1.59 \text{ m}^3/\text{s}$, $6.95 \text{ m}^3/\text{s}$, $10.0 \text{ m}^3/\text{s}$ and $20.0 \text{ m}^3/\text{s}$. These flows are attributed to the main Widawa channel that is important for the sediment transport, as well as for changes of the riverbed itself.

The presentation of the model in Power Point is given as a zipped attachment called **PRESENTATION**.

Results of contaminated sediment transport simulations are given in Report-Table 6 as attachment called **SED_TRANSP**.

Files with input data (geometry and hydraulics, and sediment properties) are given in catalogue - attachment called **Files_to_HEC-RAS**.

HEC-RAS program is accessible on **www.hec.usace.army.mil**

2.1.6. Conclusions and recommendations

The HEC-RAS model enables modelling of the contaminated sediment transport in rivers. The transport intensity of contaminants in a river is proportional to the transport rate of sediments, both bed materials and suspended load.

The following options can be analysed by using the HEC-RAS:

- concentrations of contaminants at the beginning of a studied river sector are the same as at the end
- concentrations of contaminants at the beginning of a studied river sector are different than at the end,

To analyse the contaminated sediment transport a number of subsystems and processes should be distinguished:

- inflow of contaminants is zero,
- sedimentation of contaminated particles,
- hydraulic erosion during different consolidation conditions of sediments.

Simulations of the sediment transport using the HEC-RAS for the Widawa River (see attachment 2) were estimated for the inflow of contaminants equal zero.

Contaminated sediment transport conditions depend on channel geometry, hydraulic regime, and types of bed materials. If, at the beginning and at the end of an analysed river sector, the hydraulic regime is at a steady state, and inflow of contaminants is zero, then the system can be identified and evaluated. But the intensity of contaminated sediment transport varies at varying flow conditions at the studied sector.

Preliminary estimation of the contamination concentration showed that the smallest fractions ($d < 0,063$ mm) are most of all contaminated, and the contamination level diminishes with an increase of the particle size of suspended load.

It is recommended to divide the sediments into as much as possible fractions (8-10 classes).

Prognosis of the sediment grain size variation at different flow conditions is possible by means of the TRANS program, which is based on a probability for grains to stay in quiescence according to Gessler.

The HEC-RAS can be used to calculate the total sediment transport intensity by six formulas. The analysis of calculations (in each cross-section and at a longitudinal bed profile) using these functions, showed that the formulas of Laursen, Toffaleti and Yang overestimated the sediment transport intensity compared to field data, thus they are not recommended for use.

Parameters describing the incipient motion and sedimentation, transportation, suspension and erosion of sediment in the Widawa riverbed were estimated.

Modelling of contaminated sediment transport by the HEC-RAS demands wide range of input data, which were indicated by authors. The in-situ (field) measurements and

laboratory tests (hydraulic investigations in models) are necessary to verify the HEC-RAS numerical model.

It is also recommended to estimate the changes of accumulated contaminants during sedimentation and consolidation of suspended load, and after its re-suspension due to higher flow discharges during floods.

Due to complexity of the contaminated sediment transport, more extensive studies and analyses are required.

To answer: whether bottom sediments are a source or a sink of contaminants for a particular river or a section of the river is not simple. It is very site-specific, because it depends on hydraulic flow parameters and sediment properties, thus further extensive laboratory and field investigations for each particular situation are required.

The contaminants are mainly adhered to the fine fractions of sediments. The natural cycle of transport (migration) of fine solids generally constitutes of the following processes:

- surface erosion of fine fractions of sediments in the watersheds (natural river systems and artificial sewer systems),
- transport of this wash load in rivers, canals, reservoirs, and in sewers, mainly by free water flow,
- sedimentation of grains in these systems in cases, where the mean flow velocity is too small to keep the particles in suspension,
- settlement of the sediment layer as a function of time, and many other factors causing consolidation of the layer, increase of the concentrations inside of the layer, and increase of the resistance to hydraulic erosion,
- hydraulic erosion of the layer, mainly by high flow velocities (e.g. in rivers during floods), where one can distinguish two steps: the surface erosion (mean flow velocities) and mass erosion (high flow velocities).

These phenomena are very complex and depend on many factors, mainly on the nature of the sediments (physical, chemical, rheological properties, sediment structure, organic matter content etc.), and the history of the transport, but also on the character of the eroding flow.

The erosion processes are often modelled by the comparison of the bottom shear stress τ_h exerted by the flow and critical shear stress τ_c , for example in the PARTHENIADES erosion model (Partheniades, 1965):

$$E = M_e \left(\frac{\tau_h}{\tau_c} - 1 \right) \quad \text{for } \tau_h > \tau_c$$

$$\text{and } E = 0 \quad \text{for } \tau_h < \tau_c$$

where: E – erosion rate, M_e erosion rate parameter (in many cases not constant but time dependant).

Studies concerning the erosion processes of mud indicate that the values of the parameter M_e depend on erosion type, and are different for superficial erosion and for mass erosion.

2.1.7 Literature

- Allan J. D., 1995. Stream ecology. Structure and function of running waters, Chapman & Hall.
- Banasiak R., 1999. Study of suspended load transport in open channels, Ph.D. dissertation, Agricultural University of Wroclaw (in Polish).
- Banas E., 2002. Influence of urban storage facility on water qualitative composition in Odra and Widawa rivers, M.A. thesis, Agricultural University of Wroclaw (in Polish).
- Bieszczad S., Sobota J., 1998. Hazards, protection and forming of natural-agricultural environment, Agricultural University of Wroclaw (In Polish).
- Brunner G., 2002. HEC-RAS, River Analysis System Hydraulic Reference Manual, US Army Corps of Engineers, Hydrologic Engineering Center, Davis, CA.
- Chmielewska I., 2004. The use of HEC-RAS application for flood flow modeling in the Widawa river, 3-th Polish Conference on "Close nature river valley forming", Rajgrad 2004 (in Polish).
- Dojlido J., 1995. Chemistry of surface waters, Wydawnictwo Ekonomia i Srodowisko (in Polish).
- Dz.U.2002. 02.204.1728. Rozporządzenie Min. Srod. W sprawie wymagan, jakim powinny odpowiadac wody powierzchniowe wykorzystywane do zaopatrzenia ludnosc w wode przeznaczona do spozycia. MS Warszawa.
- Głowski R., Kasperek R., Mokwa M., 2004. The measurement and analysis of contaminated sediments in Widawa river, Wroclaw (in Polish).
- Gutra-Korycka M., Werner-Wieckowska H., 1996. Guide book of hydrographical field investigations, PWN, Warszawa (in Polish).
- Manczak H., 1972. Technical basics of water protection against contaminants, Technical University of Wroclaw (in Polish).
- Mokwa M., 2002. Fluvial processes control in antropogenically modified river beds, Scientific Papers 439, CLXXXIX, Agricultural University of Wroclaw (in Polish).
- Mokwa M., Głowski R., Kasperek R., Markowski J., Chmielewska I., 2003. Numerical modeling of contaminated sediment transport, Report, Agricultural University of Wroclaw (not published).
- Molinas A., Wu B., 1998. Effect of size gradation on transport of sediment mixtures, Journal of Hydraulic Engineering, Vol. 124, No. 8, 786-792.
- Morris G. L., Fan J., 1998. Reservoir sedimentation handbook. Design and management of dams, reservoirs, and watersheds for sustainable use, McGraw-Hill.
- Olive L. J., Rieger W. A., 1988. An examination of the role of sampling strategies in the study of suspended sediment transport, In Sediment Budgets (Proceedings of the Porto Alegre Symposium, December 1988), IAHS Publ. No. 174, 259-267.
- O'Neill P., 1997. Chemistry of environment, PWN, Warszawa-Wroclaw.
- Ongley E. D., 1982. Influence of season, source and distance on physical and chemical properties of suspended sediment, In: Recent Developments in the Explanation and Prediction of Erosion and Sediment Yield (Proceedings of the Exeter Symposium, July 1982), IAHS Publ. No. 137, 371-383.
- Partheniades E., 1965. ASCE. Journal Hydraulic Division.
- Parzonka W., Głowski R., Jelowicki J., Kasperek R., Mokwa M., Radczuk L., Zyszkowska W., 2003. Estimation of the capacity of river Widawa to transfer a

- part of flood discharge of river Odra, Scientific Papers 454, Monograph XXX, Agricultural University of Wroclaw (in Polish).
- Pawlaczyk-Szpilowa M., 1980. Water and sewer microbiology, PWN, Warszawa (in Polish).
- Ratomski J., 1997. Processes connected with sediment movement in Carpathian streams, Monografie Komitetu Gospodarki PAN 13, Technical University of Warsaw (in Polish).
- Swerpel S., 1997. Flood "E bomb", Wiedza i Zycie 10, 26-30 (in Polish).
- Trybala M., 1996. Water management in agriculture, PWRiL, Warszawa (in Polish).
- Van Rijn L. C., 1984a. Sediment transport. Part I: Bed load transport, Journal of Hydraulic Engineering, Vol. 110, No. 10, 1431-1456.
- Van Rijn L. C., 1984b. Sediment transport. Part II: Suspended load transport, Journal of Hydraulic Engineering, Vol. 110, No. 11, 1613-1641.
- Van Rijn L. C., 1993. Principles of sediment transport in rivers, estuaries and coastal seas, Aqua Publications, Amsterdam.
- Walling D. E., Kane P., 1982. Temporal variation of suspended sediment properties, In: Recent Developments in the Explanation and Prediction of Erosion and Sediment Yield (Proceedings of the Exeter Symposium, July 1982), IAHS Publ. No. 137, 409-419.
- Wisniewski B., 1972. Amount of suspended and bed load in Polish rivers, Gospodarka Wodna 10-11/72, 381-386 (in Polish).
- Yang C. T., 1996. Sediment transport. Theory and practice, McGraw-Hill.

2.1.8 Attachments

1. **Input_data**: the minimum and maximum dataset for modelling of sediment transport using the HEC-RAS model (as table 7 and 8)
2. **Presentation**: work instruction of HEC-RAS model in PowerPoint
3. **Files_to_HEC-RAS**: catalogue with files for modelling by HEC-RAS
4. **Sed_transp**: results of contaminated sediment transport modelling in a table form (Table 6)

Attachment 1

The minimum and maximum input dataset for modelling of sediment transport using the HEC-RAS model

Table 7. The minimum input dataset

No.	Name
1	Geometry of river cross-section
2	Length of a river reach (segment)
3	Geometry of bridge
4	Free surface slope I
5	Water depth
6	Flow area A
7	Water width B
8	Flow velocity v
9	Flow discharge Q
10	Characteristic diameters d_i of bed materials
11	Water temperature T
12	Kinematics viscosity ν
13	Specific density of water ρ_w
14	Specific density of sediment ρ_s

Table 8. The maximum input dataset

No.	Name
1	Geometry of river cross-section
2	Length of a river reach (segment)
3	Geometry of bridge
4	Free surface slope I
5	Water depth
6	Flow area A
7	Water width B
8	Flow velocity v
9	Flow discharge Q
10	Characteristic diameters d_i of bed material
11	Water temperature T
12	Kinematics viscosity ν
13	Specific density of water ρ_w
14	Specific density of sediment ρ_s
15	Bed load transport rate
16	Suspended load transport intensity
17	Bed-material concentration
18	Roughness coefficient n or K
19	Erosion and sedimentation conditions
20	Fall velocity of grain ω
21	Tributaries on studied sector of main river

2.2 Estimation of Water Erosion Potential and Contaminant Flux at The Tarnowskie Góry Megasite

COORDINATOR OF POLISH TEAM J. Szdzuj
WP 9-LEADER OF POLISH TEAM G. Malina

J. Szdzuj , M. Korcz, J. Bronder
*Institute for Ecology of Industrial Areas, Katowice,
Poland*

G. Malina
*Institute of Environmental Engineering
Czêstochowa University of Technology, Czestochowa,
Poland*

2.2.1 Introduction

Soil erosion is a global scale problem that has both: environmental and socio-economic effects. In Europe, Mediterranean Region has been recognized as an area of special concern. Although the WELCOME project does not address the problem of erosion, it was concluded that soil water erosion could play some role in contaminants flux.

Water and eolian soil erosion, as one of soil contaminant transport mechanisms, should be taken into account in building conceptual model of objects, especially of Megasite type. Assessment should relate to potential contaminants transport capacity resulting from natural processes. For example fugitive dusts formation capacity including its respirable fraction (below 10 μm) can be an element of respiratory risk assessment. Estimation of the sediments formation capacity and rate of sediment transport with surface runoff and, in the next step, with channel runoff, constitutes an important element of contaminant migration path assessment, between contamination source and surface and groundwaters.

Soil erosion and its consequences should be analyzed at the preliminary, screening stage of risk assessment referring to highly contaminated areas. A performed assessment of contaminated sediments formation capacity should be taken into consideration when defining risk management options and creation of scenarios.

The goal of this work was to estimate water erosion potential of the soil and potential contaminant flux that is mobilized as a result of this process. The flux level was estimated for the area of the Tarnowskie Góry Megasite and should be used for improving the conceptual model as well as to assist in formulation of the final set of risk management solutions.

2.2.2 Approach

For the risk screening assessment, simple European Soil Erosion Model (ESEM) was applied. In this model erosion rate is calculated as a result of two processes: soil detachment and transport of the detached soil particles. The level of erosion is limited by one of these processes. Detailed description of this approach is presented on the internet pages of the *International Institute for Geo-Information Science and Earth Observation* [7].

To calculate the erosion rate, transport capacity and rainfall soil detachment have to be calculated. Results of the erosion modeling and data on topsoil contamination were used to calculate potential annual flux of contaminants.

The modeling was carried out for the Tarnowskie Góry Megasite area and for the Wesola water gauge basin. The Wesola water gauge is situated on the Stola river and is the first water gauge from Tarnowskie Góry direction [Fig. 4].

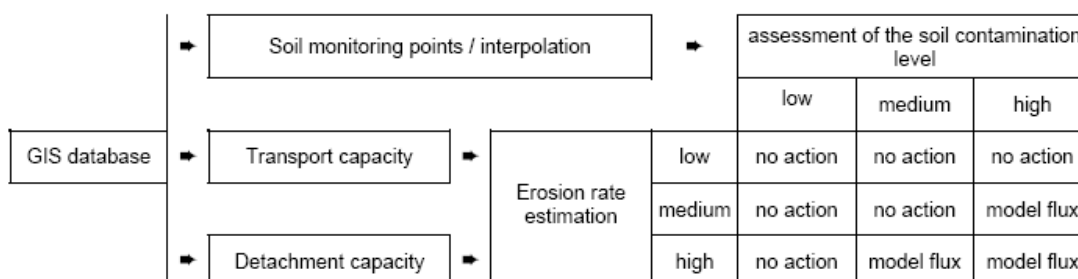
$$T = C \cdot Q^2 \cdot \sin(S)$$

where:

T	- Transport capacity	[g/m ²]
C	- Crop factor	[-]
Q	- Overland flow	[mm]
S	- Slope	[radians]

2.2.2.1 Modeling erosion and Megasite management

Assessment of the erosion rate constitutes one of the steps in a megasite model conceptualization. It can be viewed in a form as a flowchart (see below). Depending on the results of soil contamination and erosion rate evaluations, appropriate decisions are made. If the area of high soil contamination level overlays the area of high potential erosion rate a detailed hydrological modeling should be carried out to verify if the contaminant sediments pose threat to surface and ground-waters. In this case results of soil detachment capacity and soil contamination evaluations constitute an input to hydrological model. Otherwise no additional evaluation is required.



2.2.2.2 Calculation of the potential erosion rate

Transport capacity

In the ESEM model transport capacity is a function of the cover factor, the volume of overland flow and slope. Transport capacity was computed according to the following formula:

The overland flow is a function of mean annual rainfall, amount of rainfall per rainy day, soil moisture storage, and is calculated according to the formula:

$$Q = R \cdot e^{(-R_c/R_o)}$$

where:

Q	- Overland flow	[mm]
R	- Mean annual rainfall	[mm]
R _c	- Soil moisture storage	[mm]
R _o	- Amount of rainfall per rainy day	[mm]

The soil moisture storage was calculated as a function of rooting depth, field capacity, and ratio of actual and potential evapotranspiration:

$$R_c = 1000 \cdot R_d \cdot F_c \cdot (E_a/E_p)^{0.5}$$

where:

R _c	- Soil moisture storage	[mm]
R _d	- Rooting depth	[m]
F _c	- Water field capacity	[v/v]
E _a /E _p	- Ratio of actual and potential evapotranspiration	[-]

Detachment

Rainfall detachment is a function of annual kinetic energy, soil detachability index, and percentage rainfall interception. It is calculated according to the formula:

$$D = K_d \cdot K_E \cdot e^{(-a \cdot INT)^b}$$

where:

D	- Rainfall detachment	[g/m ²]
K _d	- Soil detachability index	[-]
K _E	- Annual kinetic energy	[J/m ²]
INT	- Interception	[%]
a, b	- Constants	[-]

The annual kinetic energy is a function of the mean annual rainfall and rainfall intensity:

$$KE = R \cdot (11,9 + 8,7 \cdot \log_{10} I)$$

KE	- Annual kinetic energy	[J/m ²]
R	- Mean annual rainfall	[mm]
I	- Rainfall intensity	[mm/h]

2.2.2.3 GIS coverages and data used to model soil erosion

In carrying out erosion modeling existing GIS coverages, created within the framework of the task 4.1 of WELCOME project were used [4]. The main coverages applied to erosion estimation were: digital elevation model, map of land use and map of soil textural groups. Additionally, the map of mean annual rainfall, developed on the basis of data from the precipitation gauges was used.

ARC/INFO GRID format was applied to estimate potential erosion rate. ARCVIEW software was used in calculation and spatial analyses. The size of a unique grid cell was 100m. The size of the entire modeled area was 1360 km², the size of the Megasite area was 643 km² and the area of the Weso³a water gauge basin was 214 km².

The first set of maps was created to model transport capacity of the rainwater. To calculate transport capacity, field water capacity map was used [Fig. 1]. This map was created within task 4.1 activities. Look-up table from EPA BASINS model [5] and land use map were used to create rooting depth map [Fig. 2]. A corresponding value of rooting depth was assigned to a particular type of the land use. Data from Hydrological Atlas of Poland were used in determination of potential and actual evapotranspiration [3].

As a potential evapotranspiration, a map of evapotranspiration from surface water was used. The values of these parameters were read from hardcopy maps.

Based on the two earlier mentioned maps and parameters, the map of soil moisture storage was created [Fig. 3]. To calculate overland flow, a map of mean annual rainfall was used [Fig. 4]. The map was created based on data on mean annual rainfall from 20 precipitation gauges covering the time span between 1961 and 1998. The amount of rainfall per rainy day was calculated based on data from the gauge at Tarnowskie Góry Chemical Plant in liquidation. In calculations, only days with rainfall exceeding 1mm were taken into account. Ro was equal 6,4mm. The overland flow has bimodal distribution [Fig. 5]. It takes values close to zero or values close to the level of mean annual rainfall. The last map used in the calculation of transport capacity was the map of slope [Fig. 6]. In modeling transport capacity, the crop factor was arbitrarily assumed 1. The above-described maps were used in calculation of transport capacity of flowing rainwater [Fig. 7]. The area where transport capacity is higher than zero is 88,98km². Mean annual transport capacity for the whole modeled area is 5148g/m².

The second set of maps contains coverages created to model soil detachment capacity of raindrops. The map of the annual kinetic energy was created based on mean annual rainfall map and rainfall intensity parameter [Fig. 8]. The last was derived from Hydrological Atlas of Poland and equaled 35mm per hour [3].

A crucial parameter applied in the estimation of erosion is soil detachability index [Fig. 9]. The values of the index were taken from the internet pages of Ontario Ministry of Food and Agriculture concerning application of Universal Soil Loss Equation (USLE) [6]. Because of the fact that the detachability index refers to soil textural groups of American taxonomy system, it was necessary to create a map of soil in accordance with this taxonomy system, using GIS coverages concerning sand and clay contents and information from the pedosphere online soil science magazine [8]. Eventually, values of detachability index were assigned to soil textural groups.

An interception map [Fig. 10] was created on the basis of land use map and published information on interception level [2].

The above-described three maps were used to calculate rainfall detachment capacity of the falling raindrops [Fig. 11]. Constants used in the rainfall detachment formula were arbitrarily assumed ($a=0,025$; $b=1$). The area, where detachment capacity is higher than zero is $1314,69\text{km}^2$. Mean annual transport capacity for the whole modeled area is 1228g/m^2 .

The map of erosion rate was built on the basis of transport capacity map and rainfall detachment map. For each grid cell of the two maps the lower value was selected. Five erosion classes were defined based on 20 percentiles reclassification [Fig. 12]. The final step was to create coverages concerning metal contents in topsoil. Data from

Geochemical Atlas of Upper Silesia [1] and simple linear triangulation interpolation were used. Results concerning soil contamination and estimated potential erosion rate were applied in calculation of annual contaminant flux.

2.2.3 Results and conclusion

The results show that in the extent of the Tarnowskie Góry County (primary definition of

Tarnowskie Góry Megasite) erosion may occur on the area of 21.34 km². It constitutes 3.32 percent of the entire Megasite. In the extent of the eroded soils mean erosion rate equals 1434.5g/m². It gives 30,611.4 tons per year from the Megasite and 16,362.2tons per year from the Wesola basin where area with eroded soils is 12.5km²

The highest values of potential barium flux correspond to the area of the highest barium concentrations or to areas of the highest erosion rate. These two types of areas do not overlay each other [Fig. 13]. The total annual potential barium emission from the entire modeled area is 21.2 tons, from the Megasite 6.5 tons and 4.7 tons from the Wesola water gauge basin.

The highest values of potential zinc flux correspond to the area of the highest zinc concentration and to the area of the highest erosion rate, which in this case overlay each other [Fig. 14]. The modeled zinc emission turned out to be much higher than the modeled barium emission. The area of high zinc emission rate however, is not situated within the Megasite extent. The total zinc emission from the entire modeled area is 160.4 tons, from the Megasite 18.2 tons and 8.5 tons from the Wesola basin. Assuming that contaminants concentrations above acceptable thresholds, potential erosion rate above 60 percentile (above 2313 g/m²) and distance to main rivers less than 200 m define conditions of potential risk occurrence we may point out the areas of special concern. In the extent of Tarnowskie Góry Megasite the total acreage that meets mentioned above criteria amounts to 28 hectares.

The results on contaminants flux resulting from water soil erosion were compared with results on contaminant contents in topsoil in the direct vicinity of Tarnowskie Góry Chemical Plant and with results concerning contaminant contents in the Chemical Plant landfills (see table below). The total amount of contaminant emissions due to soil erosion is comparable with annual emission of contaminants from the existing landfills. On the other hand it is about several hundred times lower than the total load of contaminants contained in the chemical plant landfills and several times lower than the load of contaminants contained in top layer of soils

Object	Area [ha]	Zn [ton]	Ba [ton]	Sr [ton]
Annual emission of contaminants - the entire modelled area (in the extent of soil contamination model)	6 746,0	160,4	21,2	4,5
Annual emission of contaminants - Megasite Tarnowskie Góry (area with eroded soils)	2 134,0	18,2	6,5	0,9
Annual emission of contaminants - Wesola water gauge basin (area with eroded soils)	1 240,0	8,5	4,7	0,5
Mass of contaminants in the topsoil – direct vicinity of the Chemical Plant	59,9	92,9	166,1	15,6
Mass of contaminants in the landfills of the Chemical Plant (only existing landfills in the extent of geo-statistical model – 50m grid)	34,0	10 929,9	5 706,7	N/A
Annual emission of contaminants from existing Chemical Plant Landfills into GW (data based on water solubility tests)	34,0	9,1	0,4	N/A

surrounding the Chemical Plant.

The estimated rates of erosion and contaminant flux (emission) have to be regarded as masses that may be displaced without defining their fate. Dedicated investigations

should be conducted to quantify the real load into the sediment system (measurements of dissolved matter, contaminant concentrations at specific river basin points). Also the erosion model should be supplemented with the whole hydrological model. This, however was out of the task scope. The obtained results of soils erosion estimation can be used in formulation of risk management solution. For example rate of erosion can be used a criterion in selection of areas suitable for specific remediation activities e.g. phytoremediation.

2.2.4 References

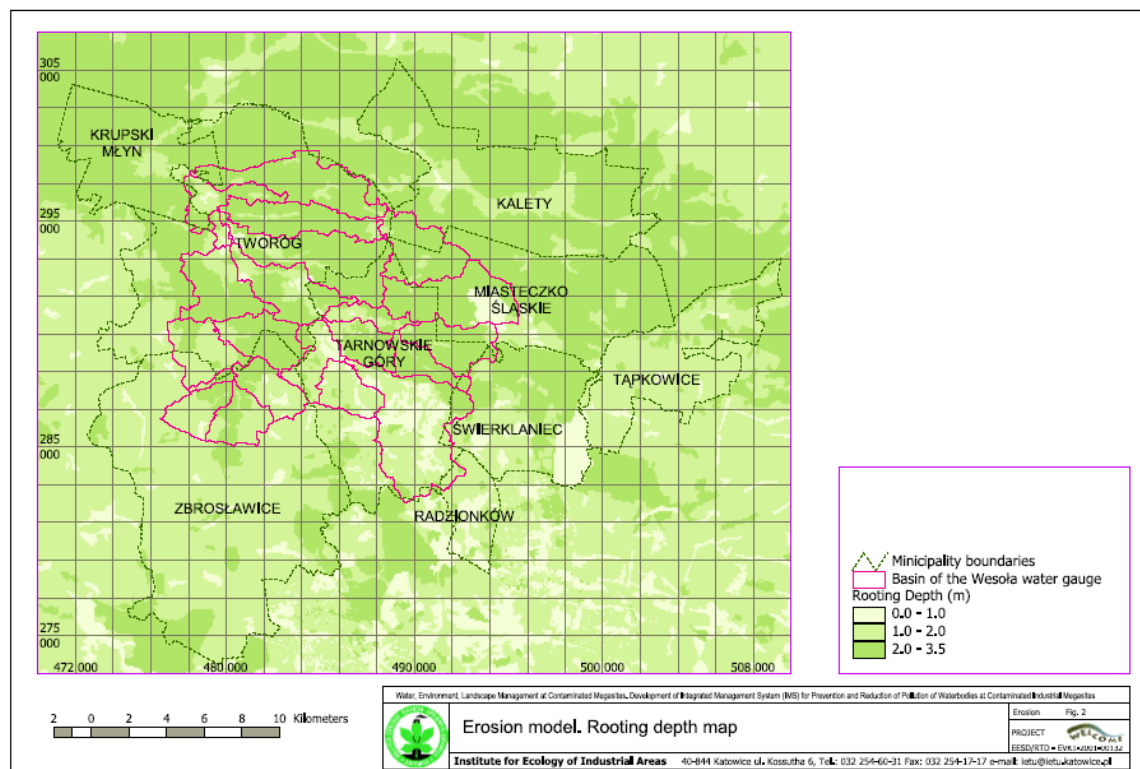
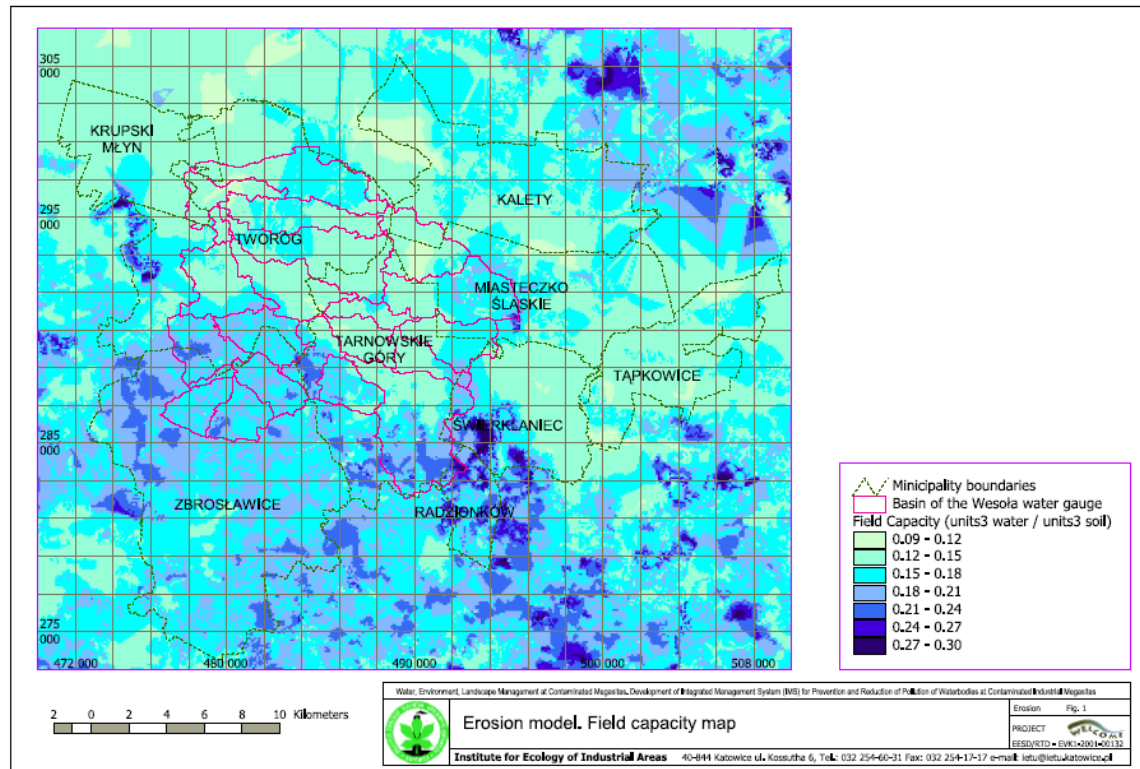
1. Lis J., Pasieczna A., 1995; Geochemical Atlas of Upper Silesia; Polish Institute of Geology, Warszawa
2. Soczyńska U.; 1989; Hydrological processes. Physical and geographical principles of modeling; PWN, Warszawa.
3. Stach. J.; 1987; Hydrological Atlas of Poland; Polish Institute of Geology, Warszawa
4. WELCOME; Water, Environment, Landscape Management At Contaminated Megsites; Development Of Integrated Management System (IMS) For Prevention And Reduction Of Pollution Of Waterbodies At Contaminated Industrial Megsites; WP4.1 GIS Description; Part; GIS development – site description

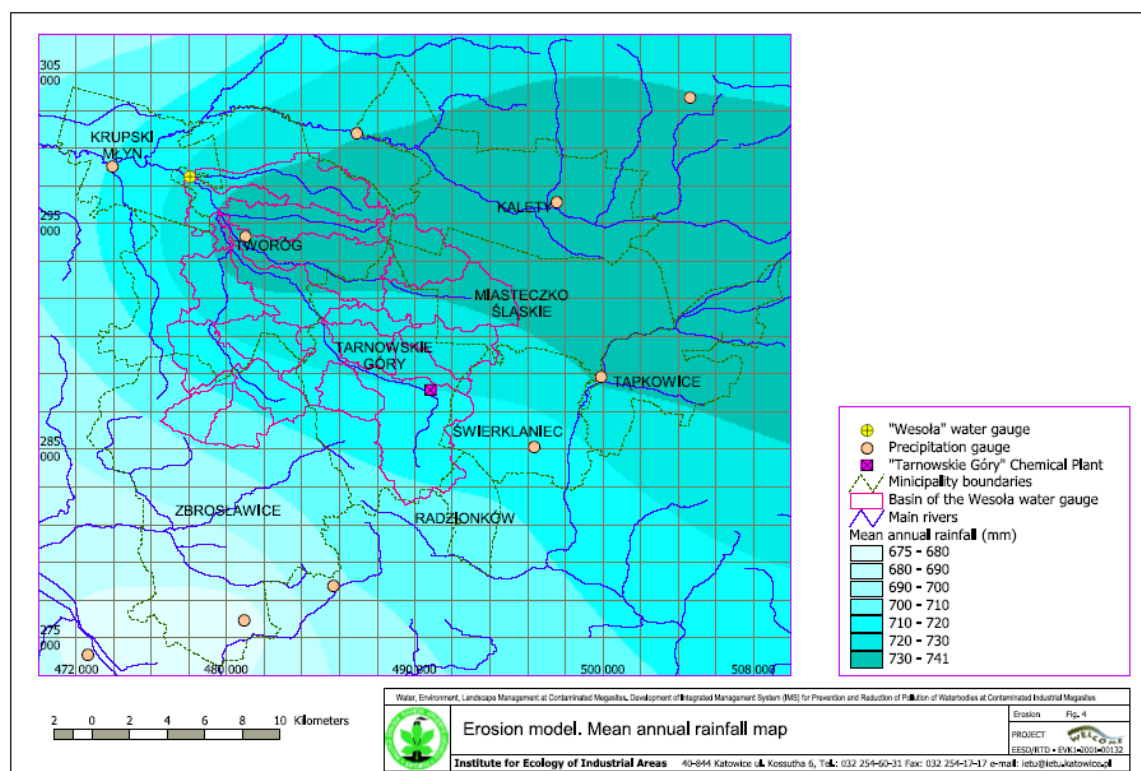
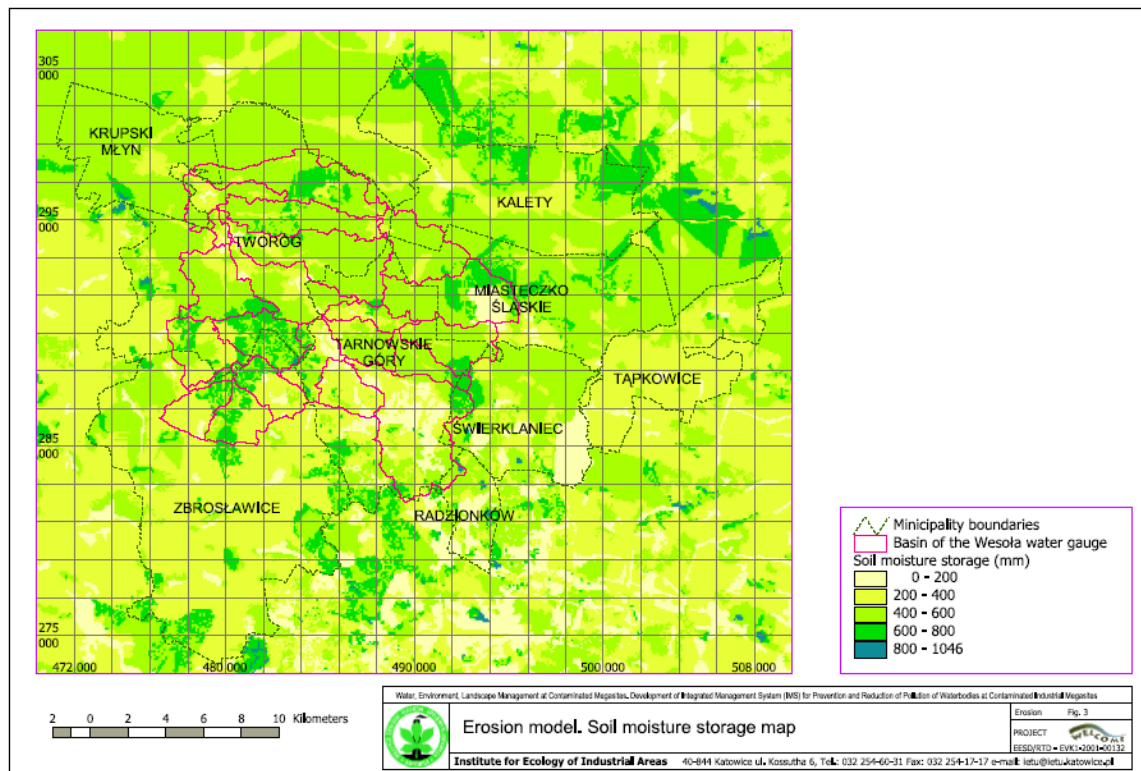
INTERNET resources:

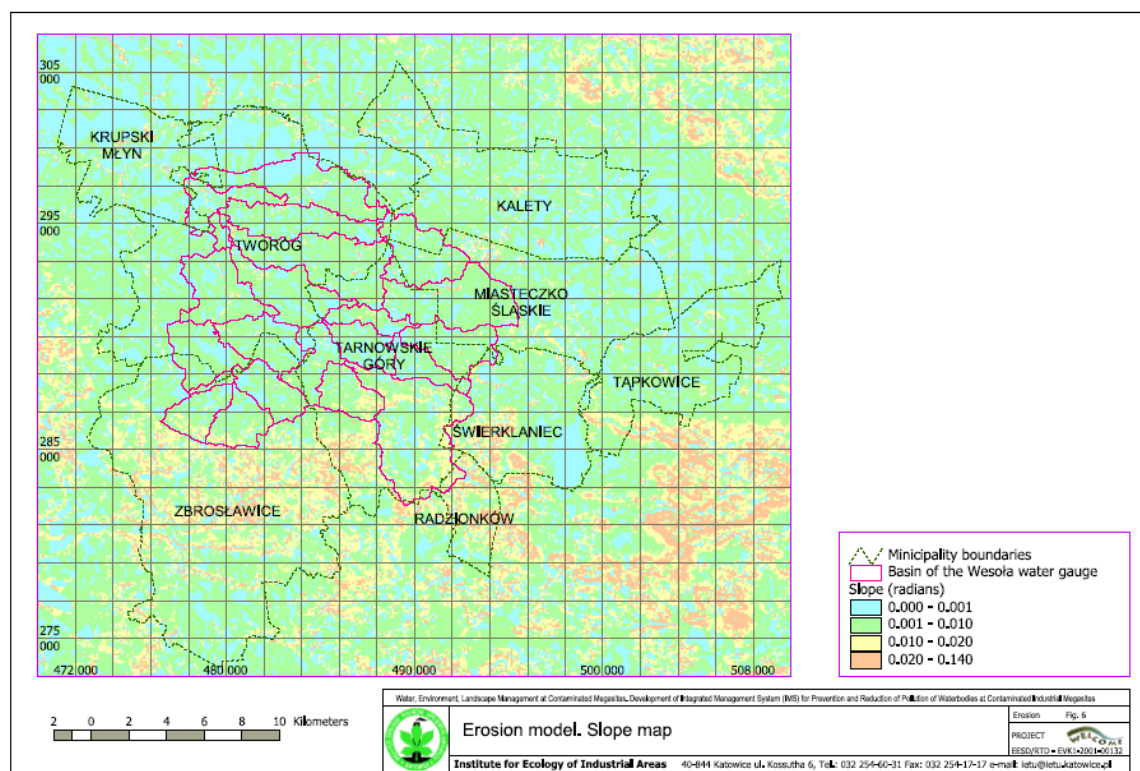
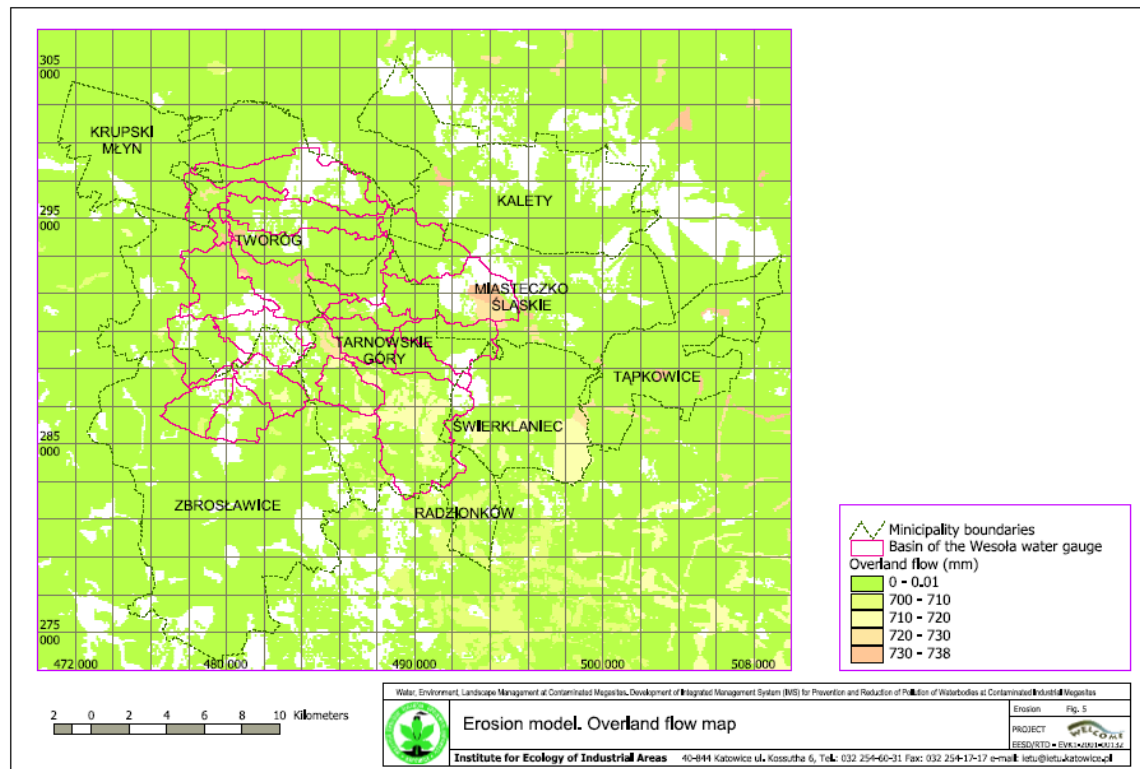
5. <http://www.epa.gov/waterscience/BASINS> - Better Assessment Science Integrating Point and Non-Point Sources
6. <http://www.gov.on.ca/OMAFRA> - Ontario Ministry of Agriculture and Food (OMAF)
7. <http://www.itc.nl> - International Institute for Geo-Information Science and Earth Observation
8. <http://www.pedosphere.com> - American Bulk Density Calculator

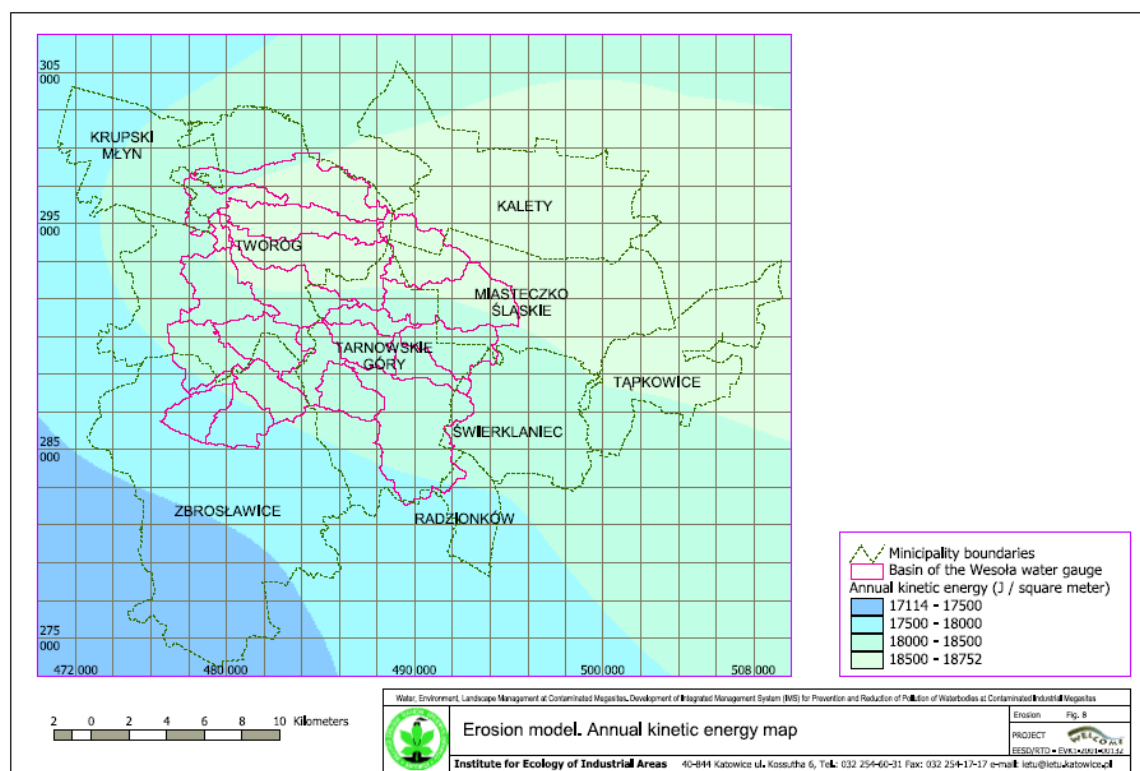
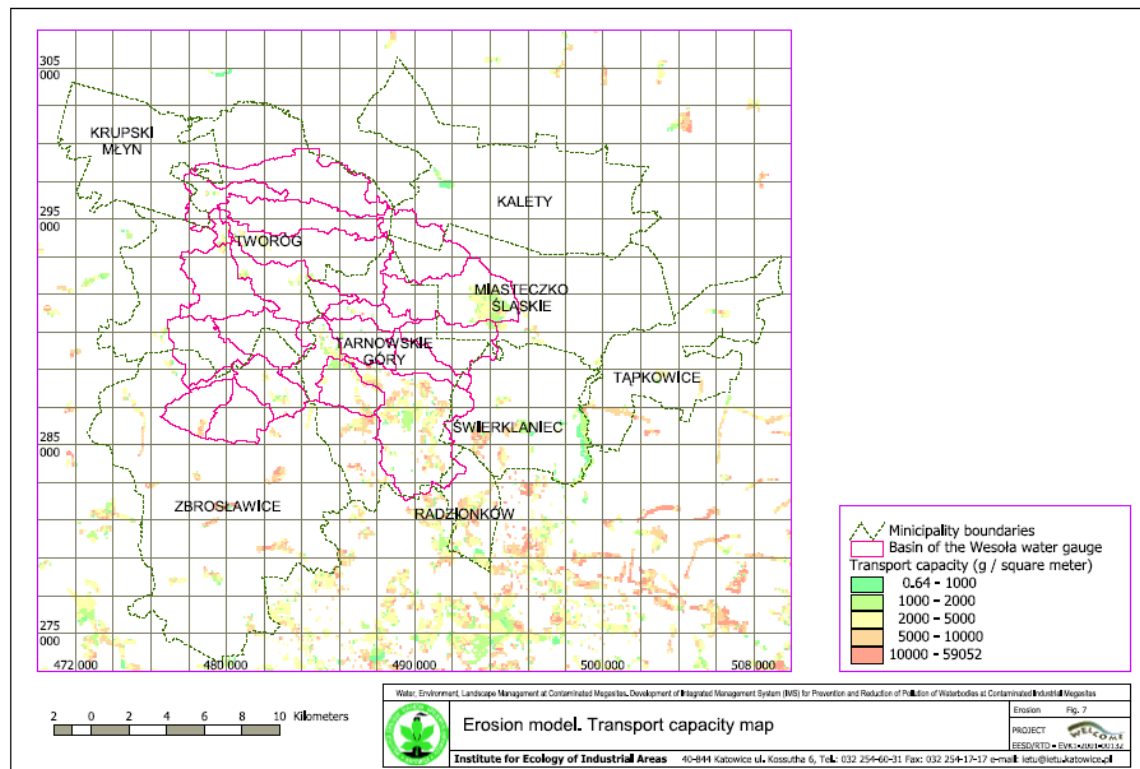
2.2.5 Appendix A. List of map compositions

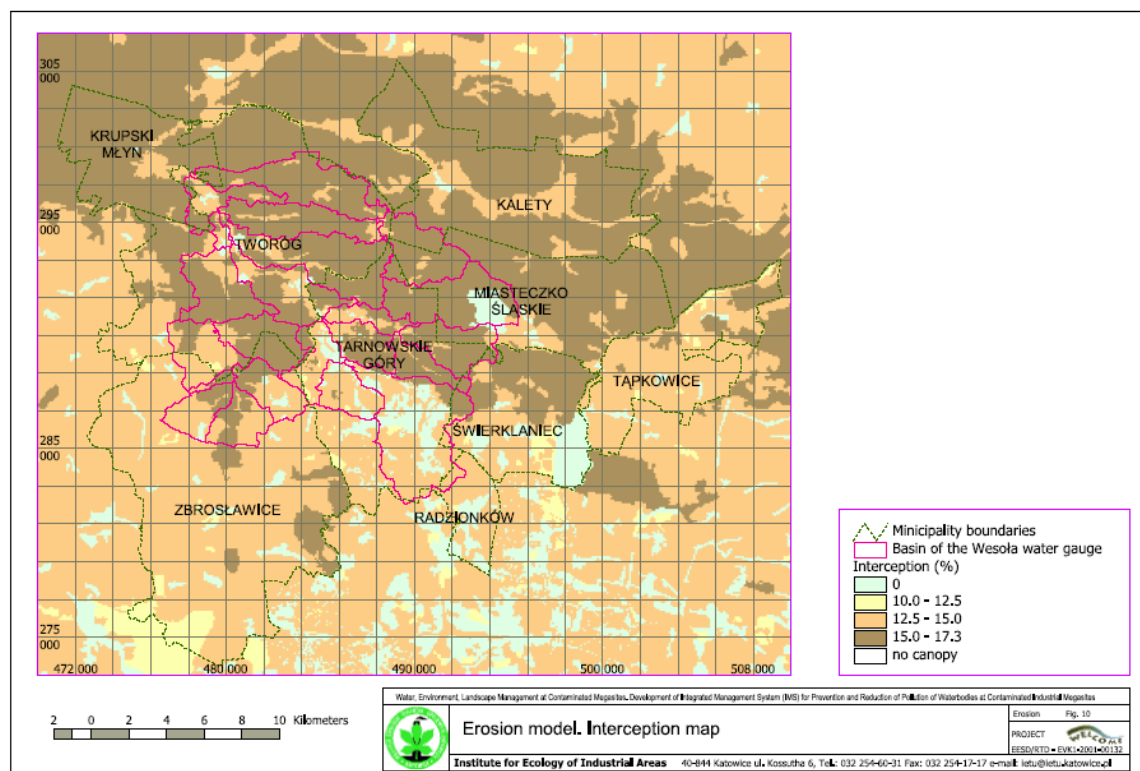
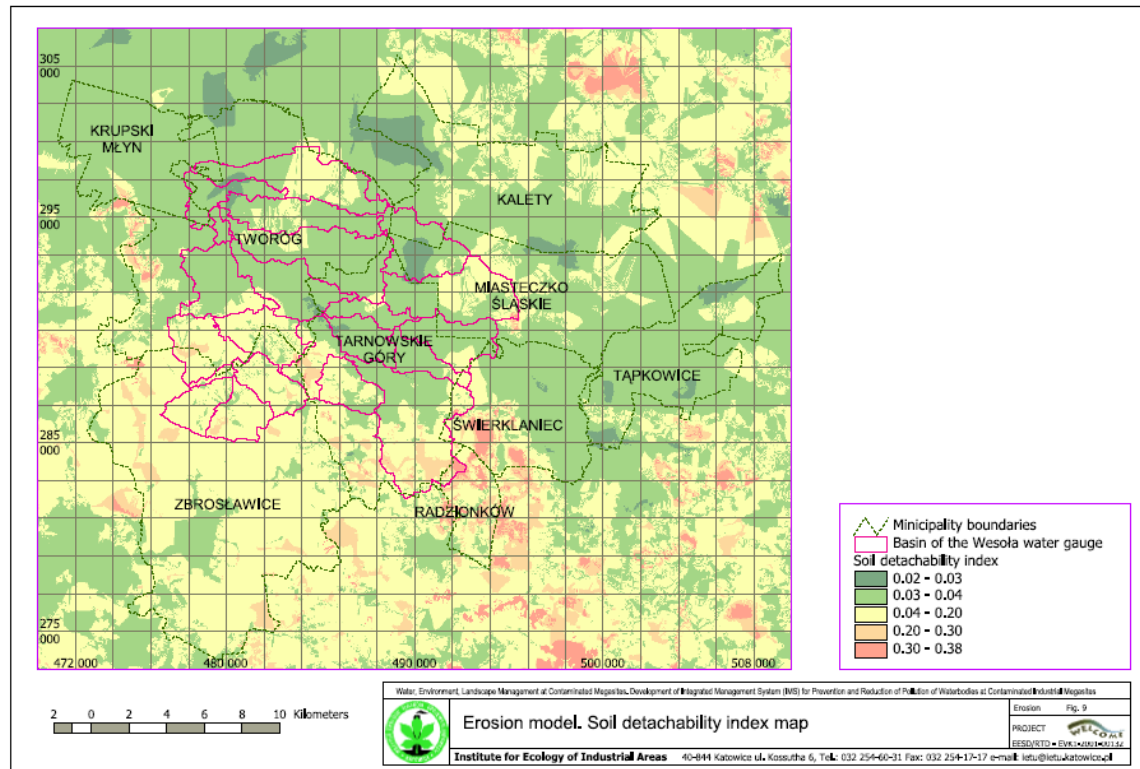
- Fig. 1 Erosion model. Field capacity map
- Fig. 2 Erosion model. Rooting depth map
- Fig. 3 Erosion model. Soil moisture storage map
- Fig. 4 Erosion model. Mean annual rainfall map
- Fig. 5 Erosion model. Overland flow map
- Fig. 6 Erosion model. Slope map
- Fig. 7 Erosion model. Transport capacity map
- Fig. 8 Erosion model. Annual kinetic energy map
- Fig. 9 Erosion model. Soil detachability index map
- Fig. 10 Erosion model. Interception map
- Fig. 11 Erosion model. Rainfall detachment map
- Fig. 12 Erosion model. Erosion rate map
- Fig. 13 Erosion model. Barium potential emission
- Fig. 14 Erosion model. Zinc potential emission

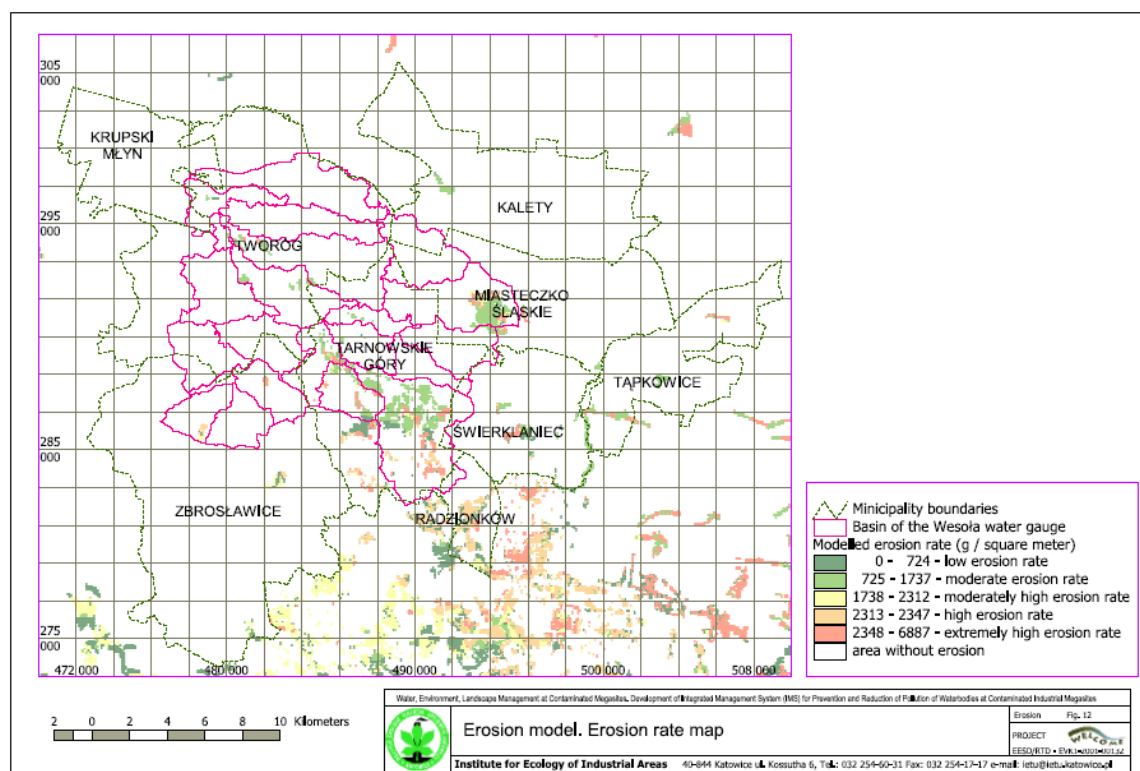
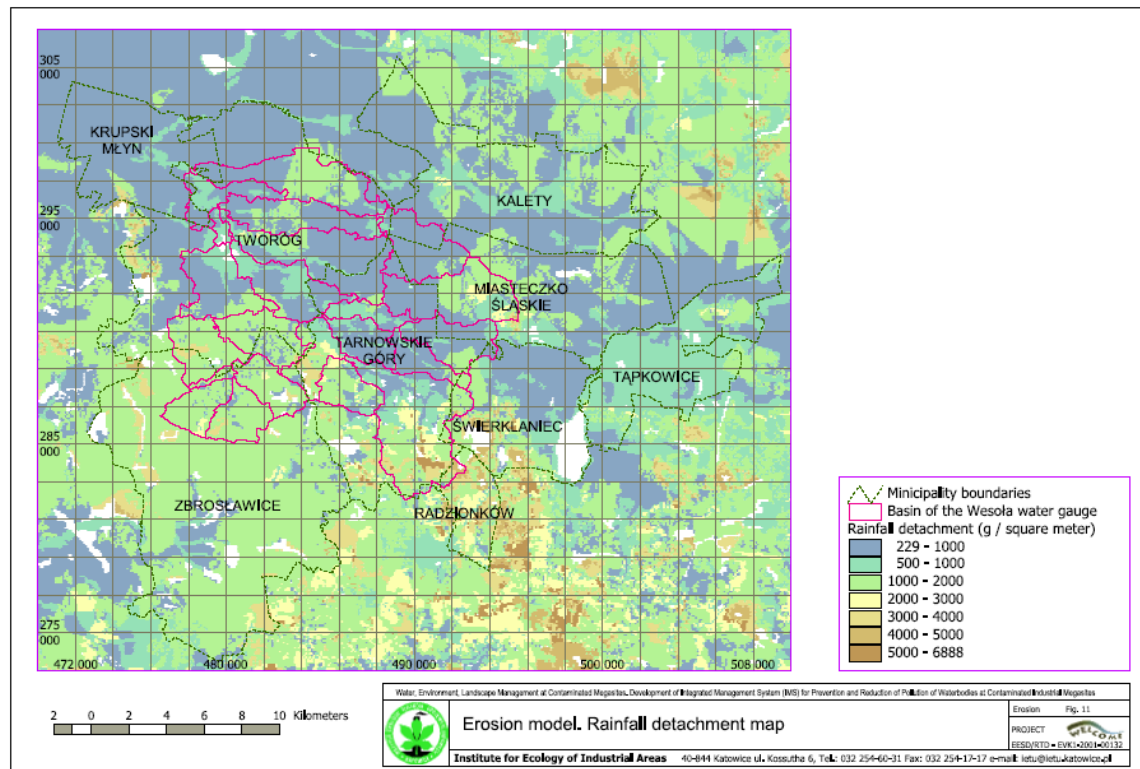


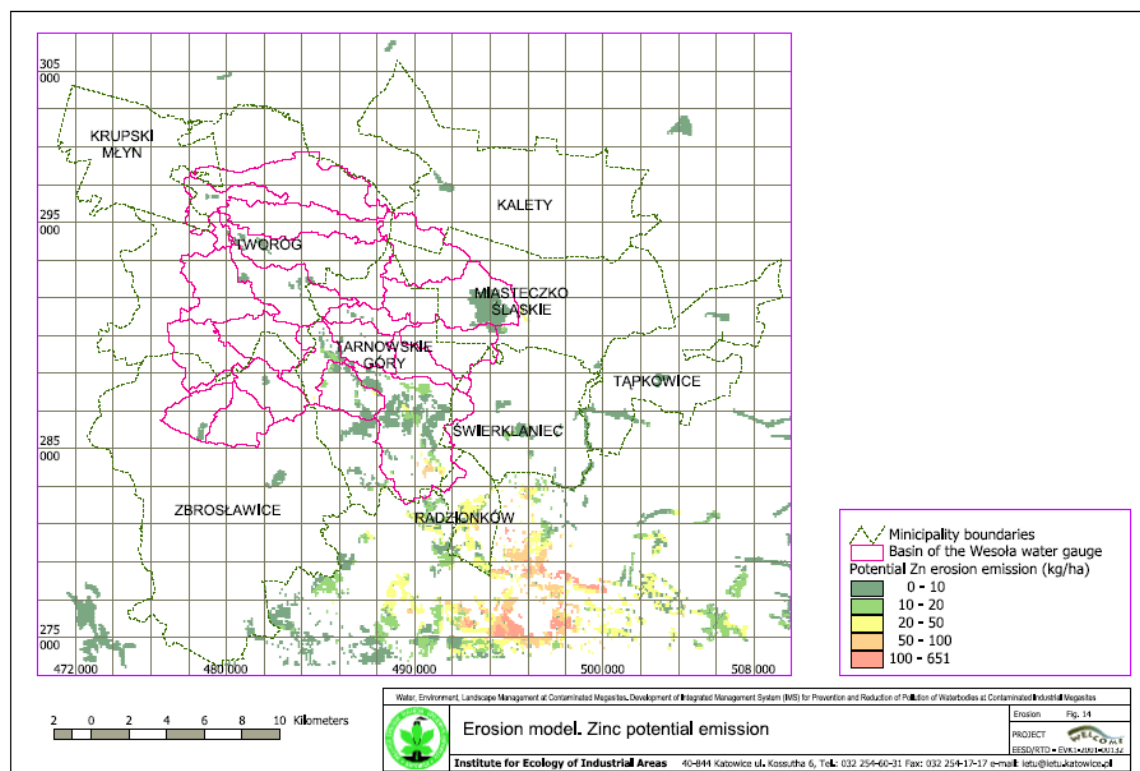
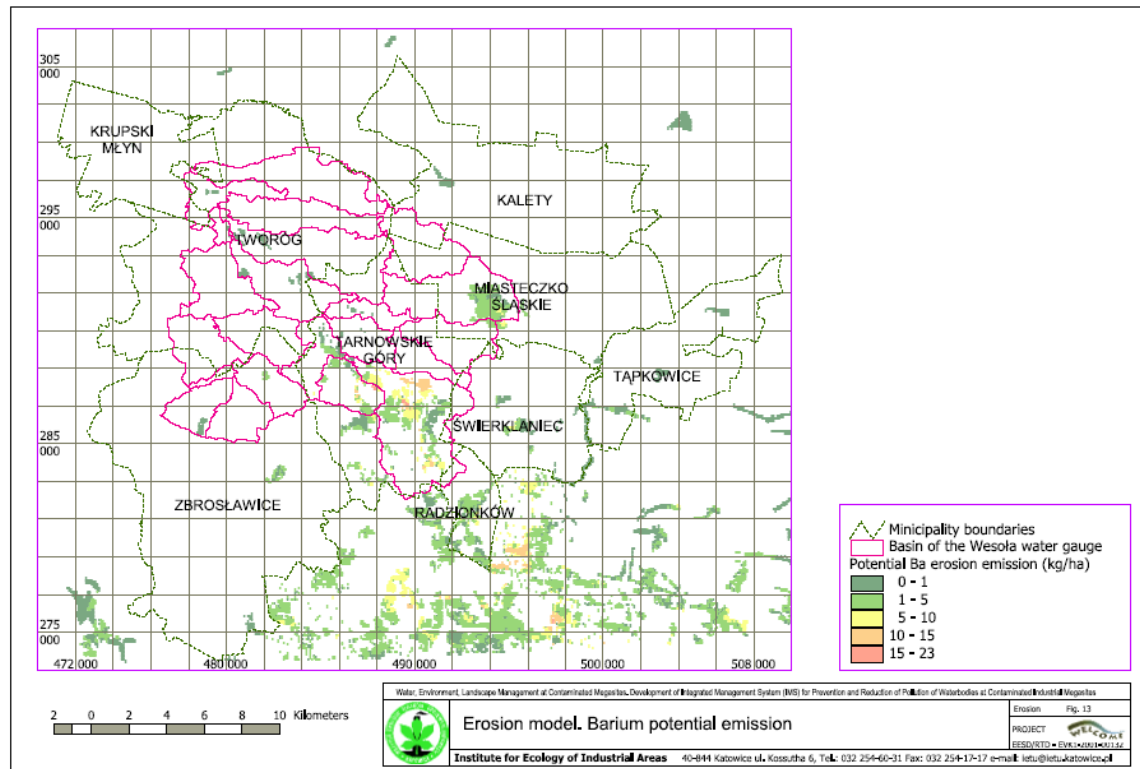












3. Contaminant transport in water systems

3.1 Heavy metal and inorganic contaminant transport

Edited by T. Grotenhuis

K. Kania, G. Malina

*Institute of Environmental Engineering
Czêstochowa University of Technology, Czestochowa,
Poland*

J.T.C. Grotenhuis

*Department of Environmental Technology
Wageningen University and Research Centre, Wageningen,
The Netherlands*

3.1.1 Introduction

Distribution, mobility and bioavailability of metals in the environment depend on their chemical and physical association and on transformation processes they undergo in natural system. Heavy metals discharged into aquatic systems are mostly accumulating in sediments, from which they can be mobilized at changing chemical conditions [1]. The major mechanism of accumulation of metals in sediment generates the existence of five binding forms: adsorptive and exchangeable, bound to carbonates, bound to organic matter and sulfides, bound to Fe and Mn oxides and residual metals [2]. Because the concentrations of heavy metals in sediment haven't got any effect on the behavior of sediments adsorbing heavy metals, the type of binding form must play an important role in release of metals [3]. Mobilization of heavy metals is strongly affected by pH and redox potential. The inorganic and organic complexing ligands, ions strength and microbial activity also have influence on the release of the metals from sediments [2]. The decrease of pH in water and sediment can be reason for release metals binding to carbonates. The decay of organic matters release metals to the water or transform them in immobile forms. The change of Eh (increase or decrease) can be reason for liberate metals binding to Fe and Mn oxides [4]. Natural and anthropogenic activities have the capacity to remobilize contaminated sediments and release contaminants from sediment and sediment pore water to the water column. Daily tidal currents, wind energies and storms in coastal and estuarine systems can cause periodical remobilization of surface sediments [5]. More turbulent flow conditions, associated with seasonal flooding or storms, can expose anoxic sediment to oxic conditions [6]. Human activities such as industrial and municipal effluents, landfill leaching, non-point source run-off and atmospheric deposition can change conditions of sediments. The speciation of metals in water is as crucial to the understanding of metal behavior in aquatic system as those of metal speciation in sediment. The forms of chemical species of toxic metals in the water column, the organic and inorganic metal complexes and the free solvated metal ions, could be used as a predictor of bioavailability to a particular aquatic organism [7].

The change of leaching of metals from sediments was observed during flooding. Due to high flow of the Lau-Che River (Taiwan) the organic matters and fine sediment particles were scoured from the bottom sediment, thus the pH and contents of heavy metals in the sediment were lower in low flow [2]. In the Odra River during the flood in July 1997, the concentrations of metals were varied. An increase of Cu, Ni, Pb, and Zn was observed in the water phase. Probably it was due to remobilizations from contaminated sediments, but also the leaching of metals from the flooded industrial areas. On the other hand concentrations of Hg decreased, whereas for As, Cr and Cd any significant changes of concentrations in the water phase were observed [8]. Wolterbeek et al. have investigated the effects of deposited metals and general quality of topsoil in flooding areas of the rivers: Meuse, Rhine and Waal. The samplings were done directly after the withdrawal of the water in February 1995. For three river regions As, Co and Cr were below the respective target values (target values are defined as reflecting the concentrations in soil at the which the soil functional properties in relation to humans, flora and fauna, are fully restored or maintained) for topsoils and river silts. The amounts of Ba and Zn were above target

values for topsoils and river silts in all regions. The deposition of river silt didn't influence in general topsoil quality [9].

The Stola River is flowing through the south part of the chemical plant at the Tarnowskie Gory megasite. Along the river were situated storage yards of hazardous industrial wastes: waste products of barium salts and lithopone (Ba), waste from factory sewage treatment plant (As, Ba, Sr and Zn) (east part of the megasite) and various waste – slag from thermal-electric power station and contaminated crushed brick (B, Ba, Cd, Cr, Sr and Zn) (in the west part and in direction south). As a result of waste deposition, the river-bed within the plant's area was displaced for ca. 100-120 m in the S direction compared to its original location [10]. Five sediments used in this study were characterized by high concentration of metals. Sediments: 2, 4, and 5 had similar properties. The characteristic of sediments 6 was slightly different as the organic matter content was much lower and Eh was higher. The Eh of sediments 10 sampled from the PA creek was much higher than in sediments from Stola River.

In this studies the influence of pH, Eh and L/S ratio on mobilization of metals from the Stola River sediments was investigated to define and evaluate the environmental risk.

3.1.2 Material and methods

Five sediments originated from the Tarnowskie Gory megasite: Stola River (sediment 2, sediment 5, sediment 4 and sediment 6) and PA Creak (sediment 10) were studied. The sediments were well buffered (pH 6,6 – 7,7) and they were characterized by varied organic mater contents (0,28 – 7,8%). Organic mater plays an important role in binding metals in sediments. All sediments were in reduced state (-187,4 mV ÷ 100,6 mV). Sediments were polluted heavy metals (Zn, Cd and Cr), metals (Sr, Ba and As) and non-metal (B).

Sediments were stored at 4°C until analyzed.

Table 3.1 The characteristics of sediments

	pH	Eh [mV]	O.M.	Total contents mg/kg d.m.						
				Zn	Cr	Cd	Ba	Sr	As	B
sed. 2	7.0	-187.4	7.8	5437	85	26	2046	702	53	51
sed. 4	7.7	-179.6	6.65	6350	119	12	2224	230	115	21
sed. 5	6.9	-226	2.9	7456	155	44	516	328	86	55
sed. 6	7.0	-64	0.28	520	5	85	709	85	2	10
sed. 10	6.6	100.6	2.07	160	4	4	1952	71	2	12

Experiments were performed using:

- different initial Eh (experiment 1),
- different initial pH (experiment 2), and
- different ratio L/S (experiment 3).

In experiment 1 two sediments: 2 and 5 were studied. The initial Eh values of +100 mV, +200mV, +300mV were obtained by flushing with air. Batch experiments were carried out for 21 days. Within the whole period samples were shaken by end- over- end shaker. 30 g of dry matter of each sediment and 300ml of 0.01 M CaCl₂ was applied (bottles 330 ml). The liquid to solid ratio was from 10 to 1. Parameters such as; Eh, pH, concentrations of heavy metals in supernatants and heavy metals contents in sediments were analyzed in 1st, 11th and 21st day.

In experiment 2 four sediments: 2, 5, 6 and 10 were used. The initial pH of 3 and 7 were obtained by adding HNO_3 (concentration: 0,014M). Batch experiments were carried out for 21 days. Within the whole period of experiments samples were shaken by end- over- end shaker. The amounts of 18 g of dry matter of each sediments and 180 ml of 0.01 M CaCl_2 solution were applied (bottles 300 ml). The liquid to solid ratio was from 10 to 1. Eh, pH, heavy metals concentrations in supernatants were analyzed in 1st, 11th and 21st day. Contents of heavy metals in sediments were analyzed after termination of the experiment.

Experiment 3 was performed for four sediments and liquid/solid ratios L/S of 5, 10, 20, 50, 100. Batch experiments were carried out for 21 days. Within the whole period samples were shaken by end- over- end shaker. The amounts of 32, 18, 9, 4, and 2 g of sediment d.m., and appropriate buffer of 160, 180, 180, 200, and 200 ml at pH 7 were applied (bottles 300 ml). Eh, pH, heavy metals concentrations in supernatants were analyzed in 1st, 9th and 21st day. Contents of heavy metals in sediments were analyzed after termination of the experiment.

The pH of sediments was measured according to PN-ISO 10390. Redox potentials were measured by inserting platinum electrode (Pt-AgCl/Ag) in the sediment paste until stable reading. The total concentrations of heavy metals and B in sediments (in mg of metal per kilogram of dry sediment) were determined after microwave destruction (CEM 2000, Matthews, USA) of pre-dried samples (40° C), subjected to digestion with aqua regia (HCl/HNO_3 , 3:1 (concentration: 0,0125M.)). After digestion, the samples were paper filtered and diluted to 100 ml. The supernatant liquid was acidified by HNO_3 to pH 2, stored at 4°C and analysed by Inductively Coupled Plasma Mass Spectrometry (ICP - MS, IRIS Interpid II XSP). The concentrations of metals in the liquid phase of supernatants were determined by centrifugation (4000 rpm 10 min). The supernatant liquid was acidified by HNO_3 to pH 2, stored at 4°C and analysed by Inductively Coupled Plasma Mass Spectrometry (ICP - MS, IRIS Interpid II XSP).

3.1.3 Results

3.1.3.1 Contaminant leaching at different Eh

In the sediments, pH varied only slightly between 6,8 -7,8 at the initial Eh values of +100mV, 6,0 - 6,8 at Eh of +200 mV and 6,3 ÷ 6,8 at Eh of +300 mV. The redox potential was not stable during the incubation period, and the changes were higher in sediments 2 than sediments 5.

Concentrations of contaminants in water for sediments 2 and 5 at the Eh range from +100 to +300mV were always below 3 mg/L. shows concentrations in liquid phase for sediments 2 versus time at the initial Eh of +300 mV.

The extraction degree (in %) for all sediments was lower than 2.5% for Sr and B, and below 1 % in the case of Zn, Cd, Cr, Ba and As.

The effect of redox potential lead to maximum extraction of less than 30 mg /kg dm in sediment 2. In the case of sediment 5 the maximum leached amounts of contaminants were even below 15 mg/kg dm (Table 2 and 3). Figure 3.2 shows leaching behavior of metals from sediment 2 at the initial Eh of +100mV. In Similar

results were found for leaching of metals from sediment 2 and 5 at the initial Eh of +100mV, +200mV and +300 mV.

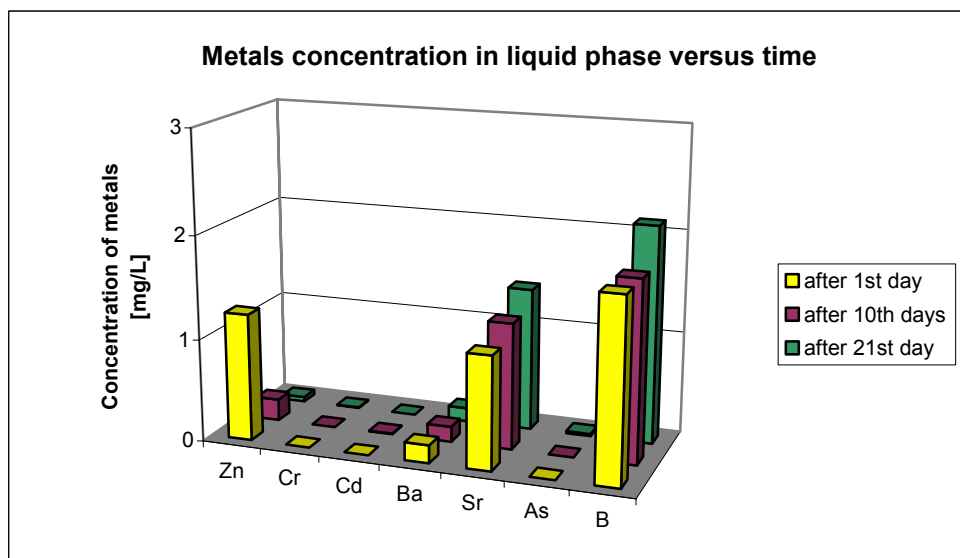


Figure 3.1 Metals concentration in the liquid phase for sediment 2 versus time at the initial Eh=+300 mV.

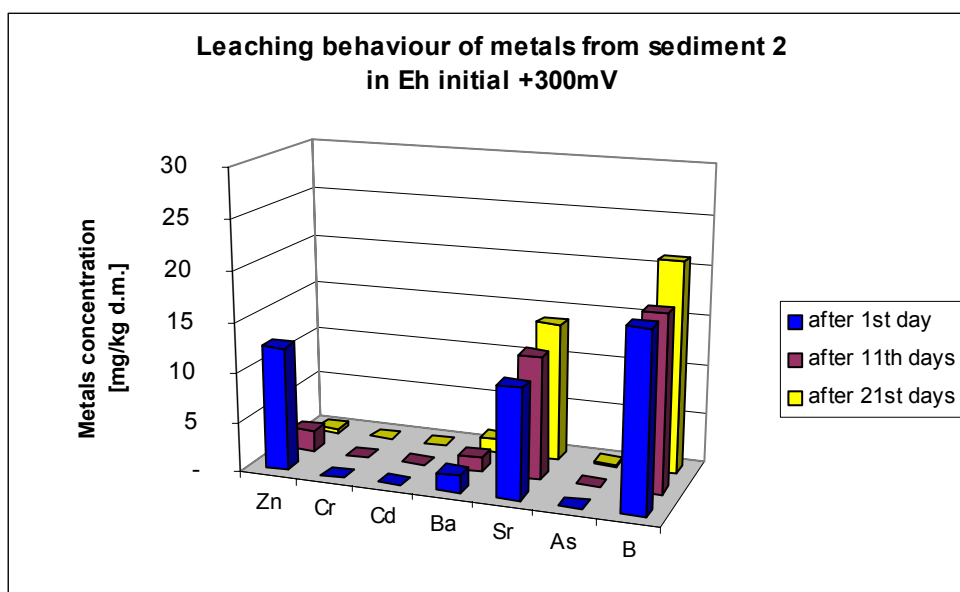


Figure 3.2 Leaching behavior of metals from sediment 2 at the initial Eh = +300mV

Table 3.2 Characterization of leaching behavior of metals from sediments 2

	Zn	Cr	Cd	Ba	Sr	As	B
mg/kg_{d.m.}							
initial +300 mV							
after 1st day	12.36	-	-	1.74	10.98	-	17.73
after 11th days	2.10	-	0.09	1.50	12.27	-	17.63
after 21st days	0.45	0.05	-	1.33	13.93	0.22	21.10
initial +200 mV							
after 1st day	3.31	-	-	0.04	13.93	0.03	24.57
after 11th days	0.26	-	-	0.11	16.13	0.15	27.60
after 21st days	0.32	-	-	0.07	16.00	0.16	25.47
initial +100 mV							
after 1st day	0.37	-	0.08	20.33	13.80	-	21.00
after 11th days	0.31	-	0.10	5.43	14.23	-	20.53
after 21st days	0.14	-	0.07	5.73	13.83	0.12	18.57

Table 3.3 Characterization of leaching behavior of metals from sediments 5

	Zn	Cr	Cd	Ba	Sr	As	B
mg/kg_{d.m.}							
initial +300 mV							
after 1st day	14.10	-	0.04	1.58	5.78	-	1.62
after 11th days	5.75	-	-	1.72	7.47	0.19	1.74
after 21st days	0.32	-	0.09	1.84	8.33	-	1.64
initial +200 mV							
after 1st day	1.08	-	0.11	5.12	4.30	-	1.72
after 11th days	0.45	-	0.11	3.31	5.82	0.15	1.78
after 21st days	0.41	-	0.06	3.13	5.42	-	1.53
initial +100 mV							
after 1st day	0.66	8.55	0.19	-	2.77	0.06	1.03
after 11th days	0.65	9.85	0.08	-	4.67	-	1.65
after 21st days	0.37	10.77	0.14	-	5.14	0.11	1.78

3.1.3.2 Contaminant leaching at different pH

After initial adjusting of pH to 3 the pH range varied between 3,09 and 6,45. . In the sediments with the initial pH of 7 its range varied only slightly from 6,86 to 7,73 (sediment 2), 6,86÷7,28 (sediment 5), 6,67 ÷ 6,98 (sediment 6) and 7,00 ÷ 7,25 (sediment 10). The changes of Eh were higher at the initial pH=3 (+39mV ÷ + 564mV) than at initial pH= 7 (+198mV ÷ + 310mV). The redox potential varied at the initial pH= 3 for sediment 2 between +39mV and +288mV (at initial pH 7 between +215 and + 250mV), for sediment 5 +133mV ÷ + 310mV (+198mV ÷ +284mV), for sediment 6 +259mV ÷ +564mV (+234mV ÷ +310mV) and for sediment 10 +276 ÷ +504mV (+210mV ÷ + 277mV).

The concentrations in water at initial pH= 3 of Cr, Cd, Sr B, Ba and As were below 5mg/L, and for Zn below 45 mg/L. (i.e. 9 times higher). The concentrations in water at the initial pH= 7 of Cr, Cd, Sr B, Ba and As were below 3 mg/L, and for Zn – below 10 mg/L (i.e. 3 times higher). In appendix Figure 6-7 (where is this appendix and

figures?) shows inorganic contaminant concentrations in the liquid phase after 21st days for both experiments (at initial pH=3 and 7).

At the initial pH= 3 leaching of metals (except Zn) was below 40 mg/kg dm. Leaching of Zn was even 450 mg/kg dm (**Error! Reference source not found.**). At the initial pH= 7 leaching of metals was lower (below 27mg/kg dm), only of Zn reached 105 mg/kg dm (Table 3.5). Figure 3.3 shows leaching of metals from sediments 2 at the initial pH= 3 and 7. In appendix 1 figure 8 – 10 show leaching of metals from sediments: 5, 6 and 10.

Table 3.4 Characterization of leaching behavior of metals from sediments at initial pH = 3

	Zn	Cr	Cd	Ba	Sr	As	B
mg/kg_{d.m.}							
sediment 2							
after 1st day	3.35	0.10	-	5.90	14.80	0.21	26.33
after 11th days	53.67	0.08	0.04	1.02	16.20	-	31.13
after 21st days	147.47	-	-	0.63	12.57	-	37.4
sediment 5							
after 1st day	38.13	0.22	-	7.03	10.57	0.96	3.32
after 11th days	141.00	0.06	-	1.12	14.27	-	4.27
after 21st days	452.67	-	0.05	0.65	14.23	-	4.84
sediment 6							
after 1st day	133.33	0.92	8.21	43.80	3.32	0.37	0.76
after 11th days	245.33	0.26	42.83	21.96	3.57	-	0.85
after 21st days	270.00	0.28	49.37	11.05	3.95	-	1.09
sediment 10							
after 1st day	35.57	0.13	0.29	47.73	7.52	0.15	1.19
after 11th days	43.33	-	0.57	44.63	8.57	-	1.48
after 21st days	64.40	0.04	4.63	34.27	8.99	-	1.56

Table 3.5 Characterization of leaching behavior of metals from sediments at initial pH = 7

	Zn	Cr	Cd	Ba	Sr	As	B
mg/kg_{d.m.}							
sediment 2							
after 1st day	0.18	-	-	8.34	10.18	-	19.57
after 11th days	0.54	-	-	1.32	15.90	-	26.43
after 21st days	2.40	-	-	0.59	13.87	-	27.03
sediment 5							
after 1st day	0.42	-	-	8.29	4.67	0.14	2.52
after 11th days	3.70	-	-	1.85	9.09	-	3.62
after 21st days	48.73	-	-	0.72	11.87	-	4.02
sediment 10							
after 1st day	5.54	-	0.42	9.09	2.15	-	0.77
after 11th days	71.77	-	13.33	12.77	2.70	-	0.92
after 21st days	105.63	-	21.47	7.44	2.89	-	0.87
sediment 10							
after 1st day	0.34	-	0.05	14.47	4.55	-	0.96
after 11th days	1.17	-	0.13	16.80	5.70	-	1.24
after 21st days	0.84	-	0.03	16.40	5.970	-	1.22

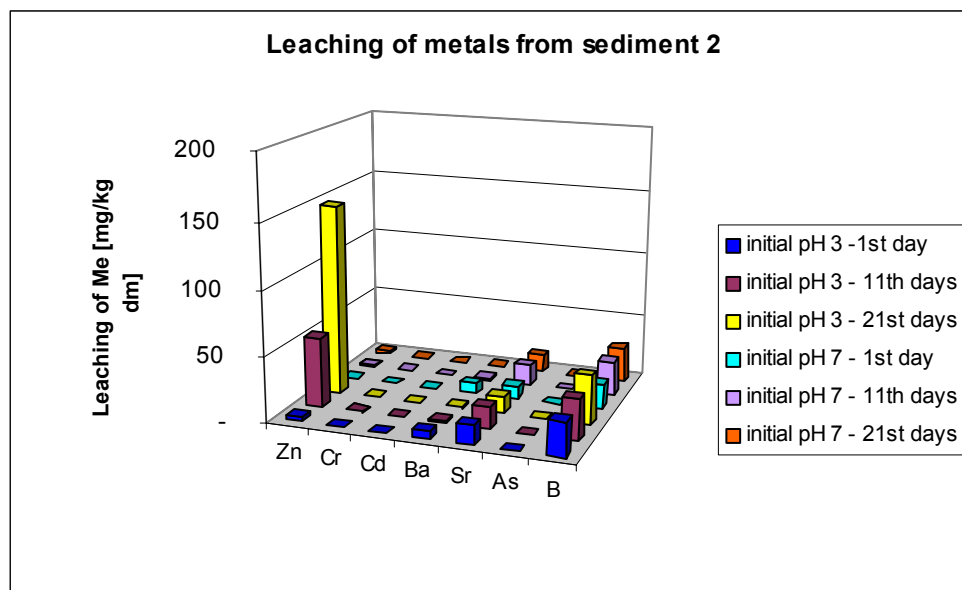


Figure 3.3 Leaching behavior of metals from sediment 2 at initial pH= 3 and 7 versus time.

3.1.3.3 Contaminant leaching at different L/S ratio

The pH of sediments varied only slightly between 6,95 and 7,22. The values of Eh varied with the L/S ratio. Eh was much lower at L/S = 5 (+110mV) than at L/S = 100 (+458mV) (Table 6).

Table 3.6 Eh in sediments at different L/S ratio.

Eh [mV]	L/S = 5	L/S = 10	L/S = 20	L/S = 50	L/S = 100
initial	+117 mV	+166 mV	+203 mV	+255 mV	+276 mV
after 1st day	+131 mV	+165 mV	+222 mV	+284 mV	+321 mV
after 9th days	+115 mV	+178 mV	+298 mV	+404 mV	+458 mV
after 21st days	+110 mV	+252 mV	+363 mV	+492 mV	+455 mV

Concentration of contaminants in water was always below 1,5 mg/L. Figure 3.4 shows concentrations in liquid phase for sediments 4 at different L/S ratio after 21st days.

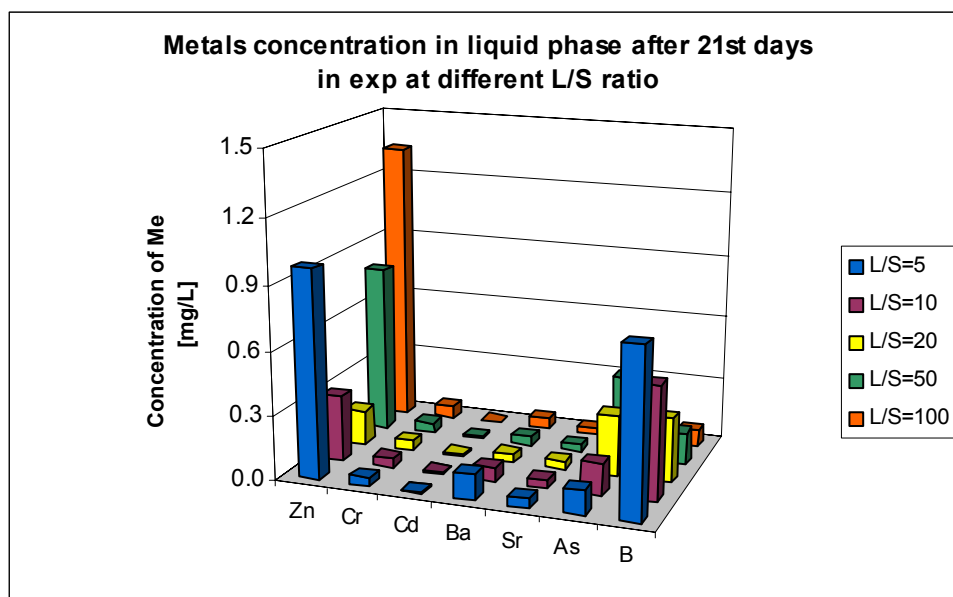


Figure 3.4 Contaminants concentrations in liquid phase for sediments 4 at different L/S ratio after 21st days

The extraction degree was increasing with increased L/S ratio. For Zn, Sr, Cd, Ba and Cr extraction was below 7%. For Ba and As was even 90% (As – L/S = 100). Desorption of contaminants from sediments increased with an increase L/S ratio. Except for Zn the maximum extraction was lower than 23 mg/kg dm, whereas in the case of Zn it was below 133 m/kg dm (Table 3.7) Figure 3.5 shows leaching of metals from sediment 4 after 21 days.

In appendix 1 Figure 11-12 shows leaching of metals from sediment 4 in the 1st and 9th day of the experiment.

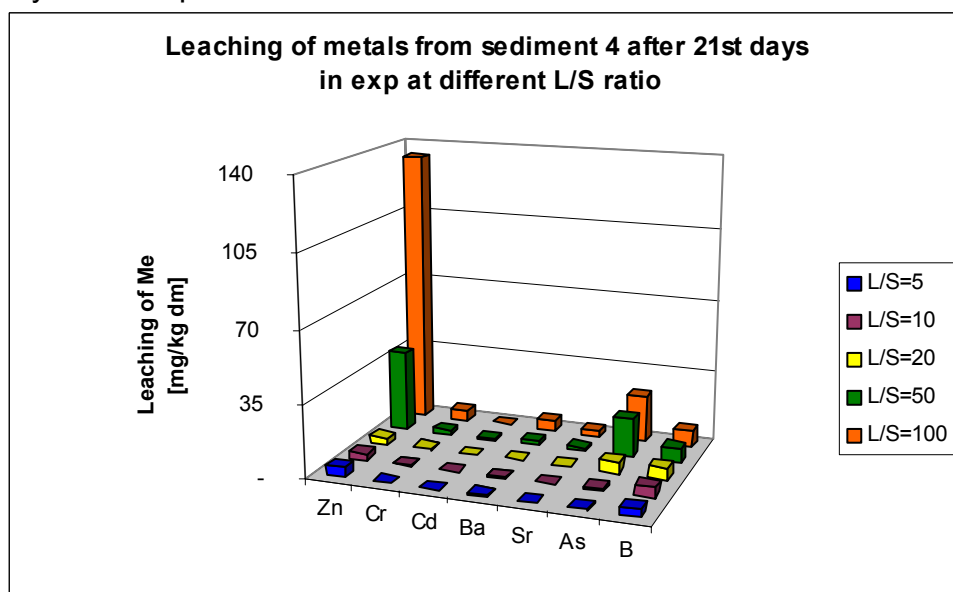


Figure 3.5 Leaching of metals from sediment 4 after 21 days.

Table 3.7 Characterization of leaching behavior of contaminants from sediment 4

	Zn	Cr	Cd	Ba	Sr	As	B
mg/kg _{d.m.}							
L/S = 5							
After 1st day	0.65	0.23	-	0.74	0.70	0.32	2.79
After 9th days	4.07	0.22	0.04	0.61	0.19	1.00	3.32
After 21st days	4.08	0.21	0.04	0.62	0.22	0.57	3.92
L/S = 10							
After 1st day	0.77	0.47	-	1.33	1.26	0.51	3.53
After 9th days	3.22	0.43	0.07	0.63	0.37	2.46	4.80
After 21st days	3.15	0.45	0.06	0.64	0.39	1.48	5.33
L/S = 20							
After 1st day	1.33	0.93	-	3.03	1.97	0.81	3.99
After 9th days	3.99	0.95	0.16	1.51	0.71	5.78	5.24
after 21st days	3.27	0.95	0.21	0.83	0.75	5.75	6.05
L/S = 50							
after 1st day	3.12	2.33	-	4.97	3.12	1.47	5.25
after 9th days	14.00	2.43	0.23	2.03	1.75	10.97	6.38
after 21st days	39.68	2.50	0.53	2.20	1.70	19.18	7.47
L/S = 100							
after 1st day	6.07	4.87	-	8.50	3.97	2.77	5.40
after 9th days	43.27	4.83	0.50	9.27	3.03	14.80	8.20

3.1.4 Discussion

In Figure 3.6 a summary of the most extreme conditions applied to the sediments is presented after a leaching period of 21 days. It can be observed that the initial pH value of 3 led to the highest extraction of contaminants from the different sediments. Especially the effect of leaching of Zn is remarkable in absolute values as 452 mg Zn/kg dm was released from sediment 5, which is 6 % of the total amount of Zn. Fortunately such extreme conditions are exceptional in the river systems.

As the effect of Zn seems to overrule the effect to all the other inorganic contaminants in the Stola River, we represented the same data with exclusion of the experiments performed at pH=3, as well as the data for Zn (Figure 3.7). The maximum extracted contaminant concentrations at these conditions are around or below 25 mg/kg dm. In relative values this means that maximum 2,1% Zn, 6 % Cd, 4.5% Cr, 2% Sr, 0.8% Ba, 20 % As and 73% of B was extracted.

Concentrations of the contaminants in the water were always below 3 mg/l for the experiments with different Eh (Experiment 2), as well as for experiments at pH 7 (experiment 1), whereas concentrations in the experiments with diverse L/S ratios (experiment 3) were always below 1.5 mg/l. Only in the experiments at pH= 3 the Zn concentration was about 45 mg/l, whereas the other concentrations were still below 5 mg/l. However, all values were above the Dutch intervention values for groundwater (Zn 0.800 mg/l, Cd 0.006 mg/l, Cr 0.03 mg/l, Sr no value given, Ba 0,625 mg/l, As 0,06 mg/l, B no value given). The Polish intervention values for potable water in all experiments were exceeded for Ba (0,1 mg/L) and Cd (0,005mg/L).

The extraction of Sr was comparable at both redox potential values, whereas Ba shows higher leaching at low Eh values. No specific differences in the two sediments were observed at the different Eh values. The studying of Ba behavior performed by van der Sloot et al showed that leaching of Ba was higher at lower Eh values, below +100mV [11]. In reduced conditions with rise of pH, the leaching was slightly decreasing. Masscheleyn et al shown that mobility of As at the Eh range between +200mv and +500 mV was very low [12]. The similar behavior was in sediments from the Stola River, where the leaching of As was below 1 mg/kg dm and Eh was higher than 100mV (at L/S up to 10).

The leaching of metals seemed not to be correlated to the concentration in the sediments. In the case of sediments 2, 4 and 5 the concentrations of the contaminants decreased in the same order from Zn to Ba, Sr, Cr, As, B and Cd, and leaching at pH = 7 shows different behavior for all these sediments. According to the results of Huang Suiliang et al. the concentrations of heavy metals in sediment have not any effect on the behavior of sediment adsorbing (desorbing) heavy metals [3]. However, increased L/S ratios had a clear effect on all the different contaminants as is demonstrated in Figure 3.8. At a high L/S ratio, which is a simulation of high tide in a river system, the extracted amounts increased for all contaminants. The same behavior was observed by van der Sloot as the leaching availability of Ba and Zn increased with increased L/S ratio. For Cr the L/S ratio did not have an influence on leaching behaviour [13]. Different results were obtained by Tack et al. for dredged sediments at L/S = 2.5, 20 and 100 [14]. The highest leaching of Cd, Cu and Zn was at L/S = 2.5. In the case of Pb the highest leaching was at L/S = 100. From these findings, it can be concluded that the sediment contamination by Zn in the Stola river at the Tarnowskie Gory meagsite is rather mobile. Although Ba and Cd were not so mobile as Zn, they also may pose risk for aqueous ecosystems. At low pH significant amounts of contaminants may be leached from sediments. However, due to high buffering capacity of the sediments it seems to be unlikely unless high amounts of acid materials enter the site. The other threat at this megasite may be due to flooding. In such a case the L/S ratios may increase dramatically, and as it is shown, may enhance the mobilization, and therefore leaching of inorganic contaminants from the sediments

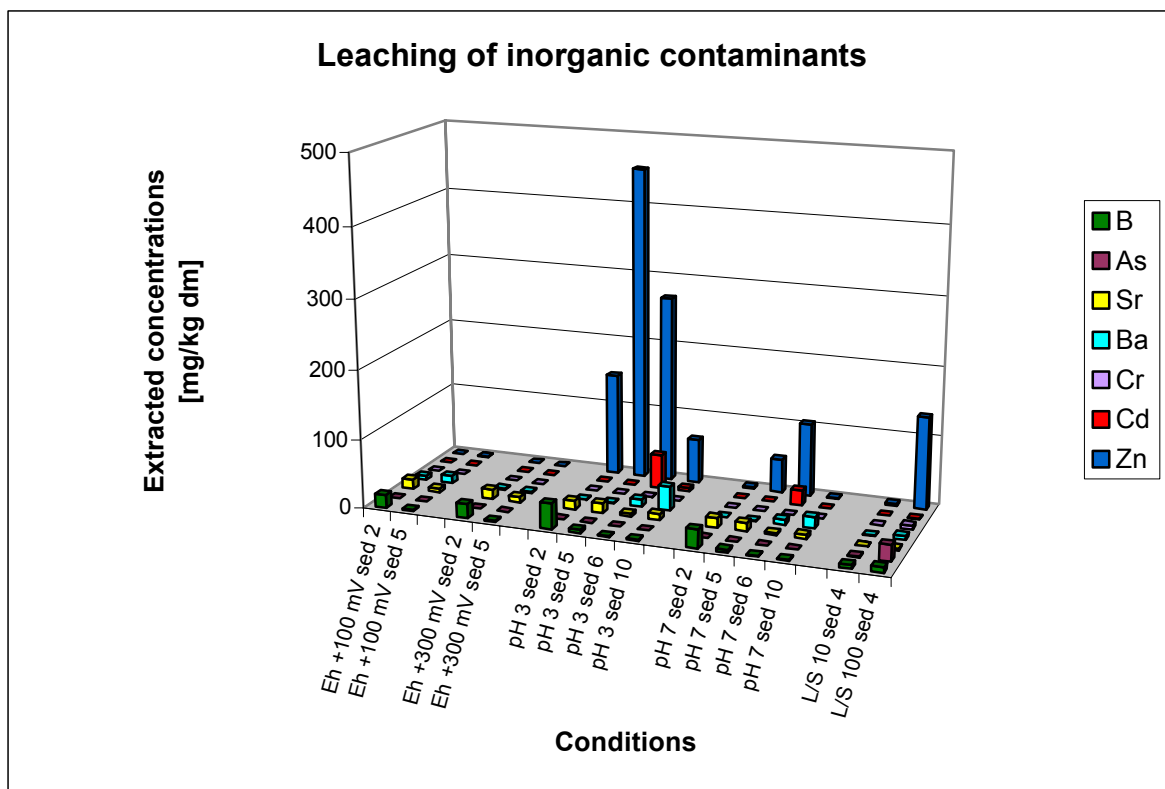


Figure 3.6 Leaching behavior of contaminants from sediments at different conditions after 21days

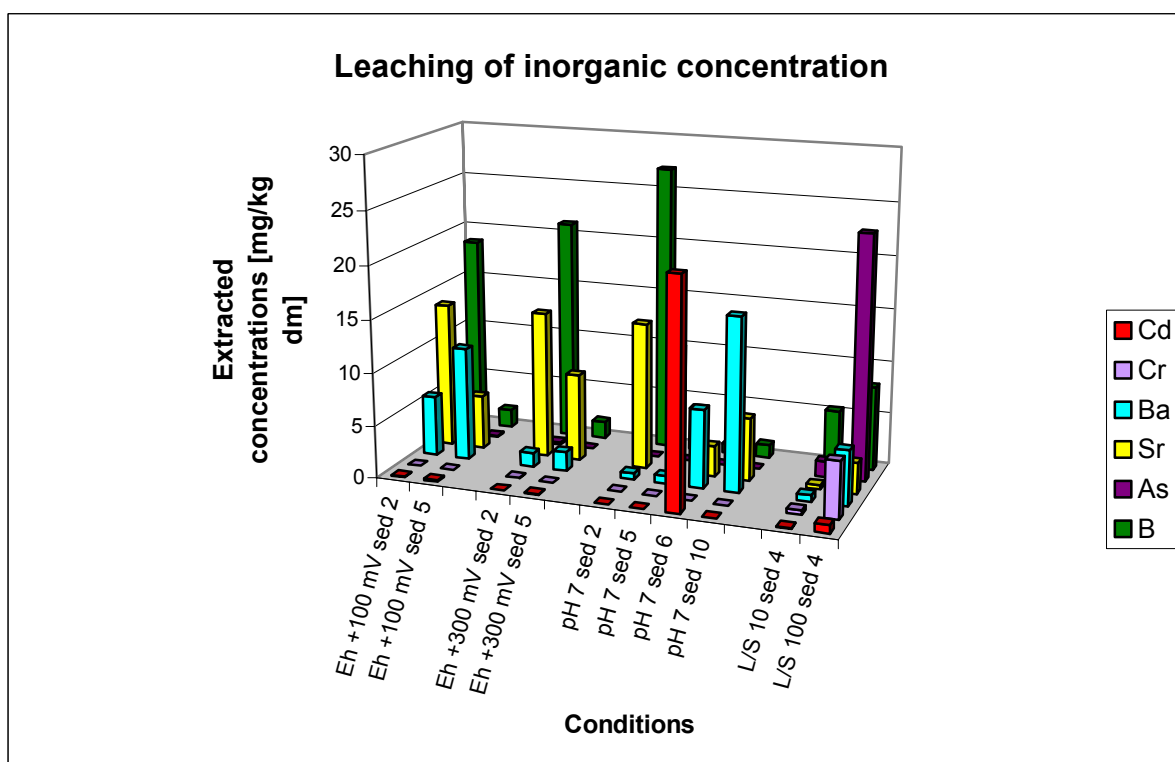


Figure 3.7 Leaching behavior of contaminants (without Zn) from sediments at different conditions after 21days

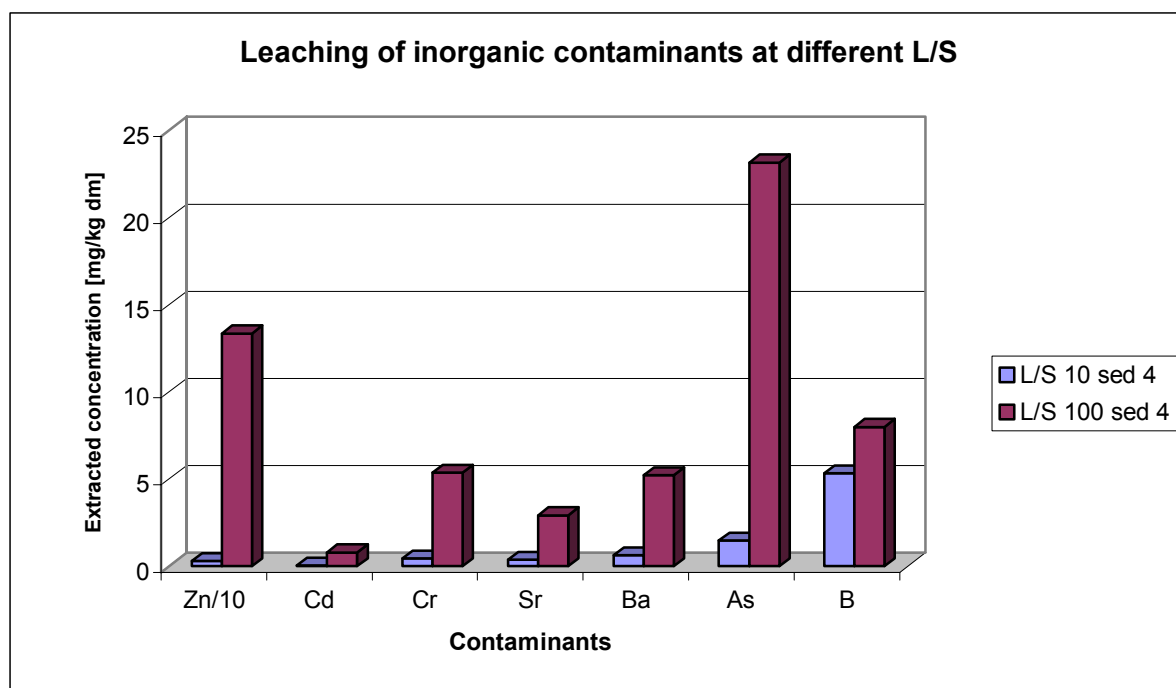


Figure 3.8 Extraction of contaminants at different L/S ratios

3.1.5 References

1. Calmano W., v.d Kammer F., Schwartz R.: Characterization of redox conditions in soils and sediments, EURO Summer School Trends in remediation of soils and sediments", 6 -11 June 2004
2. Lin J., Chen S.: The relationship between adsorption of heavy metals and organic matter in river sediments. *Environment International*, 24 (1998) 345-352.
3. Huang Suiliang et al.: The effects of concentrations of heavy metals in sediment and initially in water phase on their adsorption. *Acta Sci. Circ*, 15 910, 1995, pp 66 - 77
4. Zerbe, J., Sobczynski T., Siepak J. (1995). Metale ciezkie w osadach dennych, ich specjacja na drodze ekstrakcji sekwencyjnej. *Ekologia i technika* 3: 7-12
5. Santos Yabe M. J., de Oliveira E.: Heavy metals removal in industrial effluents by sequential adsorbent treatment. *Advances in Environmental Research* 7 (2003) 263 – 272
6. Simpson S.L., Apte S.C., Batley G.E.: Effect of short-term resuspension events on trace metal speciation in polluted anoxic sediments. *Environ Sci. Technol* 1998;32:620 – 5.
7. Korfali S. I., Davies B. E.: Speciation of metals in sediment and water in a river underlain by limestone: role of carbonate species for purification capacity of rivers. *Advances in Environmental Research* 8 (2004) 599 – 612
8. Dorzecze Odry – powodz 1997, Miedzynarodowa Komisja Ochrony Odry przed zanieczyszczeniem, Wroclaw 1999
9. Malina G. et al.: Contaminated sediment transport tool. Czestochowa 2003
10. Wolterbeek H. Th., Verburg T.G., van Meerten Th.G.: On the 1995 flooding of the rivers Meuse, Rhine and Waal in the Netherlands: metal concentrations in deposited river sediments. *Geoderma* 71 (1996) 143 –156

-
11. van der Sloot H. A, Comans R.: Pollutant leaching from contaminated soil and other materials. Guideline for Groundwater Risk Assessment at Contaminated Sites (GRACOS)
 12. Masscheleyn P., Delaune R., Patrick Jr. W.: Effect of Redox Potential and pH on Arsenic Speciation and Solubility in a Contaminated Soil. Environmental Science Technology. 25 (1991) 1414-1419
 13. van der Sloot H.A.: Developments in evaluating environmental impact from utilization of bulk inert wastes using laboratory leaching tests and field verification. Waste Management (1996) Vol 16. 65-81
 14. Tack F.M.G., Verloo M., Singh S.P.: Heavy metals in upland dredged sediment disposal sites: assessing their fate. Inaugural Conference SedNet European Research Sediment Network, Poster Abstract, Venice (Italy), 2002

3.2 Hydrophobic organic contaminant transport

Edited by T. Grotenhuis

M.P.J. Smit, J.T.C. Grotenhuis

*Department of Environmental Technology
Wageningen University and Research Centre, Wageningen,
The Netherlands*

3.2.1 Introduction

Long time industrial production in industrial area's like the Rotterdam/Antwerp harbor (NL/B), Katowice industrial area (PL) and the Bitterfeld area (Ger) affected their environment in a negative way. Direct emissions of waste products to the environmental compartments atmosphere, surface water and soil lead to major environmental problems.

Since the 1970's direct emissions to these different compartments is reduced due to a growing awareness of environmental problems. Application of gas and water treatment plants, spill control, and restrictions in the use of some chemicals lead to a rapid improvement of both air and surface water quality. Soil and sediment systems respond much slower to changes and need more time to improve their environmental quality. Moreover soils and sediments were polluted by numerous spills and landfills resulting in a diffuse pollution on a mega-site scale, which makes the active remediation of this compartment more difficult. Complete cleanup within an intermediate timeframe (25 years) is not feasible or may even be impossible for technical and economical reasons. Therefore, such megasites represent steady and long-term potential sources of regional contamination of groundwater, surface water and sediments. Until soils and sediments have acceptable environmental quality or when pollution is isolated from the relatively clean air or water surrounding it, recontamination from the diffuse polluted soil or sediment to the surrounding surface water, groundwater, and atmosphere is of major concern. Besides the threat of recontamination, direct risks can be involved for ecosystems and human health. This concept is made visible in Figure 3.9 for contaminated sediment.

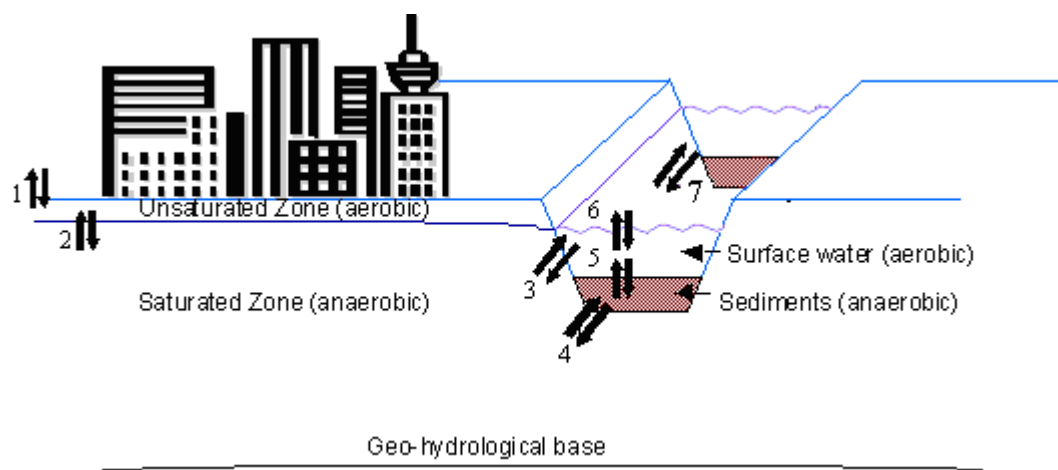


Figure 3.9 concept of contaminants transport between different compartments; flux numbers 2, 3, 4, 5, 6, and 7 are being assessed within the WELCOME project. Especially fluxes 4, 5, and 7 are studied in workpackage 9.

The fluxes drawn in Figure 3.9 are transfers of pollutants between different matrices except for flux 7. Flux 7 is the transport of surface water downstream and is including sediment particles and other suspended and dissolved materials. This flux is

described in deliverable 9.3 using the HEC-RAS model. As was described in deliverable 9.3 pollutants can be transported in several ways (see Figure 3.10).

1. transport of contaminants bound to sediment particles
2. transport of contaminants bound to dissolved organic matter
3. transport of freely dissolved contaminants

Fate and transport models (F&T models) are commonly used to describe the transport of sediment particles in a river system. Transport of pollutants is then roughly estimated by multiplying the sediment transport rate and the average concentration of pollutants in the sediment particles. To obtain insight in the effects of contaminated sediment to the surrounding environment a sediment transport tool was chosen in deliverable 9.3 (HEC-RAS). Within the WELCOME project, the HEC-RAS model is planned to include three modules (water level profiles for steady and unsteady flow and limit mobility of sediment transport). These three modules use basic geometric data for calculations of geometric and hydraulic relations. Key elements in modeling sediment transport are the shear stress

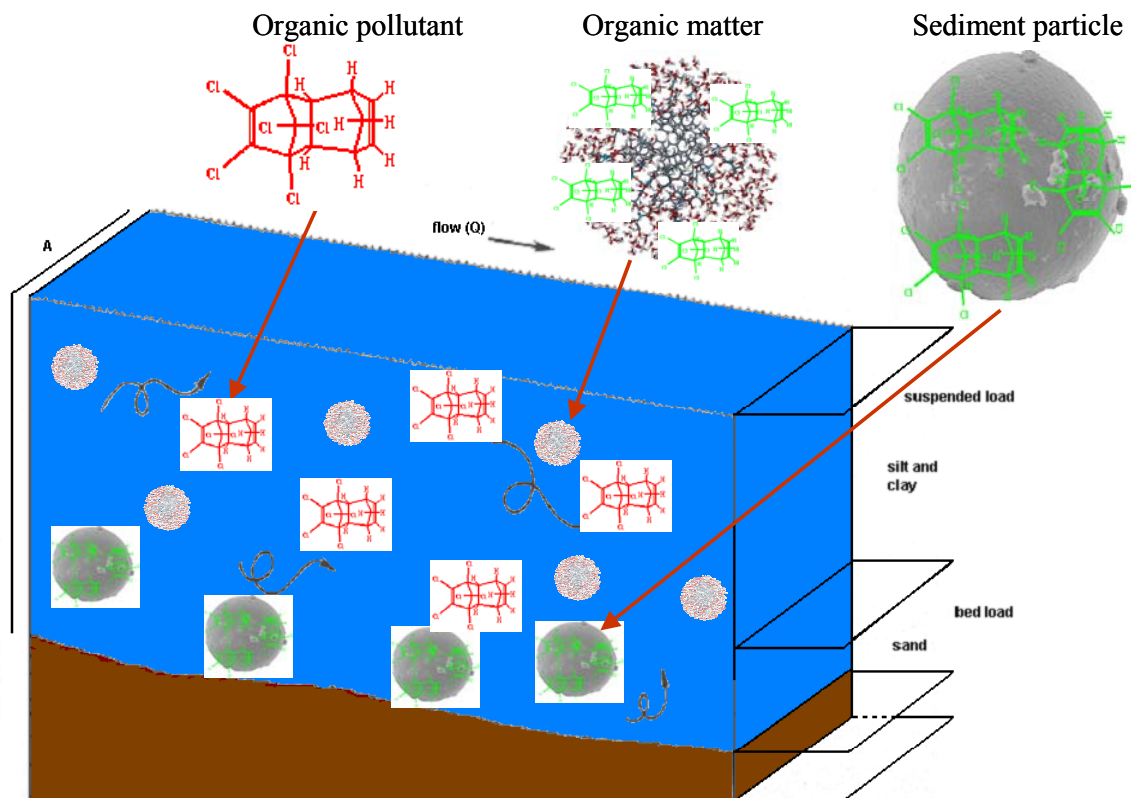


Figure 3.10: ways of transport of organic pollutants in a river system

and shear velocity. These shear forces are mainly depending on the radius (diameter) and specific gravity of the sediment particles, the flow rate of the water body, and the cross-section of the river. In deliverable 9.3 model calculations of sediment transport are demonstrated for the Stola-river. Transport of pollutants bound to dissolved organic matter or freely dissolved in the aqueous phase is however ignored.

For spreading (mobility) of the contaminants the total mass transport of these contaminants has to be considered. Depending on site-specific parameters (e.g.

hydraulic conditions, type of pollutant, sediment characteristics, etc) the major transport route has to be assessed. From a risk-based point of view (ecological and human) especially the freely dissolved contaminants are of major interest as these contaminants are readily available for uptake into the food chain.

Most pollutants (e.g. organic pollutants) are thought to have a high affinity for sorption to sediment. However at the interface of soil/sediments and the aqueous phase desorption of contaminants into the water system might be a threat for biota and human health. In deliverable 9.2 the HOC desorption method was described to assess the potential available fraction that can be desorbed from the sediment to the aqueous phase within a limited timeframe. In our laboratory we demonstrated that sediments contaminated with pesticides for more than 40 years show high contaminant availability (up to 80%). Transport of free dissolved pollutants might thus play an important role in overall transport of contaminants. Current limitations in the detection and analysis of (very) low concentrations of freely dissolved organic pollutants in water might have contributed to the possible underestimation of mass transport of freely dissolved contaminants and ecological as well as human risks related to these readily available pollutants. Although concentrations of pollutants might be very low the overall mass transport might be substantial as large volumes of water can be in contact with (polluted) sediments.

In this deliverable (9.4) a method will be presented in which the bioavailability approach is coupled with the hydraulic conditions.

3.2.2. Linking bioavailability approach to hydraulic conditions

The bioavailability approach presented in deliverable 9.2 is a refinement of traditional risk assessment. Most policies regarding soil and sediment contamination are still based on total concentration of contaminants, assuming that all contaminants are available for desorption to the water phase. Compared to the bucket in Figure 3.11A it is assumed that all contaminants present in the sediment (content of the bucket) will flow out of the sediment via the crane. In this deliverable 9.4 we focus on the transport rate of the contaminants from the sediment into the surface water. This process can be represented by the size of the crane in Figure 3.11. The goal of this study is to yield information about the risks of desorption to the water system as well as the time frame in which these risks occur.

3.2.2.1 Bioavailability approach

For hydrophobic contaminants it is assumed that desorption of contaminants to the water phase is limited to a minimal amount. Figure 3.11B schematically describes this situation. The crane is at the top of the bucket and the liquid (contaminants) cannot leave the system. Therefore there is no pollution of the surrounding environment.

However the behavior of hydrophobic pollutants is shown to be more complex: a part of the pollutants is capable to desorb rapidly to the water phase and a part of the pollutants desorbs slowly or not at all to the water phase. This situation is schematically presented in Figure 3.11C, where the crane is somewhere halfway the bucket. The liquid above the crane may flow out of the bucket to the surrounding environment, whereas the liquid below the crane will stay in the bucket. The liquid above the crane has the potential to flow out to the surrounding environment. This fraction of the contaminant is defined as 'potential available', whereas the fraction of contaminant that will be left in the sediment is defined as 'residual fraction' as well as 'non-available fraction'.

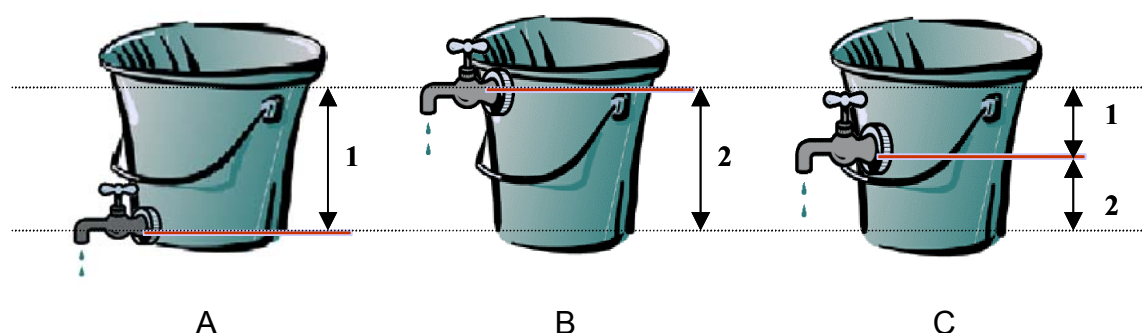


Figure 3.11 concept of potential bioavailability. The bucket presents the amount of pollutant in soil/sediment and the height of the crane represent the amount of pollutant available for desorption out of the soil/sediment. Arrow 1 is the available fraction and arrow 2 is the residual fraction

The potential availability describes the amount of contaminants that is able to enter the aqueous phase and move to possible receptors. Information on potential

availability is particularly needed to predict fate and transport of pollutants as it will determine the driving force of desorption to the water phase and therefore the timeframe in which sediments can act as a source of pollution. It also quantifies the residual concentration of contaminants in soil and sediment.

Actual availability is defined as the amount of contaminants freely dissolved in the aqueous phase. The concentration of freely dissolved contaminants is the sum of fluxes into the water system (desorption from sediment, transport of freely dissolved contaminant from upstream sources, etc.) and out of the water phase (sorption of contaminants to the sediment, downstream transport of contaminant, evaporation, etc).

The combination of both potential and actual bioavailability is needed to predict fate and transport of hydrophobic chemicals like POP and will be addressed in this chapter (Chapter 0.)

3.2.2.2 Hydraulic conditions

In the introduction a brief overview was given on the sediment transport model HEC/RAS as it was used for deliverable 9.3. Basic calculation procedures are based on the solution of a 1D energy equation. Input parameters are geometric data and flow regimes data. The driving force of water transport is the energy input (gradient, flow rate) minus energy losses (friction, contraction/expansion). Together with a momentum equation the waterlevel can be calculated. The calculated waterlevel in combination with geometric data then gives the flow rate and velocity. As reference for the transport rate of the different classes of sediment the flow velocity of the water is defined by Equation 1.

$$\text{Equation 1: } v_{\text{water}} = \frac{Q_{\text{water}}}{A_{\text{river}}} = \frac{Q_{\text{water}}}{h_{\text{water}} \cdot B} \quad [\text{m} \cdot \text{s}^{-1}]$$

In which the parameters are v_{water} flow velocity [$\text{m} \cdot \text{s}^{-1}$], Q_{water} flow rate [$\text{m}^3 \cdot \text{s}^{-1}$], A_{river} cross sectional area of the river, h_{water} waterlevel, B (average) width of the river below the water table.

The sediment transport module calculates the sediment transport based on the flow velocity and the input of sediment characteristics like specific gravity and particle size distribution (hydraulic radius). Three groups of sediment classes are defined (see also figure 2.):

1. bed load; large or high density particles that are transported by rolling, dregging, and/or saltation. Transport velocity of the bed load is generally much lower than the flow velocity of the water.
2. suspended load; part of the sediment is suspended for a long time due to turbulences of the water flow. Transport velocity of the suspended load equals to or is a bit smaller than the flow velocity of the water.
3. wash load; part of the suspended load consisting of small or low density particles. These particles are continuously suspended and are not being deposited on a riverbed. Transport velocity of the wash load equals the flow velocity of the water. This sediment class is often neglected in calculations of the total sediment transport.

The suspension of particles off all sediment classes starts when the shear velocity is close to the settling velocity of the particles. The settling velocity can be calculated using a variety of formulas for example Equation 2 (Rubey equation):

$$\text{Equation 2: } v_{s,p} = F_1 \cdot \sqrt{(s-1) \cdot g \cdot d_p} \quad [\text{m} \cdot \text{s}^{-1}]$$

Where:

$$\text{Equation 3: } F_1 = \sqrt{\frac{2}{3} + \frac{36v^2}{g \cdot d_p^3 \cdot (s-1)}} - \sqrt{\frac{36v^2}{g \cdot d_p^3 \cdot (s-1)}} \quad [-]$$

in these equations the following parameters are used: $v_{s,p}$ particle settling velocity [$\text{m} \cdot \text{s}^{-1}$], F_1 a constant [-], s particle specific gravity [-], g gravitational acceleration [$\text{m} \cdot \text{s}^{-2}$], d_p particle diameter [m], v kinematical viscosity coefficient [$\text{m}^2 \cdot \text{s}^{-1}$].

3.2.2.3 Linking bioavailability with hydraulics

Fate and transport models of hydrophobic organic pollutants in a river system usually focus on the transport of polluted sediments. This might lead to an underestimation of the total mass transport of these contaminants in the waterbody. Transport of free dissolved pollutants might play an important role in overall transport of contaminants. Current limitations in the detection and analysis of (very) low concentrations of freely dissolved organic pollutants in water might have contributed to the possible underestimation of mass transport of freely dissolved contaminants and ecological as well as human risks related to these readily available pollutants. Although concentrations of pollutants might be very low the overall mass transport might be substantial as large volumes of water can be in contact with (polluted) sediments.

With the bioavailability approach as was described in deliverable 9.2 the potential available contaminants can be measured, however to estimate and/or predict the freely dissolved concentration of pollutants additional information is required. The intense contact between sediment and water in the Tenax SPE method reduces the mass transfer resistance in the liquid phase ($1/k_b$) and leads to an overestimation of the total mass transfer at field conditions. Figure 3.12 shows the conceptual model of mass transport from a polluted sediment particle to the aqueous phase.

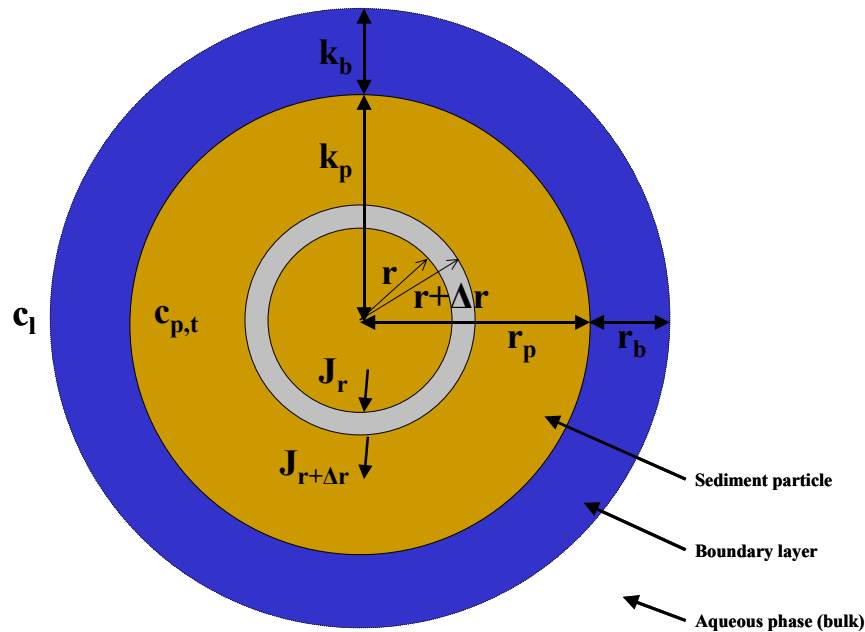


Figure 3.12: transfer of pollutants from sediment particle to aqueous phase (bulk); r_p and r_b are the radii of the particle and the boundary layer [m], k_b is the mass transfer rate in the boundary layer [$\text{m}\cdot\text{s}^{-1}$], $c_{p,t}$ and c_l are the potential available concentrations of target pollutant at position r and time t in the particle [$\text{kg}\cdot\text{m}^{-3}$] and in the aqueous phase [$\text{kg}\cdot\text{l}^{-1}$], and J_r is the mass flux at position r [$\text{kg}\cdot\text{m}^{-2}\cdot\text{s}^{-1}$].

To study the link of bioavailability and hydraulic conditions we choose the potential bioavailability approach as starting point to quantify the driving force of diffusion from the polluted sediment to the aqueous phase. We have selected a mechanistic mass transport model that can describe the kinetics of desorption and thus calculate the aqueous concentration.

In Figure 3.12 mass transfer occurs within the sediment (intra particle diffusion) and in the boundary layer. In this concept a non-stationary radial diffusion model describes mass transfer within the particle and the film theory describes the mass transfer in the boundary layer.

3.2.2.4 Mass transfer in the boundary layer

Mass transfer in the boundary layer is a function of turbulence in the aqueous phase. High turbulence leads to a decrease of the thickness of the boundary layer (r_b) and to an increase in mass transfer coefficient k_b . To calculate the mass transfer coefficient k_b in the boundary layer the dimensionless Sherwood number is used (Equation 4) which is a function of the dimensionless Reynolds number (flow conditions, Equation 5) and the dimensionless Schmidt number (mobility of a molecule in the liquid bulk and boundary layer, Equation 6):

$$\text{Equation 4: } Sh_p = \frac{k_b \cdot 2 \cdot r_p}{D_b} = C \cdot Re_p^m \cdot Sc^n \quad [-]$$

Where Sh_p is the dimensionless Sherwood number [-], k_b the mass transfer coefficient in the boundary layer [s^{-1}], r_p the radius of a particle p [m], D_b the diffusion constant in the boundary layer [$m^2 \cdot s^{-1}$], Re_p the dimensionless Reynolds number for particle p [-], Sc the dimensionless Schmidt number [-], and C , m , and n are constants [-].

The dimensionless Reynolds number for individual particles is calculated using Equation 5:

$$\text{Equation 5: } Re = \frac{(\rho_p - \rho_{\text{water}}) \cdot 2 \cdot r_p}{\eta_{\text{water}}} \cdot v_{s,p} \quad [-]$$

Where ρ_p and ρ_{water} are the density of the sediment particle and the water phase [$kg \cdot m^{-3}$], η_{water} is the dynamic viscosity of the water phase [$kg \cdot m^{-1} \cdot s^{-1}$], and $v_{s,p}$ is the relative velocity of the particle within the aqueous phase [$m \cdot s^{-1}$]. Reynolds number can be interpreted as a value of turbulence. The dimensionless Schmidt number is calculated using Equation 6:

$$\text{Equation 6: } Sc = \frac{\eta_{\text{water}}}{\rho_{\text{water}} \cdot D_b} \quad [-]$$

The Schmidt number can be interpreted as the ratio of momentum and mass diffusivity of molecules. The Schmidt number is only valid for laminar flow conditions (e.g. $Re < 1$). For turbulent flow conditions Schmidt number is ~ 0.7 .

3.2.2.5 Mass transfer within a sediment particle

Experiments in our laboratory demonstrated the validity of the of non-stationary radial diffusion model. The basic equations of this model are:

$$\text{Equation 7: } 4\pi r^2 \Delta r \frac{\partial C}{\partial t} = 4\pi r^2 J_r - 4\pi (r + \Delta r)^2 J_{r+\Delta r} \quad \text{mass balance for particle rind } \Delta r$$

$$\text{Equation 8: } \frac{\partial C}{\partial t} = \frac{D}{r^2} \frac{\partial}{\partial r} r^2 \frac{\partial C}{\partial r} \quad \text{Fick's law for radial diffusion}$$

In these equations r is the distance between the center of the sediment particle to position r [m], Δr is the thickness of a layer within the particle [m], J_r and $J_{r+\Delta r}$ are the mass fluxes at a distance r and $r+\Delta r$ from the center [$kg \cdot m^{-2} \cdot s^{-1}$], C is the concentration of target compound within the particle [$kg \cdot m^{-3}$], t is the time [s], and D is the effective diffusion constant [$m^2 \cdot s^{-1}$].

The solution of Equation 7 using Equation 8 and the appropriate boundary conditions will then be Equation 9:

Equation 9:
$$\frac{C - C_0}{C_1 - C_0} = 1 + \frac{2r_p}{\pi r} \sum_{k=1}^{\infty} \left(\frac{(-1)^k}{k} \sin \left(k\pi \frac{r}{r_p} \right) e^{-k^2 \pi^2 \frac{Dt}{r_p^2}} \right) \quad [\text{kg} \cdot \text{l}^{-1}]$$

In Equation 9 C is the average concentration of target compound in the particle at any time $[\text{kg} \cdot \text{m}^{-3}]$, C_0 is the initial concentration in the particle, and C_1 is the concentration at the particle/water interface.

From equations 4 – 9 it is clear that in a river system two processes play an important role in the mass transfer of pollutants from (or to) a sediment particle: the driving force of diffusion ($c_p - c_l$) and the mass transfer rate constants. The mass transfer rate constant (k_b) in the boundary layer is directly influenced by the turbulence (Re) and the mass transfer rate within the particle is influenced by the characteristics of pollutant and sediment. In our laboratory we made a reactor in which the effect of driving force and turbulence can be separated. By separating the driving force and turbulence the mass transfer as a function of hydraulic parameters can be analyzed. Finally this will lead to a prediction of the transfer of contaminants from the sediment to the surface water depending on the flow conditions. For example the effect of a high river tide on the release of contaminants to the surface water can be calculated.

3.2.3 Linking bioavailability and hydraulics: laboratory experiment

Based on the theoretical background as was summarized in chapter 0 a reactor was developed in which the mass transfer as a function of hydraulic parameters can be analyzed. The schematic set-up of the equipment is presented in Figure 3.13.

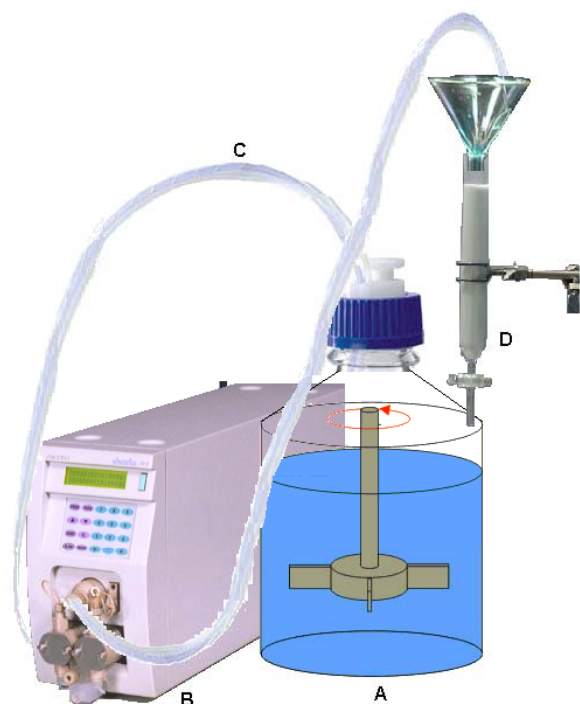


Figure 3.13: schematic overview of experimental setup to analyze mass transfer as function of hydraulic parameters. In this picture A is the standard stirred reactor, B is an inert HPLC pump, C is inert Teflon tubing, and D is a packed column with Tenax®-TA

With the experimental setup as shown in Figure 3.13 the stirring rate of the defined standard stirrer can be adjusted as well as the dilution rate (HPLC pump). All materials used are expected to be inert for the target compounds (dieldrin and endrin). In this way flow conditions in any part of a river can be simulated. As concentrations of dieldrin and endrin in the aqueous phase are very low, the water is lead over a packed column filled with Tenax® to concentrate the target compounds. The effluent of the Tenax® column is free of target compounds. The release of contaminants from the sediment to the water with time is measured by the adsorption to Tenax®. After a certain period of time the contaminated Tenax® is extracted and analyzed and replaced with fresh Tenax®.

A desorption experiment was done using sediments from the Rotterdam harbor area. The sediments contained dieldrin and endrin. For clarity reasons only results of endrin are presented in Figure 3.14 and Figure 3.15. In Figure 3.14 the removal of endrin from a sediment fraction (d_p 32 – 125 μm) with time is presented. In this experiment 400 ml of slurry ($L/S = 10$) was added in the stirred reactor (stir-rate 550 RPM, $Re \sim 7500$). Sodium azide was added to prevent biological processes. The HPLC pump was set to a flow rate of $\sim 2 \text{ ml} \cdot \text{min}^{-1}$ resulting in a hydraulic retention time of $\sim 3 \text{ h}$. As the flowrate of the HPLC pump is $\sim 2 \text{ ml} \cdot \text{min}^{-1}$ the horizontal axis is also represented as the amount of aqueous solution that passed the Tenax® column and sediment. After 200 hours at turbulent flow conditions ($Re \sim 7500$) a residual fraction of 0.6 of the initial amount of endrin was still present in the sediment. This residual fraction of 0.6 was also found experimentally by the determination of the potential available fraction with Tenax® SPE (Figure 3.15). This experiment is a first indication that sediment particles under less severe conditions than Tenax® SPE will

indeed tend to a residual fraction of contaminants in the sediment equal to the Tenax[®] SPE method.

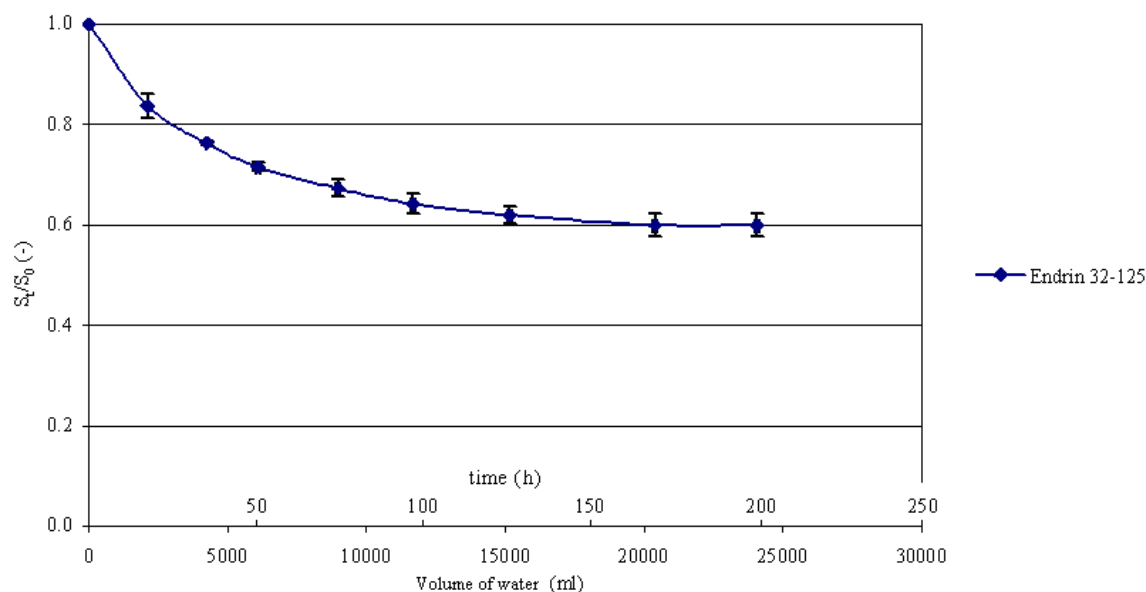


Figure 3.14: fraction of endrin remaining in the sediment particles as function of the amount of water pumped through the Tenax[®] packed column. Error bars are the std.dev. of duplicate samples.

The results presented in Figure 3.14 correspond very well with the results of the Tenax[®] SPE method presented in Figure 3.15.

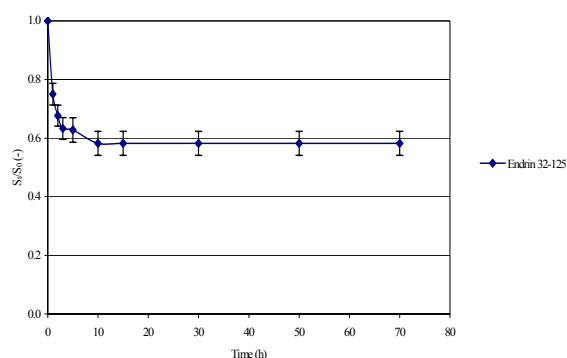


Figure 3.15: fraction of endrin remaining in the sediment particles as function of time in a Tenax[®] SPE desorption experiment. Error bars are the std.dev. of triplicate samples.

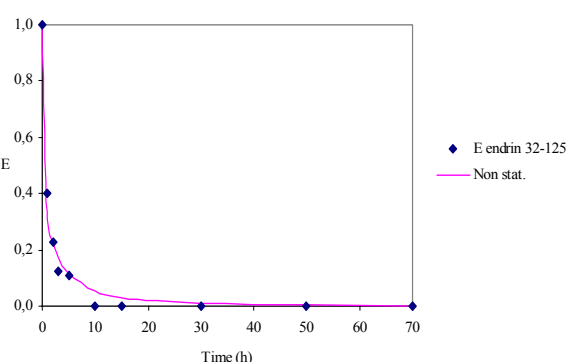


Figure 3.16: results of the non-stationary radial diffusion model (solid line) and measures data points (diamonds) using the available fraction of endrin against time. ($E=S_t/S_0$)

The experimental data of the Tenax[®] SPE method is modeled using the non stationary diffusion model described in paragraph 0 and presented in Figure 3.16. The experimental data (diamonds) and the calculated residual concentration (solid line) show a good agreement when using the bioavailable fraction of the contaminant.

A control experiment was carried out using an aqueous solution of endrin to assess the recovery of endrin in this setup (Figure 3.17). The HPLC pump was set to a flow rate of $\sim 3.6 \text{ ml} \cdot \text{min}^{-1}$ resulting in a hydraulic retention time of $\sim 1.5 \text{ h}$. As the flowrate

of the HPLC pump is $\sim 3.6 \text{ ml} \cdot \text{min}^{-1}$ the horizontal axis also gives an indication of the amount of aqueous solution that passed the Tenax[®] column and sediment. Differences of data points at the x-axis are the result of slightly different flow rates (3.2 and $4.1 \text{ ml} \cdot \text{min}^{-1}$). The time axis must be seen as indication rather than a real value, data in the graph was drawn against the volume of water that passed the Tenax[®].

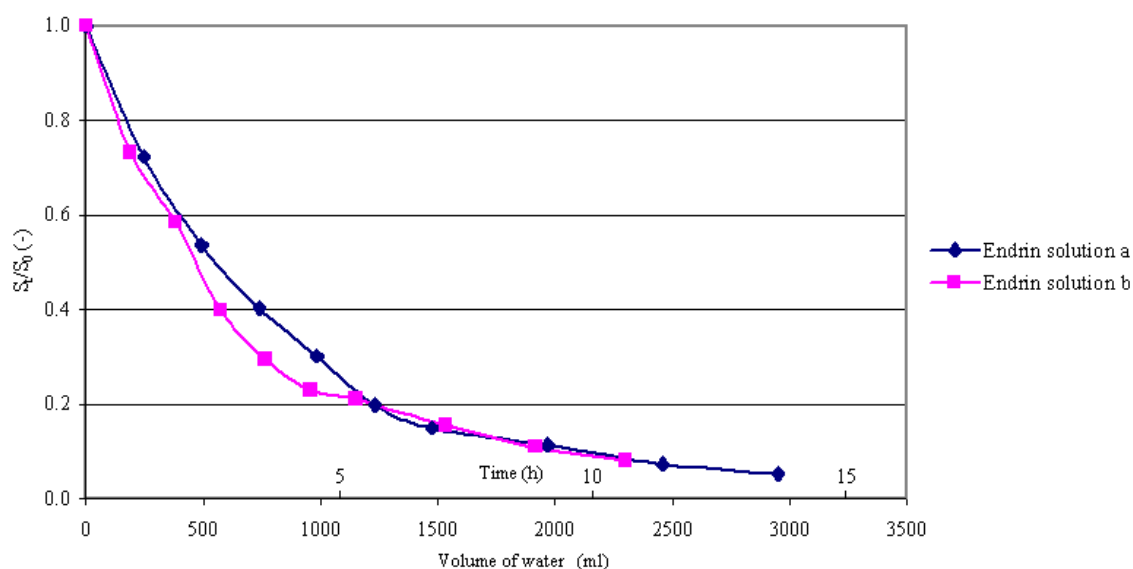


Figure 3.17: Results of a control experiment. Fraction of endrin remaining in the aqueous phase as function of the amount of water pumped through the Tenax[®] packed column.

The results in Figure 3.17 show that ad/absorption of target compounds to the reactor materials is neglectable. The removal of dissolved endrin matches very well with the dissolution model of a ideal mixed tank reactor. Therefore it can be concluded that adsorption of endrin to the reactor surfaces or losses due to evaporation or leakages will not disturb the results found in Figure 3.14. Furthermore the indication of time in the control experiment shows that recycling of the water is not the limiting factor in desorption from sediment. The time to reduce the concentration in the control experiment to low concentrations (e.g. $S_t/S_0 = 0.1$) is small compared to the time of the desorption experiment. Mass transfer from the sediment to the aqueous phase is apparently not limited because of an increase of the concentration in the bulk liquid C_l .

The link between the bioavailability approach and hydraulic conditions seem to be very promising. More experiments using different stir-rates and dilution rates as well as using soils and sediments with different contaminants are needed to test the validity and robustness of this setup.

3.2.4 Relevance of the availability-tool to the IMS

In an Integrated Management System (IMS) site-specific information on availability, mobility, and degradability (NA potential) of pollutants is of major importance. In the WELCOME project several tools are being developed to help megasite managers protect surface waters in a cost effective way. These tools can roughly be subdivided into management, communication, and technological tools, including analytical-chemistry and transport-models.

From a management perspective, knowledge about sediment transport itself (workpackage 9.3) as well as the time when a contaminant will arrive at the receptor (e.g. aquifer) and what the impact of the contaminant on a receptor will be is important. Prediction of time and impact of contamination of the receptor requires information about the pollution itself, possible receptors (e.g. surface water), and the mass-transport between pollution and receptors. Within this framework, mass transport models are important tools. These models require the input of correct data to give a solid prediction. Development of technological tools within the WELCOME project is needed to achieve a sound scientific basis for correct input in these mass transport models. The availability-tool (workpackage 9.2) is one of the technological tools and scientific research focuses on actual and potential availability of pollutants in soil and sediment systems. Both actual and potential availability are key-issues for modeling contaminant transport as is described in this workpackage of the WELCOME project.

When fate and transport models are able to describe the behavior of contaminants in a river basin they can be used to support management decisions at megasites. In the WELCOME project three types of megasites can be recognized depending on their location in the river basin. We observe an upstream megasite (Katowice (PL)), a mega site in the middle of the river basin (Bitterfeld (D)) and a megasite at the delta area of a river basin (Rotterdam/Antwerp (NL/B)).

As stated in the previous paragraph the development of technological tools within the WELCOME project is needed to achieve a sound scientific basis for correct input in mass transport models. Potential and actual availability of pollutants in soil and sediment systems are key-issues to predict time and impact of pollution of receptors.

In the SEDINA tool a first indication is given whether a sediment is functioning as a sink or a source of pollutants to the surface water. By applying deliverable 9.2 in combination of deliverable 9.3 and 9.4 insight can be obtained in the potential and actual risks as well as the effect of mitigative measures at a specific site.

3.2.5 List of publications

1. Grotenhuis Tim, Malina Grzegorz, Satijn Bert, Smit Martijn, Popena Agnieszka (2003): Surface water as receptor for POP and heavy metals from sediments. In: 8th International Conference on Contaminated Soil (ConSoil). May 12 – 16. Gent, Belgium.
2. Grotenhuis T., L. Diels, M. Ruhland, G. Malina, H. Rijnaarts (2003): WELCOME, an EU-project concerning the development of an Integrated Management System for soil, sediment and groundwater at Megasites: Presentation of a bioavailability method of organic pollutants in sediment and soil. Presentation at SedNet working group 2: CONTAMINANT BEHAVIOUR AND FATE, 3-5 April, 2003, Berlin, Germany, 2nd WORKSHOP: Impact, bioavailability and assessment of pollutants in sediments and dredged materials under extreme hydrological conditions.
3. Hendriks, Janneke (2004): Possible application of Solid Phase Micro Extraction for determination of pesticide availability in sediment, MSc thesis, Wageningen University, Wageningen, the Netherlands.
4. Pacak, Ania (2003): Bioavailability of drins in soil and sediment, MSc thesis, Technical University Czestochowa, Czestochowa, Poland.
5. Smit M.P.J., Steinbusch K. and Grotenhuis J.T.C. (2003): Fate of drins in sediment with anaerobic sludge. In: Contaminated Sediments. September 30 – October 3, 2003. Venice, Italy.
6. Smit M.P.J. and Grotenhuis J.T.C. (2004): Potential bioavailability of pesticides in soil and sediment. In: Soil and Water. June 2 – 3, 2004, Zeist, the Netherlands.
7. Steinbusch, Kirsten (2003): Bioavailability and biodegradation of drins in soil and sediment, MSc thesis, Wageningen University, Wageningen, the Netherlands.

4. Relevance sediment and contaminant transport to IMS

With the Integrated Management System (IMS) of the WELCOME project a general procedure is described how to act when dealing with a contaminated megasite. As many megasites are located in a delta area or along the river course, they all have to deal with the role of polluted sediment related to the quality of surface water that is regarded as one of the major receptors for contaminants in the environment. The study performed within deliverable 9.4 interacts mainly with the IMS sections related to 'Risk Management' and to the section 'Risk Management Scenarios'.

The step 'Risk Management' starts with the section 'Characterization' of megasites. To perform an initial assessment of the risks caused by sediments in a megasite the so-called SEDINA tool can be used. By comparison of the total concentrations of pollutants upstream, at the megasite and downstream of the megasite area, the role of the megasite as a sink or a source of contaminants can be defined (see the IMS; Tools; SEDINA). When the megasite functions as the sink of contaminants no specific measures related to the sediments have to be undertaken, although monitoring of the surface water and sediments quality is recommended. However, if the output of the SEDINA tool reflects that the megasite may function or functions as a source of contaminants further investigations are necessary as described in the section 'Modeling' of the step 'Risk Management'.

In the section 'Modeling' several details can be found upon fate and transport modeling. The amount of contaminated sediment that can be transported to or from the megasite can be calculated, as it is performed for the Widawa case (D9.4 Chapter 2.1). This is based upon the selection of a proper sediment transport models as described in D9.3.

Also the erosion by water may affect the risk management as such. The ESEM model used for the description of the water erosion at the Tarnowskie Góry megasite in D9.4 (Chapter 2.2) is an illustration of this phenomenon.

Except the flux of contaminated particles into and from the megasite, information is necessary about the transport of contaminants (heavy metals, HOC) within the sediments and from the sediments to the water system.

In WP9 the remobilization of heavy metals from sediments was studied in D9.4 (Chapter 3.1). Remobilization occurred when pH was decreased, and also remobilization was found when the liquid/solid ratio was increased. This last finding indicates that during flooding conditions, when the flow of water is increased, remobilization and, therefore, an increase of risk for heavy metal transport to the surface water as a receptor may occur.

Still most often risk assessment is based upon total concentrations of contaminants, which may lead to overestimation of risks.

In several scientific disciplines like ecotoxicology, biology, as well as in biodegradation studies in microbiology and environmental technology, it was shown in the last ten years that only part of the contaminants cause risk and only the risk-

causing fractions of organic contaminants are bioavailable and, in consequence can be biodegraded.

It is stated that only part of the contaminants is bioavailable. Only the bioavailable fractions of contaminants have to be taken in account for risk assessment.

Therefore, in future it is expected that legislation will be based on 'real' risks of contaminants in the field. For determination of these risks, the sound based scientific methods have to be developed. Several research groups work on development of such bioavailability tools for heavy metals, as well as HOC.

In D9.2 a method is presented, by which the availability of HOC can be determined at specific sites. In this specific case, a tool for persistent organic pollutants (POP) is presented. This group of contaminants is of interest as they may pose more risks compared to other HOC as these compounds are not biodegradable.

All bioavailability methods based upon physical/chemical techniques show that much less than the total concentrations of the pollutants can be desorbed. Therefore leading to less risk compared to the use of total concentrations of HOC. For example about 50 to 60 % of the HOC contaminants can be desorbed, and so the risks of these contaminants are reduced compared to risks of total concentrations. Therefore the application of bioavailability methods will lead to an improvement of the risk assessment and subsequently to more cost effective remediations.

In D9.4 an attempt is made to link the bioavailability method developed in D9.2 to the hydrological conditions in the field (D9.4 Chapter 3.2). As the HOC desorption method described in D9.2 is performed under optimal desorption conditions in the lab this may lead to an overestimation of the mobility of the bioavailable fractions in the field. The proposed set up in D9.4 is intended to improve the prediction of bioavailability at field conditions, which may be lower than determined with the HOC desorption method (D9.2).

The determination of the bioavailability is included in the section 'Tools' at 'Support Natural Attenuation' as a Bioavailability meter. This tool, as well as the results developed in D9.4 (Chapter 3.2), can be used to build 'basic scenarios' in the step 'Risk Management Scenarios' of the IMS.

5. Appendix 1. Heavy metal and inorganic contaminant transport

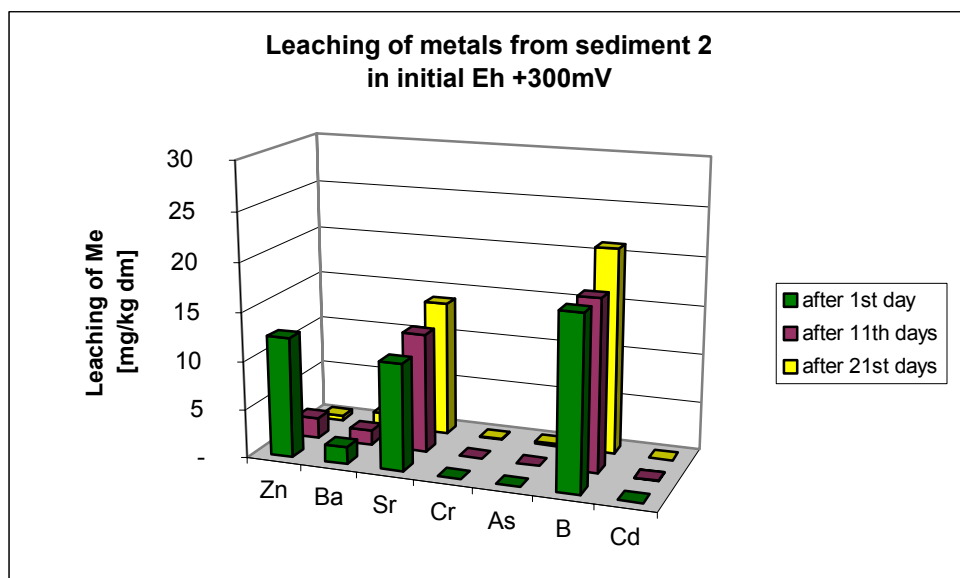


Figure 1. Leaching of metals from sediment 2 in exp at different Eh initial

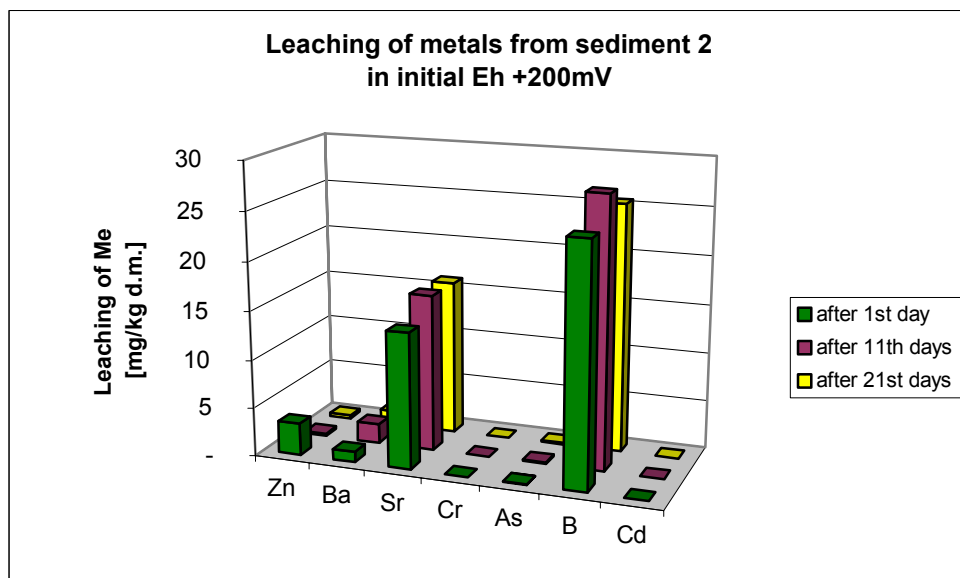


Figure 2. Leaching of metals from sediment 2 in exp at different Eh initial.

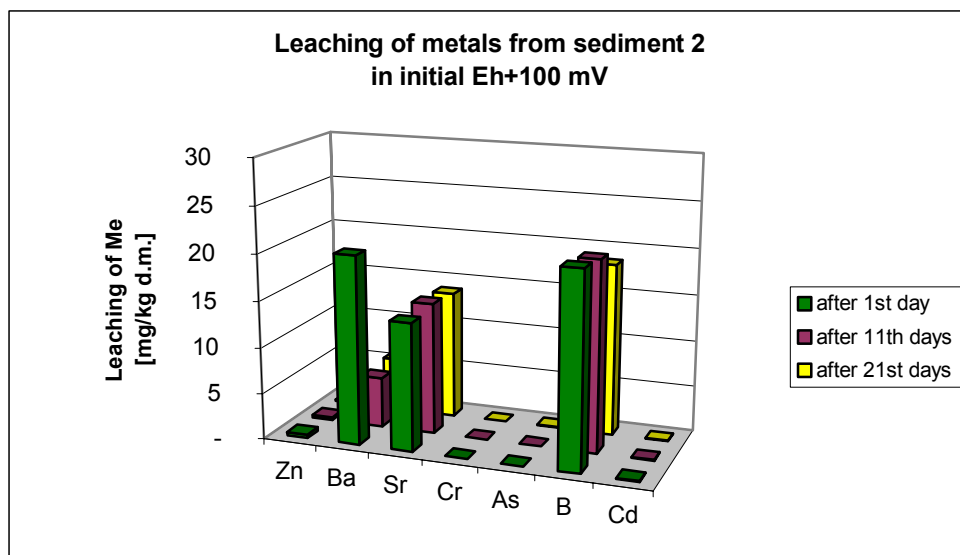


Figure 3. Leaching of metals from sediment 2 in exp at different Eh initial

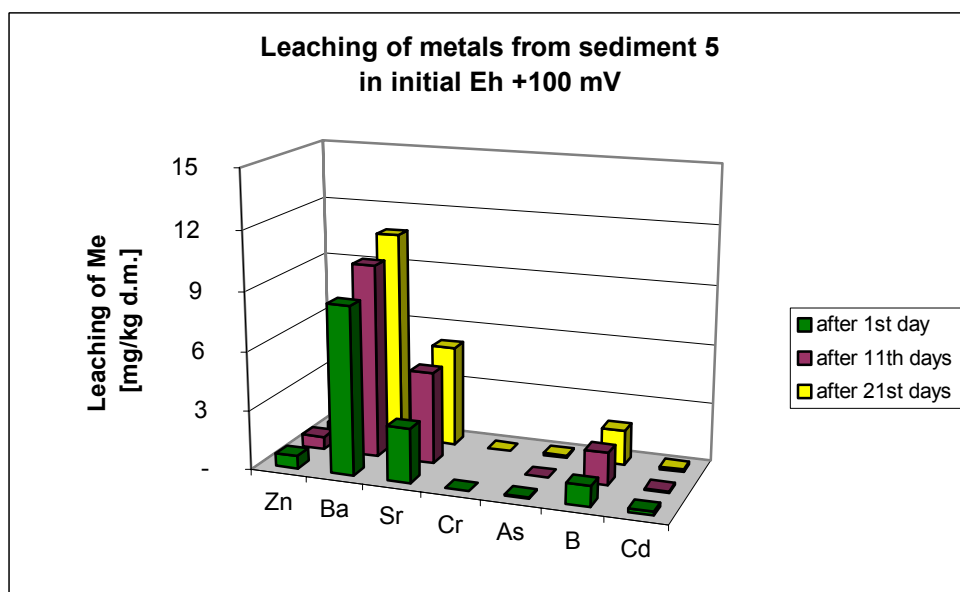


Figure 4. Leaching of metals from sediment 5 in exp at different Eh initial

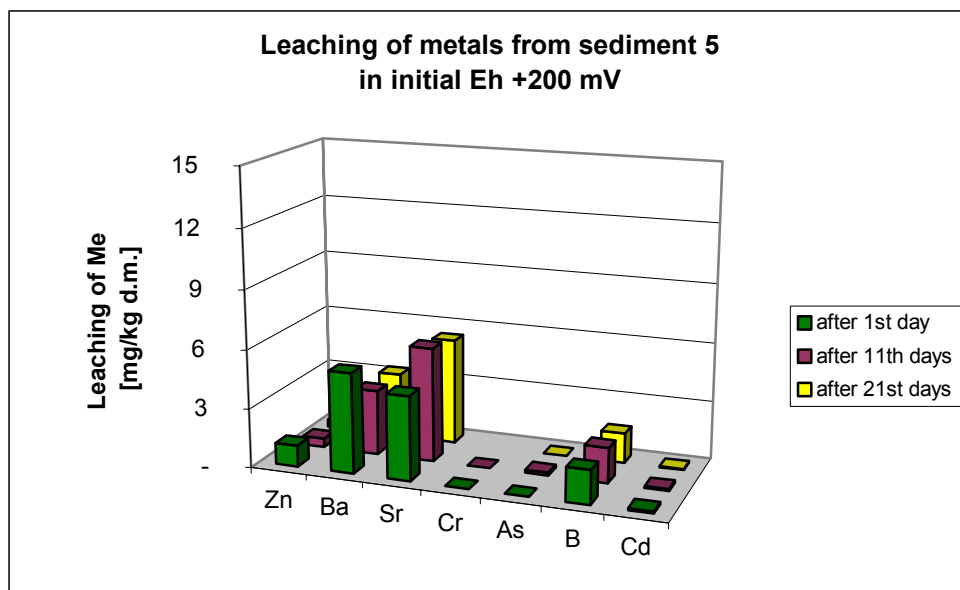


Figure 5. Leaching of metals from sediment 5 in exp at different Eh initial

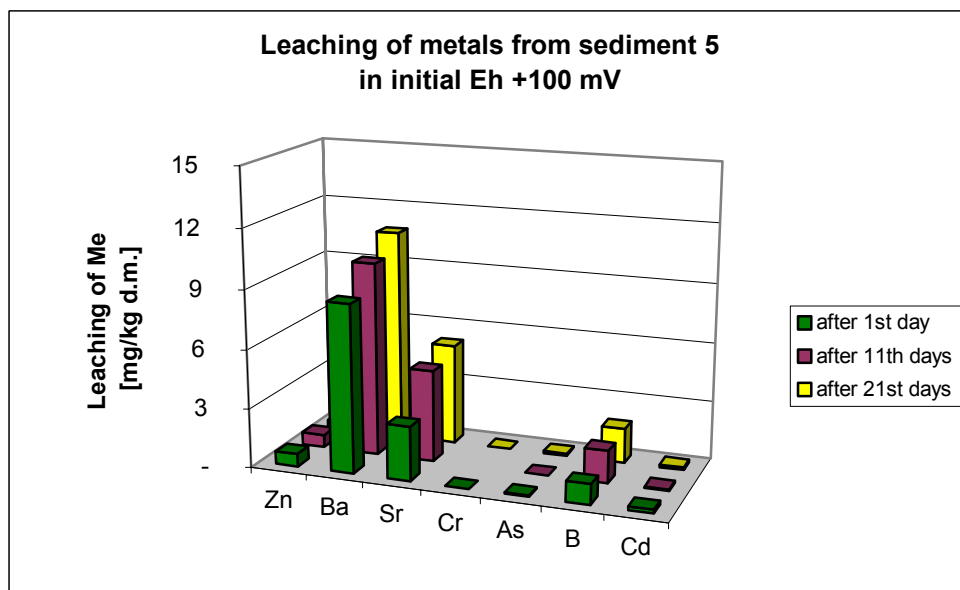


Figure 6. Leaching of metals from sediment 5 in exp at different Eh initial

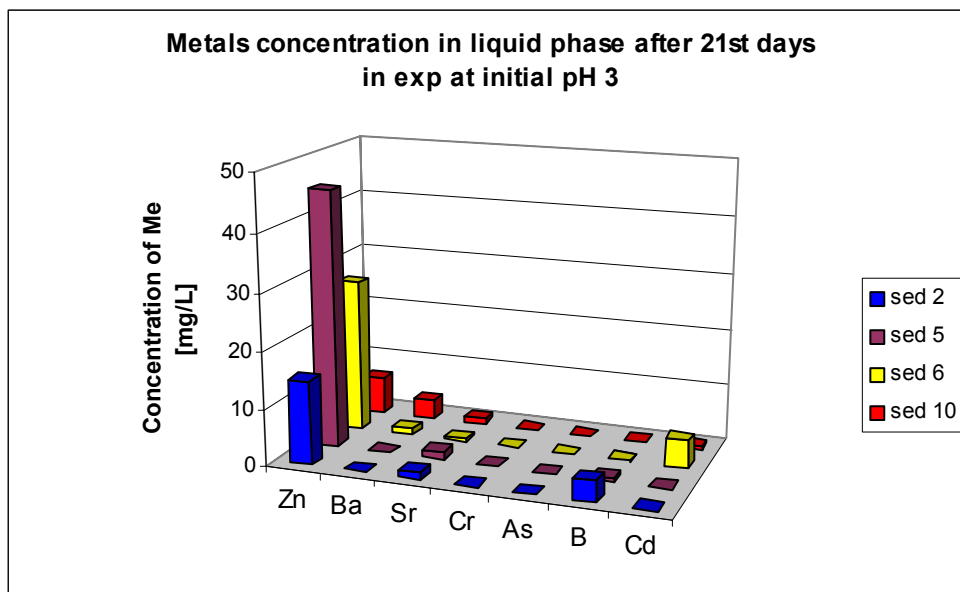


Figure 7. Metals concentration in liquid phase after 21st days in exp at initial pH 3

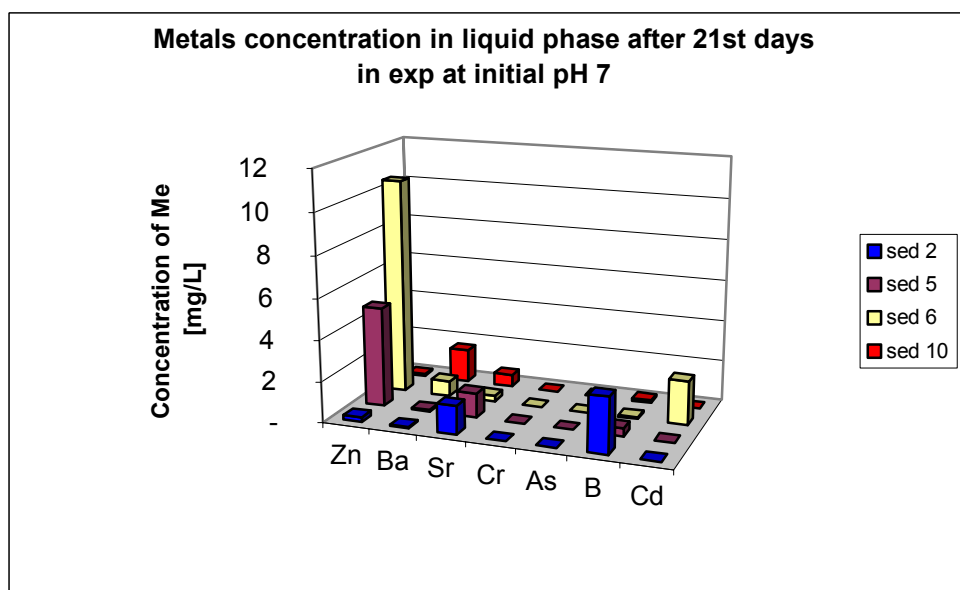


Figure 8. Metals concentration in liquid phase after 21st days in exp at initial pH 7

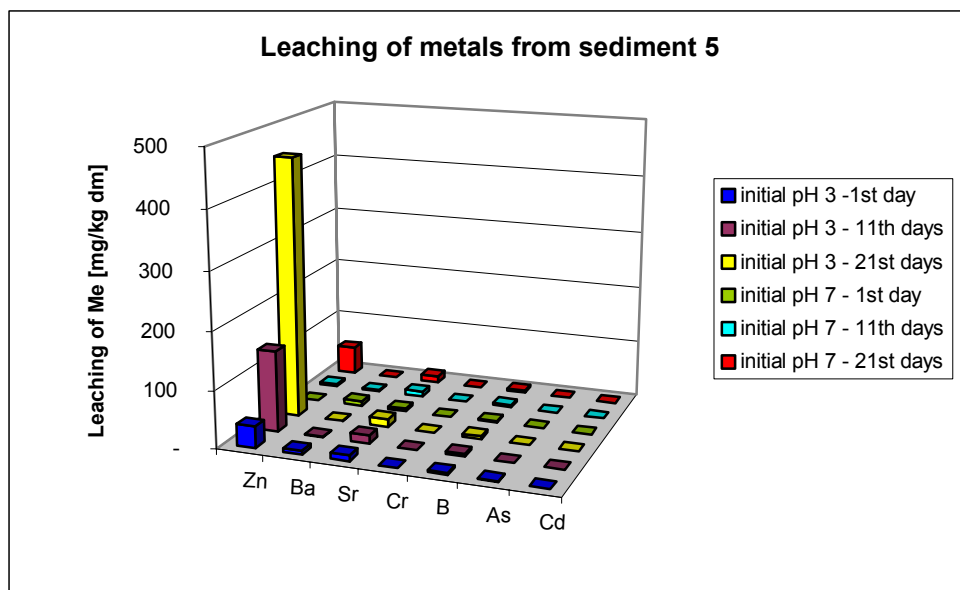


Figure 9. Leaching of metals from sediment 5 in exp at different pH initial

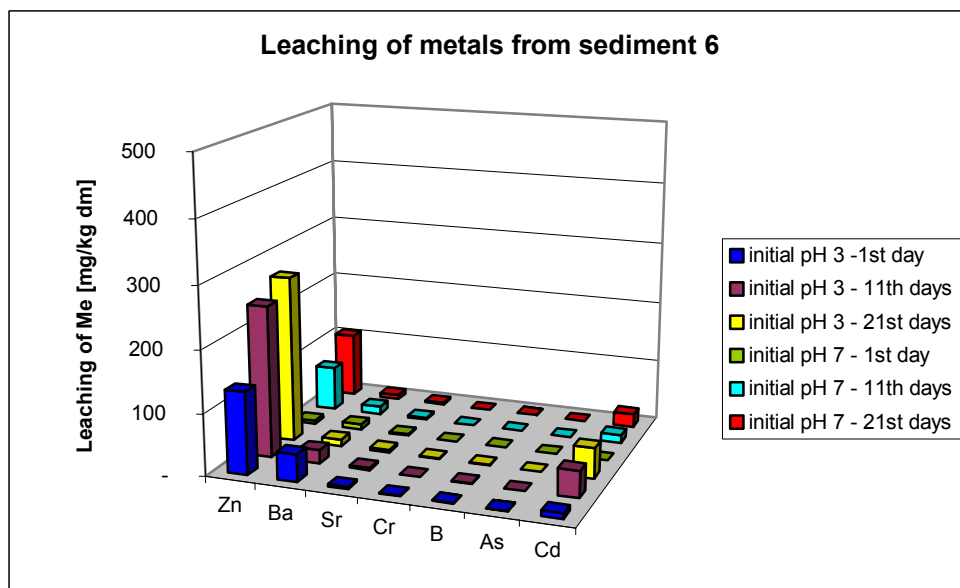


Figure 10. Leaching of metals from sediment 6 in exp at different pH initial

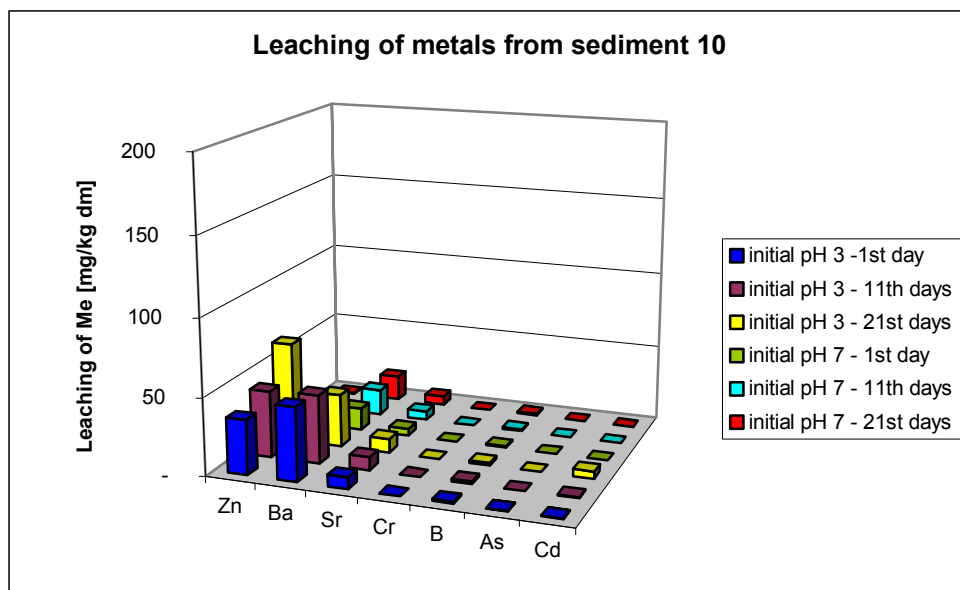


Figure 11. Leaching of metals from sediment 10 in exp at different pH initial

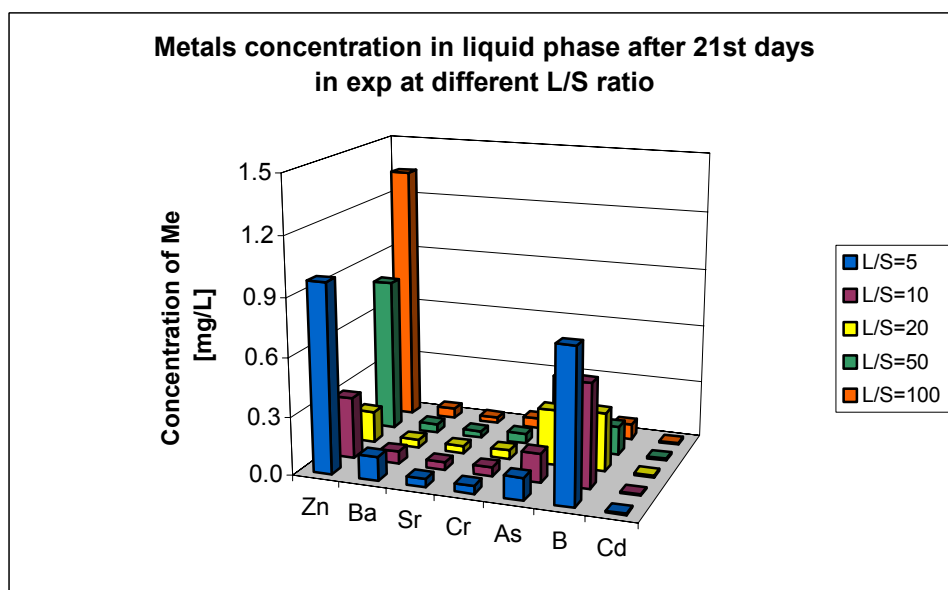


Figure 12. Metals concentration in liquid phase in sediment 4 at different L/S ratio

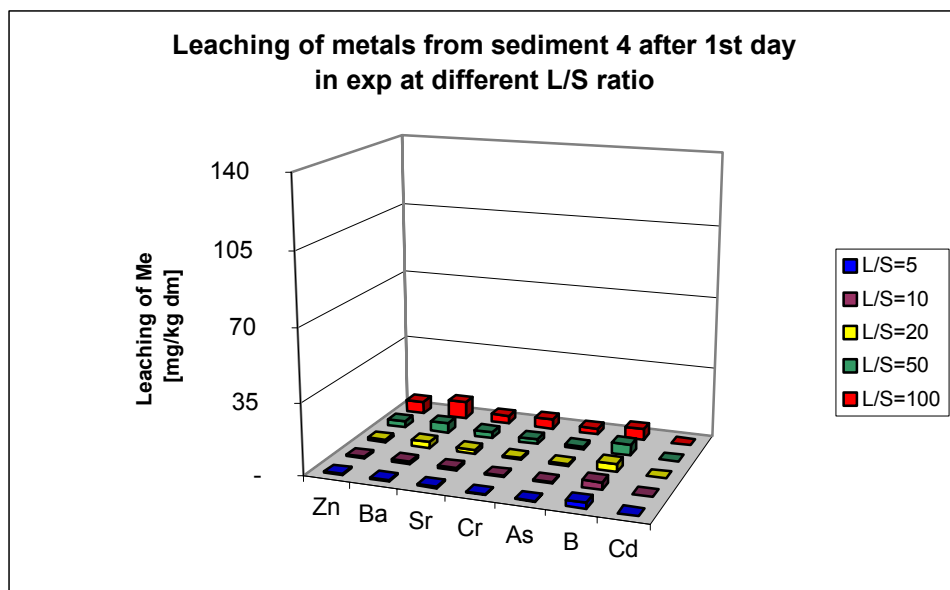


Figure 13. Leaching of metals from sediment 4 in exp at different L/S ratio

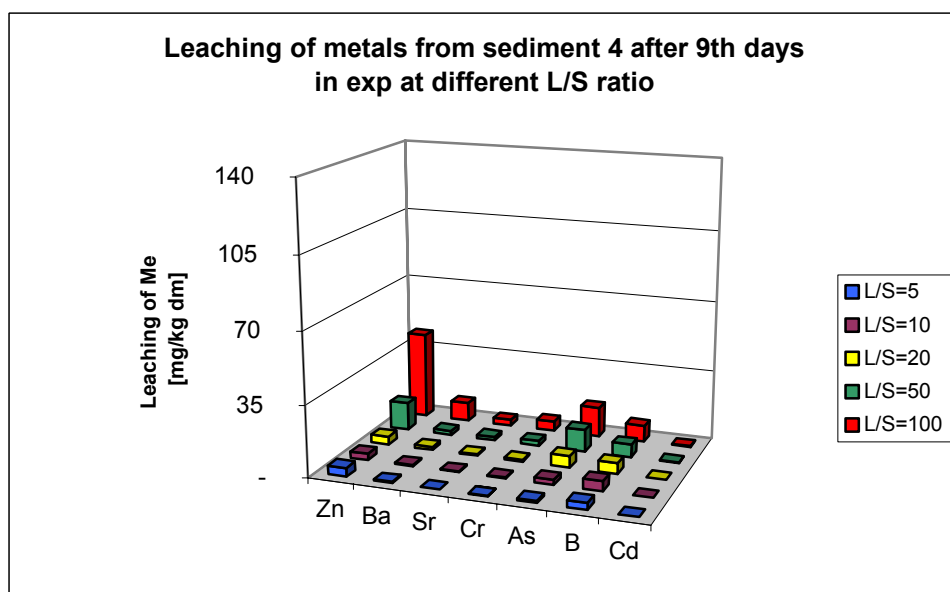


Figure 14. Leaching of metals from sediment 4 in exp at different L/S ratio

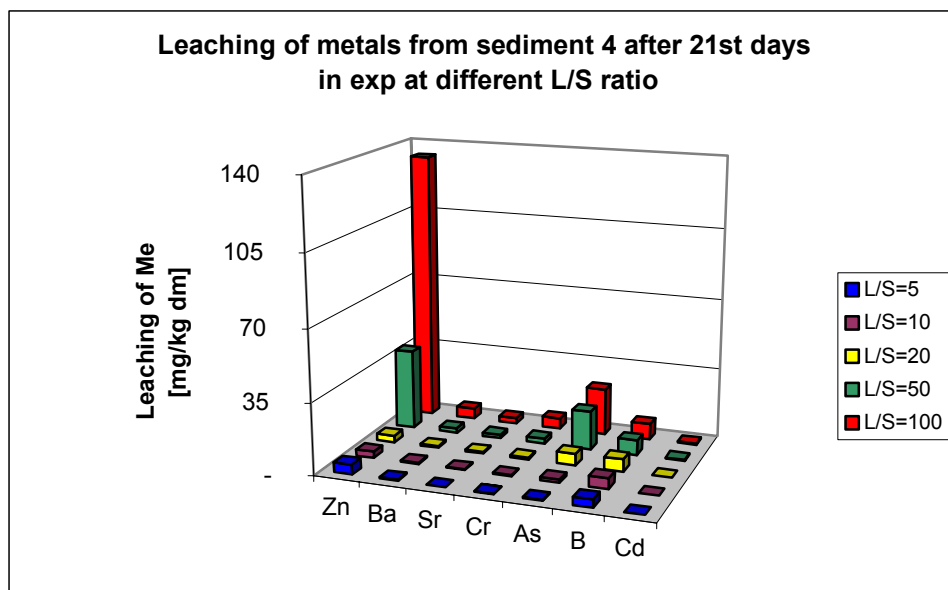


Figure 15. Leaching of metals from sediment 4 in exp at different L/S ratio